S P A R K B R E A K D O W N

O F A

R O D - P L A N E G A P

M. M. C. COLLINS

Thesis submitted for the degree of

Doctor in Philosophy

in the

Faculty of Engineering Science

THE UNIVERSITY OF LIVERPOOL

April, 1966

CONTENTS

CHAPTER I

INTRODUCTION

I. Historical Introduction

Electrical discharges in gases, in the form of lightning, are assumed to have been occurring since early geological times and there is speculation that these lightning discharges in the atmosphere may have played an important role in the origin of life on this planet. Miller[1] has shown that organic compounds which make up living systems can be synthesized by passing an electrical discharge through an atmosphere of CH_4, NH_3, H_2O and H_2, the gases which Urey[2] has postulated as being the components of the primitive earth's atmosphere. Apart from this early importance of lightning little, if anything, is known of electrical discharges until the early recorded history of man when lightning was considered to be created in various manners by the gods which were in vogue at the time. An interesting account of some of these beliefs is given by Schonland[3].

Although man-made electricity was known to the early Greek philosophers it was not until 1600 that the first scientific study of electricity was made by William Gilbert

and, according to Chalmers[4], it remained for Wall in 1708 to be the first to suggest that lightning was an electrical phenomenon. In the years that followed there was considerable speculation on this point and in 1749 Benjamin Franklin[5], who was convinced that lightning was due to electricity, proposed a method by which this could be proven. Franklin's suggestion was taken up by d'Alibard who in 1752, one month prior to Franklin's famous kite experiment, successfully showed that thunder-clouds were in fact electrified.

The problem of destruction by lightning, a brief historical account of which is given by Schonland[3], has been known to man since earliest times but it was not until lightning had been equated with an electrical discharge that Franklin, acting in the capacity of an high voltage engineer, was able to develop a lightning rod to provide protection against this destruction. Franklin's works[5] indicate that the first fully recorded successful per-formance of the lightning rod was in 1760 although it was suggested that unrecorded successes had occurred some years earlier. In spite of this fact that protection from electrical dischargeswas initiated over 200 years ago it is still a major problem in high voltage engineering

which indicates the need for more information on the discharge processes so that the engineer will be better able to develop the protection required.

The actual study of lightning discharges progressed little until the end of the nineteenth century when Hoffert[6] in 1889 and Walter[7] in 1903 published pictures taken by moving a camera, with the lens open, while waiting for a lightning flash to occur. These pictures showed the multiple stroke nature of lightning but were not able to resolve the development of the stroke. The time resolution was greatly increased by Boys[8] who in 1926 published details of his camera, incorporating twin rotating lenses, which he had invented in 1900. Boys himself only obtained one picture with his camera and that in 1928[8] after 27 years of failure but Schonland and Collens[9], in the early 1930's, successfully used a Boys camera in South Africa and from their results were able to put forward a widely accepted picture of the lightning development.

Laboratory studies of electrical discharges were ahead of the study of lightning and some early interesting results were reported by Harris[10] in 1834 and Faraday[11] in 1837 on D.C. discharges and by Steinmetz[12] in 1898

on A.C. discharges. In 1900 and succeeding years a tremendous breakthrough was made by Townsend[13] who developed the theory of ionization by collision. This theory was the basis for a vast amount of research on electrical discharges continuing to the present day. The application of Townsend's theory to higher pressures and longer gaps showed that it was inadequate to cover all discharges and in the late 1930's a further breakthrough was made when Meek[14], working with Loeb, developed the streamer theory.

One other early important development should be mentioned in this brief historical outline and that is the multi-stage impulse generator by Marx[15] in 1924. This invention with its subsequent improvements (see Craggs and Meek[16]) has been a standard tool in impulse breakdown research and undoubtably will continue to be so. The steady development of the cathode ray oscilloscope and more recently of photomultipliers, image converters and high speed film for various types of time resolving cameras has given engineers and physicists a wide range of tools with which to continue the study of electrical breakdown phenomena and a review of the recent work pertinent to this thesis will be found in the following chapter.

II. Outline of Present Problem

As power requirements grow electrical engineers have found that in order to meet demands, it is technically and economically necessary to go to higher and higher transmission voltages. Attendant on these higher voltages have been increased problems of insulation and protection of equipment from high voltage surges, and although a considerable amount of work has been done on the impulse breakdown of non-uniform field gaps there is as yet no complete understanding of the breakdown mechanism.

In the author's opinion, an understanding of the nature of the impulse breakdown is necessary if the best protection is to be developed for power systems and it is therefore the aim of this thesis to provide new information on the impulse breakdown of non-uniform field gaps in air. Since gaps encountered in engineering are generally of a non-uniform field nature this type of gap was studied and in order to separate positive and negative breakdown effects the rod-plane gap was used. During the course of this research a new probe technique (see chapter 3) for measuring the electric field at either of the gap electrodes was developed and this technique has been used to study the breakdown of positive rod-plane gaps up to 200 cm in length using short

front impulses. For comparative purposes some work was done using a negative impulse with a 50 and 100 cm gap.

The results provide new information from which a better understanding of the breakdown mechanism has emerged and it is hoped that further use will be made of the field measuring technique to provide new information on other gap geometries and using long wave front impulses.

CHAPTER II

REVIEW OF PREVIOUS WORK

I. Introduction

Meek and Craggs[17] in their book "Electrical Breakdown of Gases" have given a comprehensive coverage to the work up until early 1951 and several sections of this book are of particular interest with regard to the work of this thesis. A brief resume of these chapters is therefore given including some of the more important references contained in their extensive bibliography. Chapter IV gives a descriptive account of the various techniques employed to study the growth of spark discharges and as these techniques have been used to provide most of the present knowledge of the spark discharge a summary will be given.

(i) Suppressed discharges

Suppressed discharges which are obtained by applying a voltage to a gap for a limited time only have been used to study the growth of sparks in a non-uniform field. The technique employed is to photograph the discharge with the voltage applied for varying lengths of time and then to compare the advance of the spark with the time of voltage

application. This technique necessitates averaging a number of shots since each photograph refers to a different discharge but it does permit an average velocity of propagation of the spark to be determined. A further disadvantage has been shown to exist by recent studies of Gorin and Stekolnikov[18]. They show that when the applied voltage is chopped a reverse discharge occurs due to the space charge in the gap. With time integrated photography this discharge may be confused with the forward discharge.

(ii) Cloud chambers and Kerr cells

Although the cloud chamber has been used mainly to study avalanches and streamers in uniform field gaps, Nakaya and Yamasaki[19] have used one to study short point-plane gaps with results similar to those of Raether in uniform field gaps.

The Kerr cell[20,21], first used in 1875, consists of two polarizing sheets between which is a liquid such as nitrobenzene which is capable of changing the plane of polarization of light passing through it depending on whether or not it is electrically stressed. This cell is used as a shutter with a fast response time, notably of the order of 4 nsec to close. This shutter has been used

to study the growth of sparks but the results quoted are all for uniform field gaps.

(iii) Time resolving cameras

A number of investigators have used time resolving cameras of the rotating lens, rotating mirror or rotating film type. A considerable amount of work was done on the non-uniform field gap up to 2 metres in length with the results showing a leader stroke starting from the anode (in a positive point, negative plane gap) and branching in the downward direction until reaching the cathode. The main stroke then follows in detail the path of the leader stroke but it does not branch as frequently, only following the more prominent branches. The leader stroke is seen as an intense filamentary channel accompanied by a less light, but more diffuse, voluminous shower of discharge. The importance of this shower of discharge has been stressed in several papers[22,23]. The nature of the breakdown was quite variable from shot to shot and in some cases the positive leader stroke did not cross the entire gap but was met by a negative leader propagating from the plane. If a point electrode was placed on the negative plane a negative leader was always seen to grow from the point although it was much slower than the positive leader and

did not start until the positive leader was partway across the gap.

This technique has made possible a good measurement of leader velocity and a graph of initial and final leader velocity is given as a function of series resistance.

Komelkov, by putting a slit between the discharge and the camera, was able to view various parts of the gap individually and thus showed separately the two parts of the leader stroke. Komelkov states that the first part, a zone of large diameter, low intensity ionization corresponding to the voluminous shower of discharge visible on earlier photographs, consists of streamers emerging from the tip of the second part which is the leader channel of relatively small diameter and intense illumination.

(iv) Photomultipliers

Meek and Craggs[24] suggested the use of a photomultiplier to study the growth of the leader stroke which precedes the spark breakdown of a gap and this technique gave a considerable advantage in time resolution over the rotating camera technique. Saxe and Meek[23] studied a positive point, negative plane gap and give curves of distance travelled against time for the leader in two different gaps with varying circuit resistance.

For voltages below breakdown value they showed that a corona discharge emits light from a roughly hemispherical volume with the positive point at the center of the plane face which is parallel to the negative plane and with the curved surface towards the plane. The light intensity was found to decay continuously with distance from the point.

Two other methods of studying the breakdown mechanism are mentioned, namely oscillographic studies and the use of Lichtenberg figures. No results pertaining to rod-plane gaps are given for the former but mention is made of some work by Allibone[25] and by others on rod-plane gaps using Lichtenberg figures. Allibone's results, obtained by placing a piece of film between the electrodes, show that the initial corona may cross the gap without the formation of a leader. This indicates that the photomultiplier used by Saxe and Meek was not sufficiently sensitive to enable them to observe all the corona.

(v) <u>Other chapters of particular interest</u>

Chapter VI, "Theory of the Spark Mechanism", deals mainly with the basic breakdown theories which are more readily applied to uniform fields. A brief section is however devoted to non-uniform fields and Meek and Craggs state about the point-plane gap " ..... the breakdown

why not use software packages?

voltage cannot be computed theoretically, as it depends on the conditions governing the propagation of streamers for which no quantitative mechanism has yet been proposed." Although a great deal of work has been done on point-plane gaps since 1951 the position is still the same in that the breakdown voltage cannot be computed theoretically.

Chapter VII deals with breakdown voltage characteristics and includes curves showing breakdown voltage-vs-gap length for both positive and negative impulses. These values will not be enlarged upon here as this work is concerned mainly with obtaining new information on the mechanism of breakdown rather than on the breakdown voltage values. It must be noted however, that any proposed theory of breakdown must be capable of explaining the observed breakdown voltage characteristics.

The chapters not mentioned specifically were found valuable in providing a general background to the problem of electrical discharges.

II. Swedish Work

Norinder and Salka published a series of papers on non-uniform field breakdown using a chopped impulse voltage and studying the growth of the discharge in a sphere-plane and

point-plane gap using a camera with a quartz-rocksalt lens. Their results for the positive case[26] showed the discharge to occur in three phases. The first is a corona consisting of a short stem from which grows a long crown developing in a time less than they could resolve. They considered the possibility of radioactive substances in the air to create electrons away from the high field region in this first phase. The second phase is a high conductivity channel starting from the base of the corona stem and branching downwards with the aid of "fine luminous tufts" at the ends. In addition a "luminous bundle of rays" develops and traverses the whole gap at the sparking voltage. The third phase or main stroke occurs when a branch of the second phase crosses the gap and it follows the path of the branch or in some cases two branches in parallel. No growth from the plane was observed in these experiments. These results are in good general agreement with earlier work.

The negative case[27] gave an initial phase of corona which crossed the gap in a single or in several stages. When this occurred a leader developed from the plane and was met by a leader developing from the cathode. These leaders form the track of the main stroke which follows

when they meet approximately in mid-gap, the positive leader generally covering the greater distance.

The third paper[28] in the series, dealing with insulating screens in the long discharges brings out the interesting fact that the corona from the positive point is stopped by a screen whereas the corona from a negative point is not. That is to say the positive corona tends to spread out along the screen while the negative corona causes a corona to start on the opposite side of the screen even though the screen is not punctured. An explanation of this is given in terms of a higher space charge density in the negative case and it is pointed out that a screen in the negative case decreases the breakdown voltage value while it increases the breakdown voltage in the positive case.

The final paper[29] again deals with the negative case using limited current to slow down the process and to make the main stroke less intense as was done by earlier workers[30].

III. Further Work Using The Techniques Described By Meek and Craggs

(i) Photomultipliers

In 1955 Saxe and Meek[31] published a paper giving further results using the photomultiplier technique which they had developed and reported on earlier[23]. They also used an inverted gap, i.e. the plane was at a high potential and the rod was earthed (through a resistor), in order to facilitate current measurements. The results show the similarity between the current pulse shape and the light pulse shape corresponding to the impulse corona. The impulse corona and the diffuse, voluminous discharge ahead of the leader channel are shown to be generally similar indicating that the two are different aspects of the same phenomena.

(ii) Suppressed discharges

Park and Cones[32] give an interesting theory of the breakdown mechanism after giving a set of experimental results correlating current measurements, made in an inverted gap as was done by Saxe and Meek, to still photographs obtained by chopping the applied voltage before breakdown. The photographic results agree generally with those published earlier by Norinder and Salka using the

same technique. The corona is seen to be made up of a large number of "streamers" so-called because of their appearance on the discharge pictures but which, according to their theory, are actually photographic traces produced by balls or regions of high space-charge density with high ionization and excitation activity at their leading surface. These balls are projected from the sphere electrode towards the plane along lines of force of the applied field. The ball should be thought of as a travelling wave of high charge density propagated by new charges being continually produced in the high field of the leading edge. A high concentration of positive and negative ions is left behind with an excess of positive ions for the sphere positive and an excess of negative ions for the sphere negative. This space charge reduces the field so that ionization is inhibited and thus the passage of the high charge density does not produce a conducting path.

They go on to postulate that this process is initiated (considering the positive case) by an electron being produced from a negative ion by the high field near the sphere and being accelerated towards the sphere forming an electron avalanche. As soon as this ionization process starts it produces photons which liberate electrons in the nearby high

field region and thus a large number of avalanches are formed. The electrons are drawn into the sphere leaving the regions of high positive charge density which then propagate across the gap. This theory accounts for the high speed of propagation of the streamers across the gap. After the corona streamers the leader stroke starts but the reason for it starting is not explained.

The paper includes an appendix giving the calculation of the voltage distribution between the sphere and the plane. This distribution is plotted along with a curve which is estimated to be the voltage distribution after the space charge has entered the gap and the corona has propagated to the plane.

(iii) Time resolved photography

Waters and Jones[33] did considerable experimental work on non-uniform field breakdown in air. They used a rotating mirror camera with an f/1.0 aperture and in order to prevent the film being fogged by the final breakdown, the voltage was chopped by a triggered sphere gap. They also measured the current in the gap and studied the time lag to breakdown using an impulse with a wave-tail of several millisec to half value.

They observe the positive corona to fill a volume roughly hemispherical in shape and having a filament growth rate of 10^8 cm/sec. In general their results are in agreement with previous work.

For the negative case they show the corona completely crossing the gap before the positive leader is initiated from the point where the negative corona hit the plane.

(iv) Lichtenberg figures

Baatz, Böcker and Fisher[34] did some work on a rod-rod gap of 35 cm in length in order to get results which could be compared with an investigation done for CIGRE Study Committee No. 8. They give results of current and voltage measurements and they studied the corona growth using a film stretched between the electrodes on which Lichtenberg figures were produced. Again the final discharge was suppressed by chopping the voltage so as to prevent fogging of the film.

IV. Work Done Under Loeb

Hudson and Loeb[35] have studied the breakdown of a point-plane gap in air using a high speed photomultiplier technique and although the study was done using a D.C. voltage the results of the prebreakdown study are of interest.

Their technique was to use two photomultipliers, one to trigger the oscilloscope and one to observe the corona growth. The trigger photomultiplier was focused on the space near the anode tip so that the oscilloscope would be triggered at the instant corona was initiated in the gap. The signal photomultiplier was moveable so that it could view any portion of the gap and by a succession of observations at different points in the gap the growth of the corona was observed.

The results show that the corona discharge consists of "a fast primary streamer or dendrite" (a dendrite is defined as a "more or less tree-like configuration of a large or small number of streamers which start at the electrode as either separate filaments or as a single trunk which then develops into multiple streamers by branching") "and a slower secondary which are not at first resolved. The primary emerges and increases in amplitude as it proceeds at high speed into the gap." "The initially very bright but slower secondary dendrites at first mask the primaries but attenuate rapidly ....." The mechanism of this primary-secondary dendrite process is discussed but no definite conclusions are reached.

In a later paper Nasser and Loeb[36] state that from the Lichtenberg figure technique there is no evidence of primary and secondary streamers and they go on to suggest that the phenomena observed by the photomultiplier technique are in fact due to the branching of the corona streamers. The primary streamers would then be the streamers travelling axially which pass a given horizontal plane before the more radial streamer tips which travel further and more slowly and would be observed as the secondary streamers.

More recently still Dawson[37], working in Loeb's laboratory, has used an image converter and photomultipliers to show that the primary-secondary streamer pattern is in fact a real phenomenon and not due to the method of observing streamer branches as suggested by Nasser and Loeb. Dawson reduced the photomultiplier slit to a square aperture and then observed the edge of the region in which streamers were observed. Although a signal was obtained only occasionally when a signal did occur it always consisted of a primary-secondary streamer sequence.

Dawson also observed, using an image converter, that when the primary streamer tips reached the cathode the secondary streamers started to increase in length almost instantaneously. "This", he says, "is explicable if the

presence of a very fast, unobserved return stroke from the cathode is assumed."

Returning to the paper by Nasser and Loeb, they show interesting results using Lichtenberg figures produced on film. The branching of the corona filaments is studied and the number of branches as a function of distance from the anode and of gap length is shown. They consider that the length of the Lichtenberg figure produced by any given streamer is a function of the voltage on the streamer tip and use this to determine the voltage at the tip of streamers which have crossed the gap. If these streamer tips are considered to be regions of high charge density isolated from the anode as has been suggested[32] then it seems more likely that the important factor is the charge of the streamer tip rather than the potential of the tip.

V. Russian Work

Considerable work has been done in Russia on rod-plane gaps and much of this has been translated in Soviet Physics - Technical Physics and Soviet Physics - Doklady. Stekolnikov and Shkilev[38] published results relating current in the gap to streak photographs taken using an "electron-optical converter" or image converter. This paper deals mainly

with the development of the leader in a positive rod-negative plane gap of length from 3.0 to 5.75 metres. Stekolnikov[39], in a later paper, using the same technique gives results of a study of the impulse corona including propagation velocities which vary from 5×10^9 cm/sec to 2×10^8 cm/sec. The velocity of the "beams of filaments" from the head of the leader stroke is given as an average of 4×10^7 cm/sec. In two more papers, Stekolnikov and Shkilev[40,41] deal with the negative rod-plane gap using the techniques employed for their earlier work on the positive rod-plane gap. In the second of these papers they discuss the effect of varying the rate of rise of voltage which has been found to have a large effect on the breakdown voltage value. Other work on the effect of wave front duration on long rod-plane gaps is reported in two papers by Bazelyan, Brago and Stekolnikov[42,43]. They find the breakdown voltage is a minimum for a wave front of from 150 to 250 μsec with a minimum average gradient of from 2.25 kV/cm to 4.7 kV/cm for gaps ranging in length from 590 cm to 50 cm. This compares with an average gradient of 5.35 kV/cm using a standard impulse wave. This work was continued by Stekolnikov and Shkilev[44] who give a comparison of image converter photographs taken with short and long wave fronts.

Two papers closely associated with the present thesis work were published after the present work had been under way for about a year. The first of these, by Bazelyan[45], describes the measurement of the space charge injected into a gap by the corona pulse using an inverted sphere-plane gap. The sphere was divided into sections and the integral of the current flowing in each section was measured. With this technique Bazelyan measured the current in the very small section of the sphere from which the corona originates, thus eliminating the error caused by the displacement current in the remainder of the sphere which previously caused a lower than actual value to be obtained. The integral of the current in the other sections of the sphere was used to determine the field at the surface of the sphere and the change in that field due to the space charge of the corona. From these field changes, Bazelyan concludes that the hypothesis, put forward by Park and Cones[32], that the space charge moves along with the ionization front leaving behind a neutral or weakly charged medium is correct.

The second paper, by Bazelyan and Stekolnikov[46], uses the equipment of the first paper to study the effect of injecting a space charge into a gap. This is done by

superimposing a short impulse voltage on a slowly rising impulse wave. The results showed that by injecting a charge of between 8.5 and 10 μcoulombs into the gap an increase in the breakdown voltage of up to 20% could be obtained.

Gorin and Inkov[47] have investigated the development of the leader channel by means of an insulated probe projecting a short distance from the rod in a positive rod-negative plane gap. This effectively isolated a short section of the discharge channel so that the voltage gradients could be measured. The current densities were measured by measuring the current in the rod and determining the channel diameter from image converter records.

VI. Theoretical Papers

Wright[48] has developed a theory of the propagation of positive impulse corona based on a model in which electrons produced by photoionization initiate avalanches in the strong fields near the tip of the corona filament. He compares the results with experimental results obtained by Kritzinger[49] and gets a reasonable agreement. However, he assumes the corona filament has an electrically conducting channel which has not been shown to exist and which, in fact, probably does not exist so his model would need some modification in this respect.

Aleksandrov[50] published a paper on the corona to spark transition in long air gaps. He concludes that the condition for breakdown of the gap is the condition for the appearance of a leader which he states is determined entirely by thermal processes.

Dawson and Winn[51] have presented a model for the corona streamer propagation which assumes negligible conductivity of the path behind the filament head. This is in agreement with the hypothesis originally put forward by Park and Cones[32]. The criterion given for the propagation of a corona streamer is that the tip should contain an excess charge of 10^8 ions and the radius of the tip should be about 3×10^{-3} cm. This is compared with experimental results of the present work in Appendix I. In a following paper, Dawson[52] describes an experiment in which it is found that corona filaments do in fact continue to grow after the applied voltage has been removed which gives further support to the hypothesis that the corona filaments are isolated regions of charge propagating because of their own high field.

VII. First Use Of A Field Probe

Kritzinger[53,54] first used a field probe protruding above the plane in a point-plane gap in conjunction with photomultiplier studies in which he claims to have shown that a region of ionization activity moved from the point to the plane and then back towards the point. These regions of ionization, which he called "globules", were observed by using a photomultiplier to scan various levels in the gap so that an average picture of the movement could be built up by taking several shots at each interval of distance from the point. No explanation of the mechanism causing the "globules" to return to the rod from the plane was given but for the forward growth he suggested, on the basis of experiments using various gas mixtures, that photoionization played an important role.

Using a high impedance probe protruding above the plane he obtained field values of about 15 kV/cm when the field due to the geometry of the gap would only be 1 kV/cm. This showed definitely the enhancement of the field by the corona space charge. By scanning the region just above the probe with the photomultiplier he showed that a step occurred on the voltage oscillogram coincident with the occurrence of a light pulse at the probe. This showed that

the light pulse of the corona "globules" was associated with the space charge effect. Using a low impedance current probe mounted level with the plane a current pulse was found to be coincident with the light pulse and from both the current and voltage measurements the charge associated with a "globule" was found to be from 2 to 5 x 10^{-9} coulombs.

VIII. Summing Up

This review of the literature has been to indicate the state of the art when the present work was begun and includes work published while the present program was in progress. Although some comment has been made in this chapter, in general where previous results have a direct bearing on the work of this thesis comment and comparison will be given in that section following which deals with the specific results.

One further recent work must be mentioned and that is the new book by Loeb[55]. It gives an interesting review of the work up to 1964 in a typically enthusiastic manner which leads one to believe that a better picture of the non-uniform field breakdown has been developed than actually exists.

CHAPTER III

EXPERIMENTAL EQUIPMENT

I. DEVELOPMENT OF A NEW FIELD PROBE TECHNIQUE

(i) General

The field probe used by Kritzinger[53] protruded above the surface of the plane in order to measure the potential drop, $\triangle V$, over a small distance, $\triangle d$, which gives the field as $\triangle V/\triangle d$ volts/cm. This technique has several disadvantages, the main one being that a small portion of the field will be short circuited by the lead which connects the probe to the oscilloscope and by the finite thickness of the probe itself. The result is that the potential of the probe is lower than that of the space would have been if the probe were not there so that the probe will not give the correct value of field and it will cause a distortion of the field in the gap. In order to minimize this effect the probe diameter must be large compared with the diameter of the supporting lead. This, however, introduces another problem in that changes of field over a small distance horizontally cannot be measured. It is these factors which the author wished to overcome in the development of a new probe technique.

A probe mounted flush with the plane surface was considered and from the following it can be seen that the field at the probe surface is proportional to the integral of the displacement current flowing in the probe. Taking any arbitrary electrode configuration with a small insulated probe mounted flush with the surface of the earthed electrode, when a voltage is applied to the high voltage electrode an electric flux, ψ, will link the high voltage electrode with the probe of surface area A. This electric flux is equal to Q, the charge which has flowed into the probe, and is equal to $\int i dt$ where i is the displacement current in the probe. Since E, the electric field at the probe surface is proportional to the flux density D which is equal to ψ/A it follows that $E = \int i dt/\epsilon_o A$.

In order to assess the value of this technique a probe, 2 cm in diameter, was made and current oscillograms obtained. It was found, however, that the oscillograms were generally not of a sufficiently high quality to permit an accurate integration to be made and that when an interference free oscillogram was obtained the time involved in the integration made the method impractical.

A simple solution to this problem was found by doing the integration electrically. By connecting the probe to earth through a capacitor instead of a resistor the voltage, as measured on the oscilloscope, was proportional to the integral of the current instead of to the current and thus since $\int idt = Q = CV$, where C is the capacitance from the probe to earth and V the voltage measured on the oscilloscope, $E = CV/\epsilon_o A$. For any given probe arrangement $C/\epsilon_o A$ is a constant and will be called the probe constant, K_p, with units of kV/cm/volt. This means that oscillograms of the capacitor voltage will be oscillograms of the field at the probe surface differing only by a constant K_p. Tests of this technique showed that consistent results could be obtained and an assessment of the accuracy and limitations involved was begun.

(ii) Errors in field probe technique

Three sources of error were considered. Firstly the insulation required between the probe and the surrounding electrode will cause some distortion of the field but experiment has shown that this can be taken into account by considering the effective probe radius to include approximately half of the insulation thickness. For probes smaller than 1 cm diameter this is a very appreciable

factor and, as will be seen later, it is better to measure K_p than to compute it from A and C. The second source of error is due to the time constant of the probe capacitance and the recording oscilloscope input resistance. With a varying field this is difficult to correct so it is necessary to have the time constant long enough to make its effect negligible. Thirdly, the voltage on the probe will cause a field distortion since the surface should be at the same potential as the remainder of the electrode surface. This effect is equivalent to a depression in the electrode surface of $1/K_p \times 10^{-2}$ cm and in practice is negligible.

(iii) Limitations of field probe technique

There are two limitations on the use of this probe technique which must be considered. The first is that the field measured is the average field over the surface area of the probe. If the field along the plane varies rapidly then obviously a small diameter probe must be used. Since the probe can be made any diameter desired this overcomes one of the disadvantages mentioned in connection with the Kritzinger probe. The second limitation is the fact that there must be no conduction current to the probe since the measurement of field is dependent on the integration of the displacement current. Experiment has shown that

this is not a problem as long as any discharge is confined to the region around the high voltage electrode but once the corona filaments cross the complete gap or if a discharge starts from the earthed electrode care must be exercised in interpreting the results. Practical results show that for a probe 2 mm in diameter the chance of a conduction current to the probe is very small unless breakdown occurs when the chance increases to almost 100%. It has been found however that the field can be measured, even under breakdown conditions, by covering the probe with a perspex dome which prevents any conduction current to the probe. Although this cover will change K_p it can be taken into account by calibrating the probe in a uniform field with the cover in place.

(iv) Calibration of field probes

Initial calibration tests were made on a probe of 2.22 cm diameter by placing a uniform field electrode, 42 cm in diameter, 5 cm above the plane in which the probe was mounted. The applied voltage was measured on the resistance voltage divider (which will be described in a later section) and the voltage over gap length, which gave a field value of 21.8 kV/cm, compared to the field value measured with the probe.

The insulation around the probe was an air gap of 0.50 mm so that the actual probe radius plus one-half of the insulation thickness gives an effective probe radius of 1.135 cm. This gives an effective probe area of 4.04 cm^2. These dimensions were measured with a micrometer so the values are $\pm$ 0.010 mm which gives an accuracy in the area of about $\pm$ 1/4%. Initially the capacitance of the probe to earth was the stray capacitance including the oscilloscope input capacitance. This stray capacitance was measured using a Q meter and found to be 33 pF but the accuracy of this would at best be $\pm$ 3% so a further 339 pF was added giving a total of 372 pF with an accuracy of about $\pm$ 1/2%

From these values K_p was computed for each case and the result is $K_{p1} = 0.0924$ and $K_{p2} = 1.040$ kV/cm/volt. The voltage applied to the uniform field electrode was 109 kV which gave probe voltages of 227 and 20.8 volts corresponding to 21.0 kV/cm and 21.6 kV/cm respectively. This result indicates that the value of the stray capacitance was too low but with the improved accuracy of C the agreement is within 1%.

It is interesting to note that if the field value is used to compute the stray capacitance from $C = EA\epsilon_o/V$ the

result of 34.3 pF when used with the additional capacitance of 339 pF gives K_{p2} = 1.045 and E = 21.75 kV/cm. This agreement does not include any oscilloscope error since the impulse voltage and probe voltage were both measured using the same oscilloscope. The calibration was done with positive and negative polarity and with insulating barriers up to 3 mm thick covering the probe. The results were the same for all cases.

A further calibration was done for a probe 1.930 mm in diameter using a uniform field electrode 1 m in diameter 9.75 cm above the plane in which the probe was mounted. The applied voltage was 146 kV giving a field of 14.98 kV/cm. The probe insulation was 0.089 mm so that the effective probe radius was 1.010 mm and the effective area 3.30 mm^2. The stray capacitance was again used as the integrating C and it was measured on a Wayne Kerr bridge and found to be 30.9 pF $\pm$ 0.5 pF. This gives a value of K_p = 10.6 kV/cm/volt and E = 14.05 kV/cm which is a difference of 7% from the value obtained using the applied voltage and the gap length. The large difference is undoubtedly due to not knowing the effective probe area sufficiently accurately. A 7% error in area representsa 2.6% error in radius which is only 0.026 mm. The actual radius of the probe is known

to a sufficiently high degree of accuracy so it is likely that the effective probe radius does not include exactly one-half of the insulation thickness for small diameter probes. From this it can be concluded that if a high degree of accuracy is required the probe should be calibrated in a known field.

(v) Probes used in experimental work

Three probes, mounted as shown in Fig. 1, were used for the majority of the work and had nominal diameters of 2 cm, 1 cm and 2 mm. The insulating block, which was threaded so that the probes could be easily changed, was cemented to the plane with Araldite. The copper screening box, a cube of 13 cm, was screwed to the insulating block and contact with the plane was made through spring "fingers" which pressed against the lower surface of the plane. The hole in the plane was the correct size for the 2 cm probe so it was necessary to use inserts to reduce the hole size for the smaller probes. The shank of the probe was connected to a BNC connector in the screening box and from this connector a short length of 75 Ω cable took the signal to the oscilloscope screening box. This cable could not be terminated in its characteristic impedance so it was necessary to keep the length of cable short to prevent

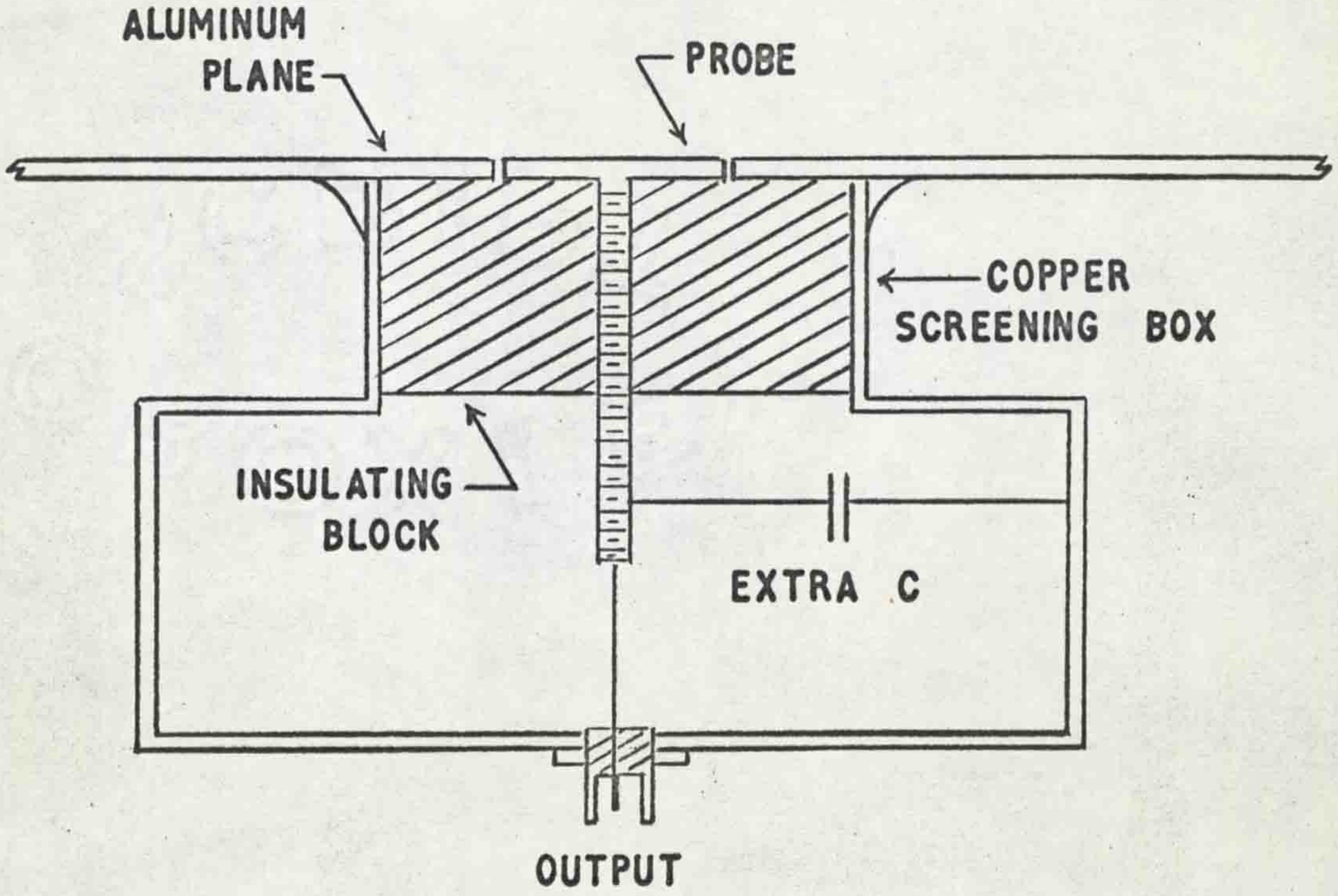

FIG. 1 MOUNTING OF FIELD PROBE

oscillations in the cable. This made it necessary to use the oscilloscope 10X attenuating probe to connect the signal to the oscilloscope but this had the advantage of a 10X increase in input resistance.

After the initial calibration the oscilloscope attenuator probe was changed and this reduced the integrating capacitance to 31 pF. Using this value the following probe constants were obtained.

2 cm probe - K_p = 0.0865 kV/cm/volt

1 cm probe - K_p = 0.449 kV/cm/volt

2 mm probe - K_p = 11.30 kV/cm/volt

2 mm probe covered by perspex dome

K_p = 12.63 kV/cm/volt.

The value of K_p with the perspex cover was obtained by calibration in a uniform field. A check was then made in a non-uniform field and the same ratio of K_p (not covered) to K_p (covered) was obtained.

For measurements of the field at the rod an inverted gap was used as shown in Fig. 2B and the probe constant calculated to be 9.82 kV/cm/volt. It was not practical to measure K_p for this probe so the calculated value was used even though experience had shown that it could have an absolute error of 5 or 10%. This absolute error is not of

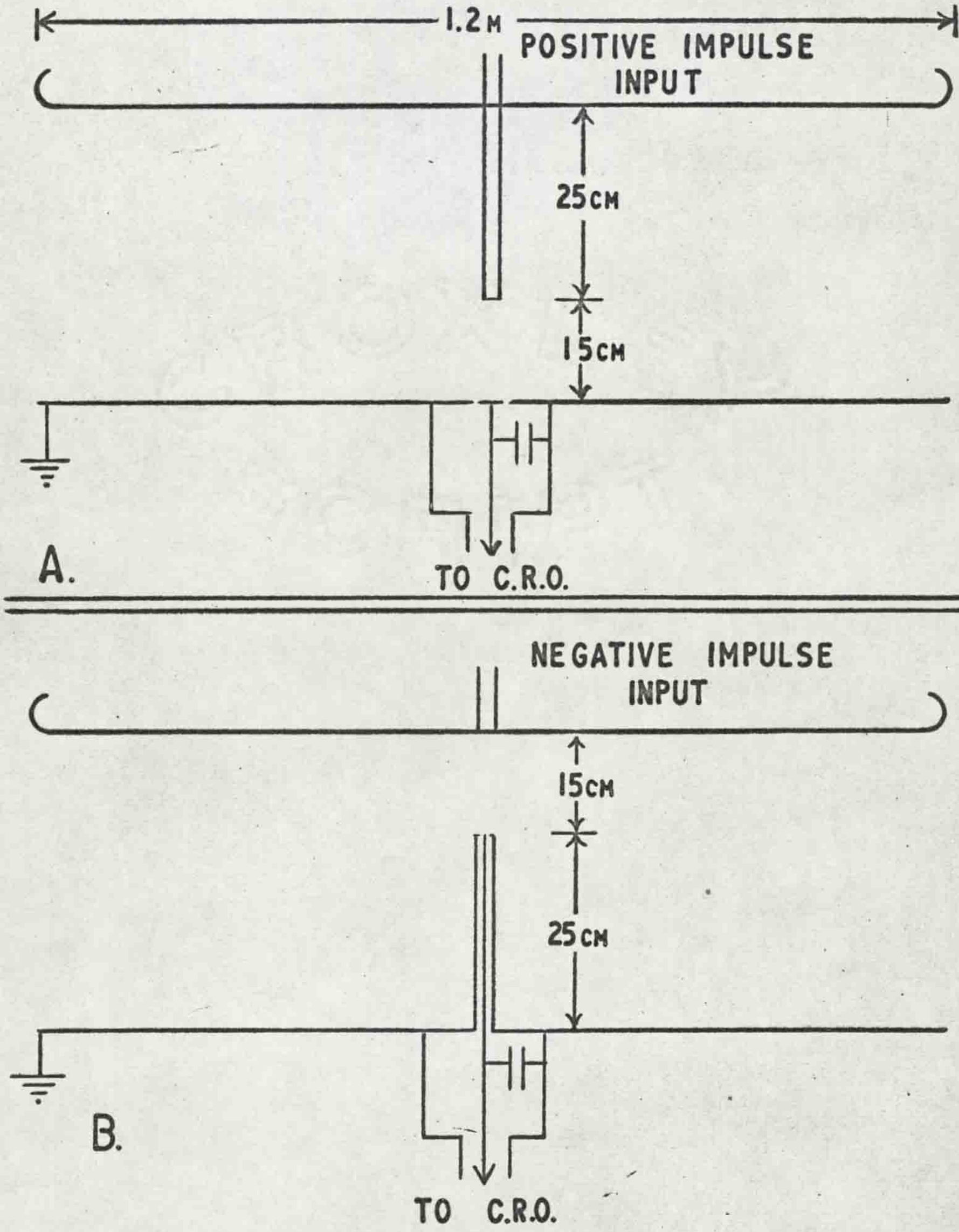

FIG. 2 INVERTABLE TEST GAP

A. FOR FIELD AT PLANE

B. FOR FIELD AT ROD

great importance since the same probe was used throughout and the comparative error would be small.

II. Oscilloscope

The oscilloscope used was a Hewlett Packard Type 175A with a specified bandwidth of D.C. to greater than 50 MHz and a sensitivity of 50 millivolts per cm. The screen had an internal graticule which could be illuminated by an ultra-violet light source which was mounted in the polaroid camera. The ultra-violet light also served to pre-fog the film which gave an improved writing rate. The lens on the camera could be shifted to eleven different vertical positions (five either side of a normal center position) so that eleven traces could be recorded on one polaroid picture. This was very convenient for comparison as well as economy reasons. All the oscillographic results were taken on polaroid film, mainly type 410 which is specifically for oscillographic work and has a film speed of ASA 10,000. Some of the slower work was done using type 47 film which has a film speed of ASA 3,000.

Initial experiments showed that the oscilloscope was not adequately screened to prevent interference caused by the firing of the impulse generator from affecting the

oscilloscope trace. It was therefore necessary to build a screening box to house the oscilloscope. A box, 91½ cm wide, 84 cm deep and 56 cm high was constructed from copper sheet and mounted on a Handy-angle trolley to facilitate its movement. Access to the oscilloscope was through hinged doors on the front which were made of copper mesh. The doors were held shut with four spring clamps which covered the complete length of the top and bottom and which provided quick access while maintaining good screening. The power input was taken from an isolating transformer and fed through a mains filter as shown in Fig. 3. The signal was fed into BNC feedthrough connectors mounted on the box. As mentioned earlier the signal was taken from the feedthrough connector to the oscilloscope by means of a 10X attenuating probe in order to eliminate oscillations in the 75Ω cable and to raise the input impedance seen by the field probe. This attenuating probe and lead introduced interference on to the signal and it was found that an extra earthed screen on the whole probe and lead was necessary to eliminate this interference. The mechanism of this interference was not determined. With the screening as outlined the interference was reduced to an acceptable level over the complete range of impulse voltages and oscilloscope sensitivities.

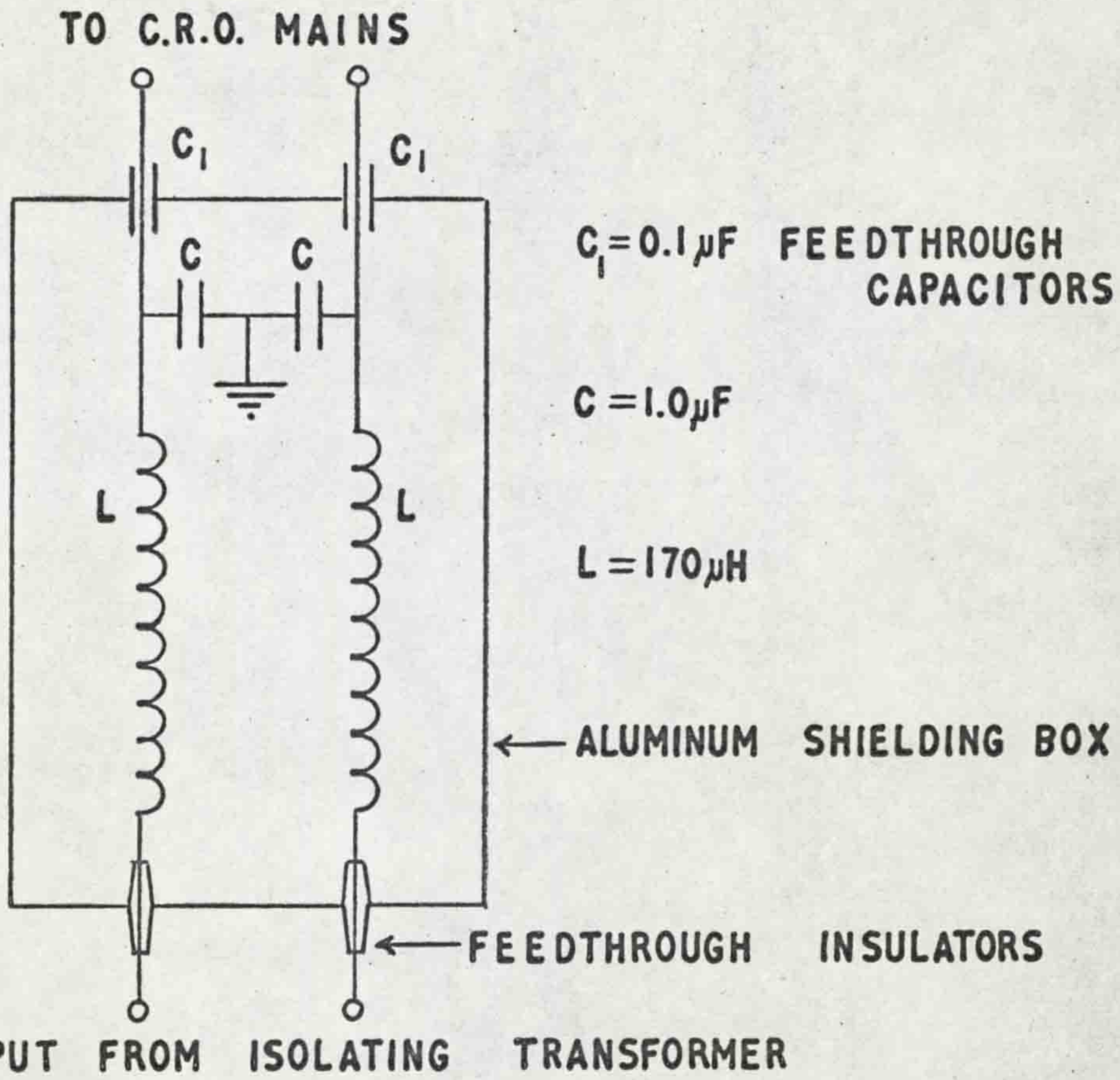

FIG. 3 MAINS FILTER FOR C.R.O. SHIELDING BOX

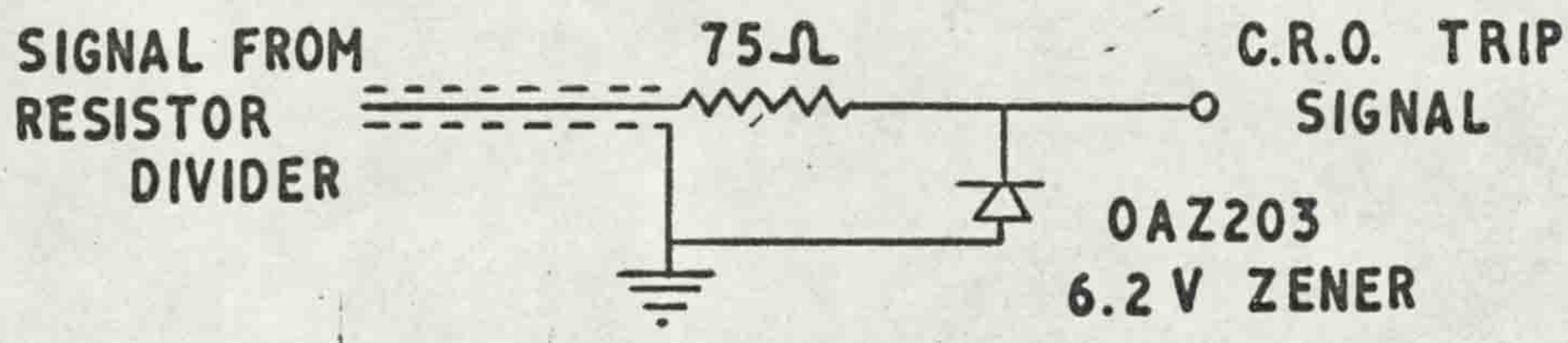

FIG. 4 C.R.O. TRIPPING CIRCUIT

Several methods of triggering the oscilloscope were tried and different methods were used for different conditions. When the resistor divider was used a signal was taken from it and fed through a circuit as shown in Fig. 4. Initially this circuit applies the full voltage from the divider to the trigger input. When the voltage rises to 6.2 volts the Zener diode conducts preventing the pulse from rising further. The trigger pulse is thus independent of the voltage input (providing of course that the input is greater than 6.2 volts) and therefore gave very reliable triggering without requiring any change for different impulse voltages. When the resistor divider was not used a short piece of wire acting as an antenna to pick up a signal from the firing of the impulse generator was used to provide the triggering signal and again reliable results were obtained. A third method was to trigger the oscilloscope from the incoming signal. This method was mainly used to study the pulses caused by charge hitting the field probe since a fast sweep speed was used and a variable delay after the firing of the impulse was necessary. The disadvantage of the internal trigger is that the settings of the controls must be changed to suit the signal and for very small signals the triggering was not reliable.

In order to photograph the oscilloscope traces the shutter of the camera was locked open in the B position and the screening doors clamped shut. If a series of shots was taken on one picture the lens position could be altered from outside the box. For the type 410 film the lens was set for its widest aperture for sweep speeds greater than 1 μsec/cm with a corresponding reduction in aperture as the sweep speed was decreased. The graticule was illuminated and exposed for 1/100 sec at an aperture of f/8 in order to pre-fog the film and record the graticule. This was done with the lens in the central position.

III. Experimental Gap

(i) Rod

The rod used was circular in cross-section with a diameter of 1.1 cm and a length of 1 metre. The lower 9 cm was threaded into the upper part so that the end could be hemispherical, a 30° cone, or square cut which was used for the majority of the work. The rod was suspended by a copper braid from a 2.5 cm diameter aluminum pipe which was the connection to the impulse generator.

(ii) Plane

The earthed plane was made up of three aluminum sheets on a Handy-angle frame. The center sheet, in which the probes were mounted, was 1.22 m wide by 3.66 m long and could be slid back and forth along the framework so that the probe could be situated at any horizontal distance from the rod center-line. This center sheet overlapped the two edge sheets which were 2.44 m by 0.91 m and which were fastened to the 2.44 m by 2.44 m framework. Experiment showed that the spark did not tend to terminate at the point of overlap so it was assumed that the slight discontinuity in the earth plane did not affect the breakdown. The framework was mounted on legs 1.37 m high so as to enable the oscilloscope to be used beneath the plane which was necessary in order to keep the length of cable from the probe to the oscilloscope as short as possible. The legs were set on insulating blocks and the plane was earthed by a single heavy copper braid to one end of the center sheet.

IV. Lichtenberg Figure Technique

Most of the Lichtenberg figures were produced on perspex by coating it with Xerox powder before subjecting it to the corona streamers. The technique involved wiping

Xerox powder onto the perspex sheet using a piece of cotton. The powder tended to stick to the perspex so a thin layer was easily applied. The perspex was then set at the appropriate height in the gap, parallel to the plane, and the required impulse applied to the gap. The perspex was then wiped lightly with the cotton which brushed aside the excess powder leaving clear Lichtenberg figures. The figures could be removed and the perspex readied for another shot by rubbing the sheet vigorously until a thin layer again covered it. If a flashover occurred which caused a heavy tree shaped Lichtenberg figure on the sheet considerable effort was required to rub the sheet back to its original condition. An example of a Lichtenberg figure on perspex is shown in the photograph, Fig. 5.

More permanent Lichtenberg figures were produced on X-ray film. It was found that for negative impulses the film could be covered by a light proof barrier and the figures could still be obtained but for the positive case the film could not have any cover so it was necessary to do the work in darkness. For this the double emulsion of the X-ray film proved to be a great asset as it did not matter which side of the film was exposed to the corona. An example of the Lichtenberg figures produced with the film is shown in Fig. 6.

FIG. 5 POWDER LICHTENBERG FIGURE ON PERSPEX

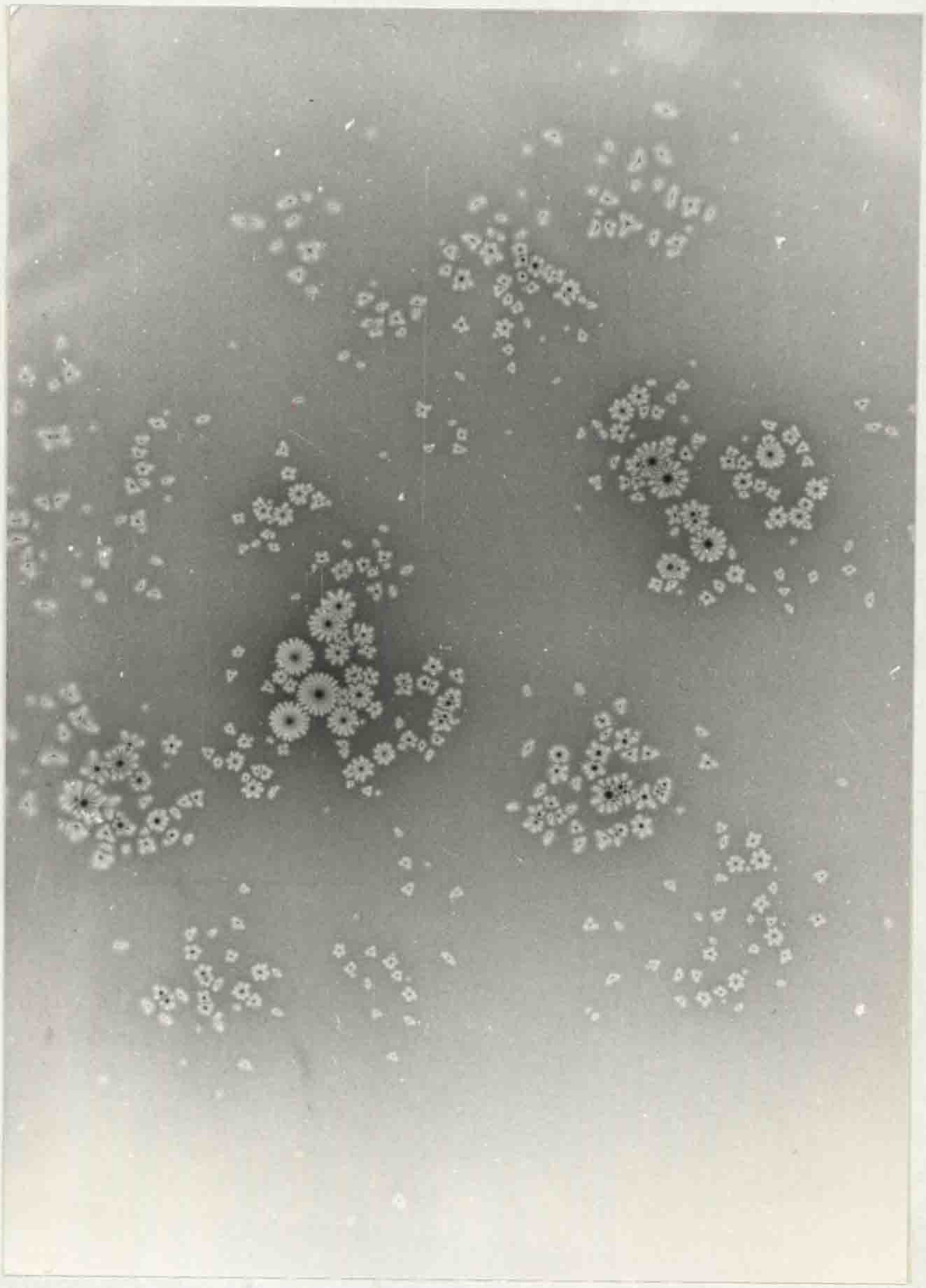

FIG. 6 LICHTENBERG FIGURE ON X-RAY FILM

Lichtenberg figures were also produced with the film perpendicular to the plane and an example of this is shown in Fig. 7.

V. Impulse Generators

Due to the fact that the department moved in the middle of the experimental work it was necessary to use three different impulse generators during the course of this investigation. The initial work was done on an 8 stage, 0.20 μF, 125 kV per stage generator shown in Fig. 8. This generator was designed to be used with a high capacitance load so the only wave front capacitor was the 100 cm sphere gap. With the low capacitance of the test gap this gave a wave front duration of approximately 0.4 μsec with some oscillation near the wave crest. The voltage wave shape is not shown as it is the same as the geometrical field shape shown in Fig. 22B of the results.

The voltage was measured using a screened resistor divider, shown in Fig. 9C, which was designed and built using an existing 6 kΩ resistor. The resistor was mounted on a moveable 1.22 m square earth plane in order to provide a constant earth reference and the screening ring assembly was added to the top of the divider in order to improve

ROD

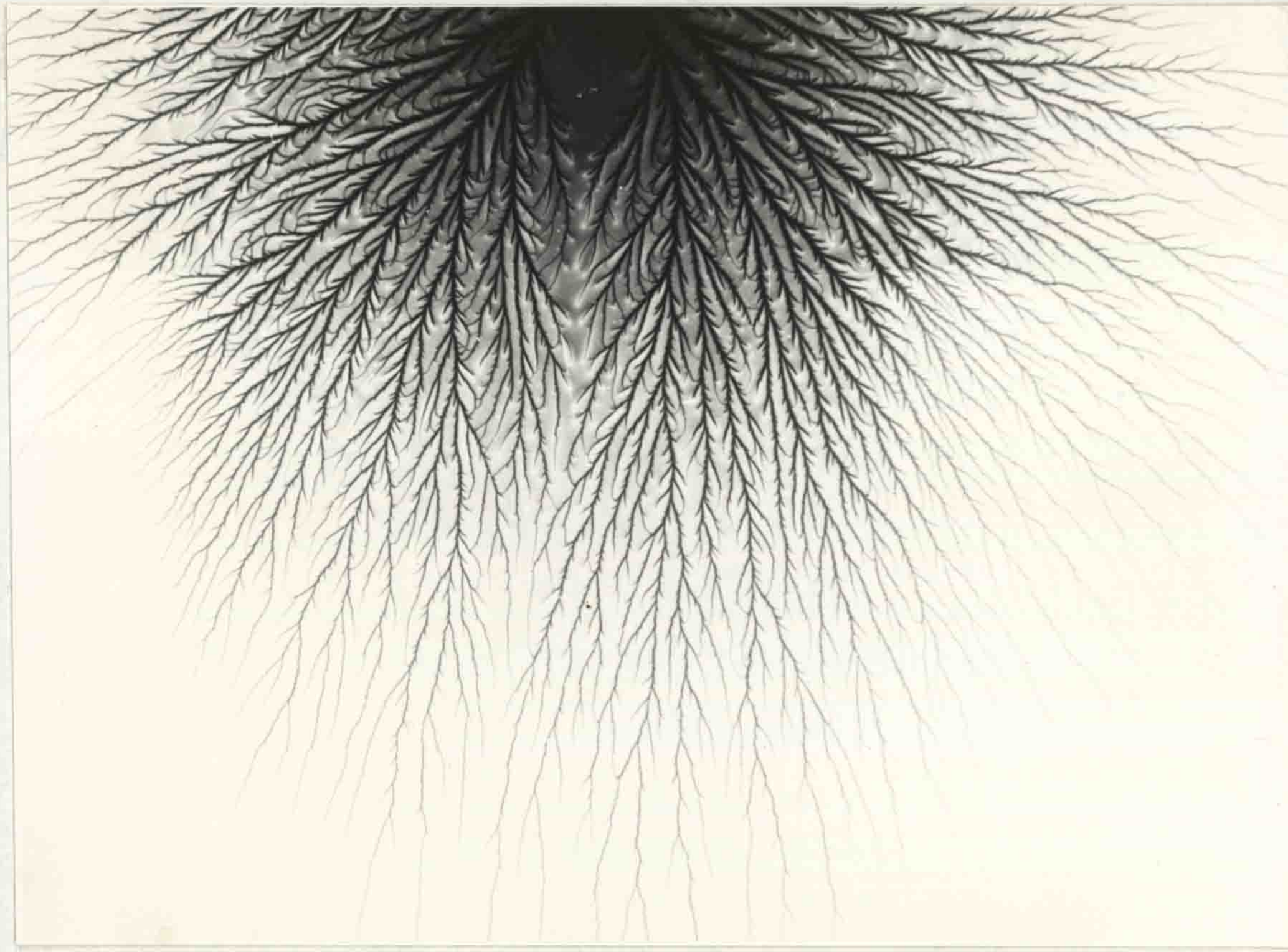

PLANE

FIG. 7 LICHTENBERG FIGURE WITH FILM VERTICALLY BETWEEN ROD AND PLANE

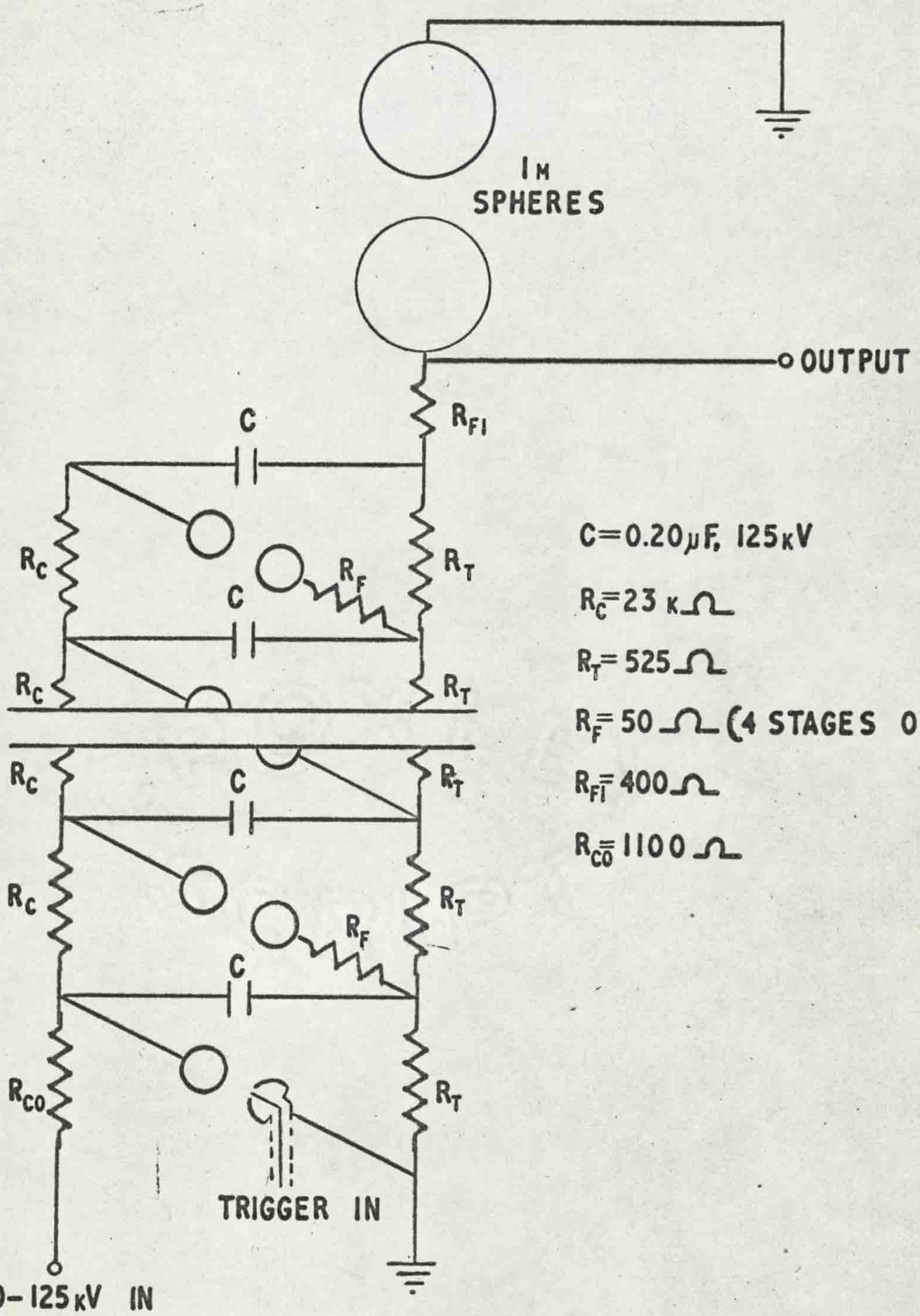

C=0.20μF, 125kV

R_C=23 kΩ

R_T=525Ω

R_F=50Ω (4 STAGES ONLY)

R_{FI}=400Ω

R_{CO}=1100Ω

FIG. 8 8 STAGE IMPULSE GENERATOR

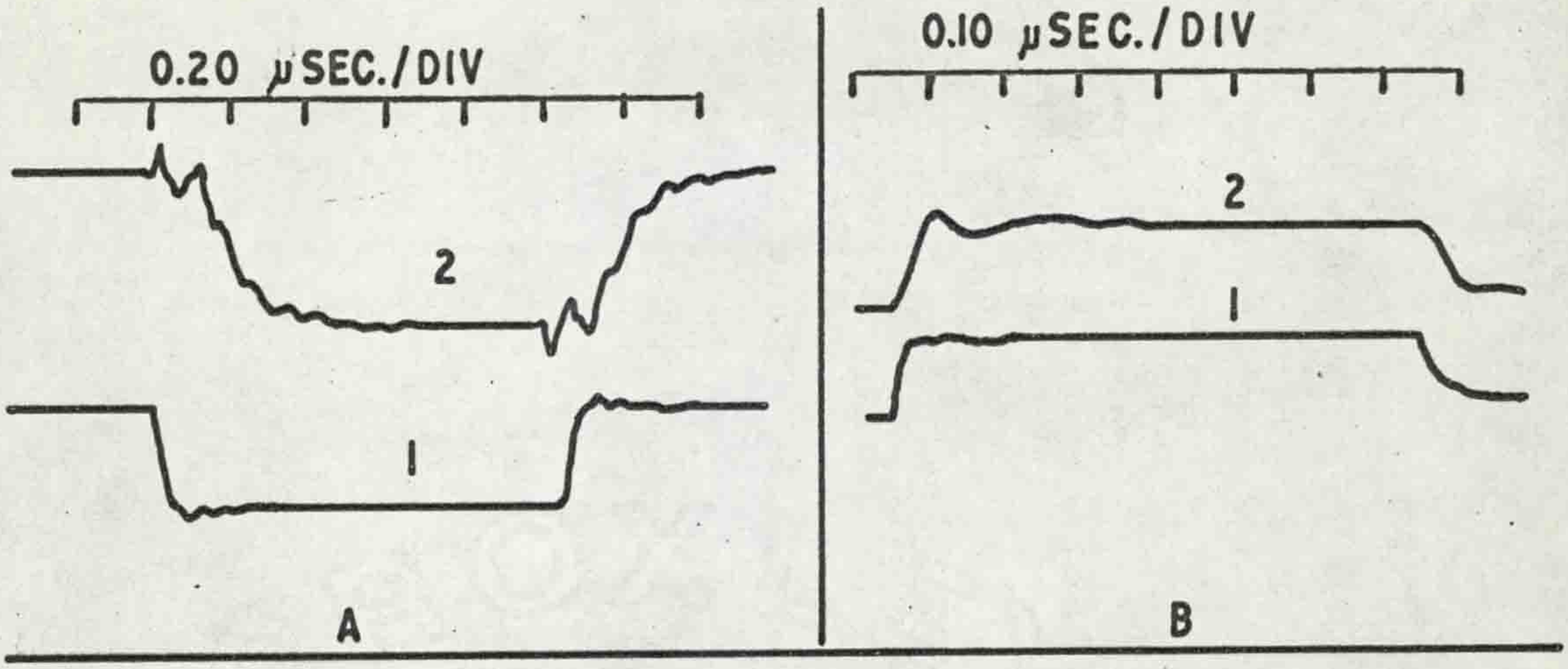

FIG. 9 SCREENED RESISTOR DIVIDER

A. RESPONSE OF RESISTOR ALONE

1. INPUT 2. OUTPUT

B. RESPONSE OF RESISTOR WITH SCREENING

1. INPUT 2. OUTPUT

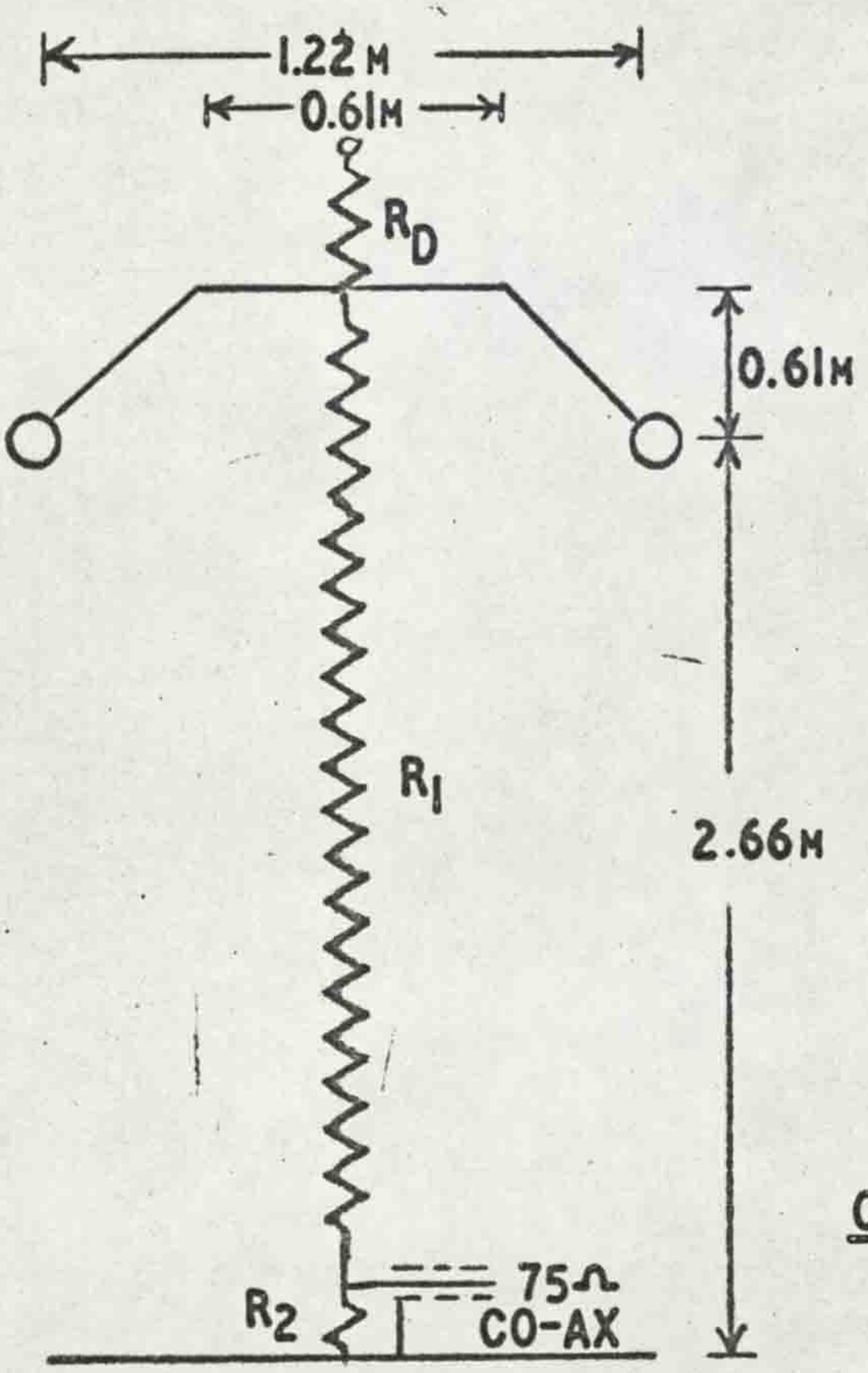

C. DIAGRAM OF DIVIDER

the response time. The improvement obtained is shown in Fig. 9A and B where part A shows the response to a unit step of the straight resistor used as a divider and part B shows the response to a unit step after the addition of the earth plane and screening ring. The unit step was obtained from a Marconi nano-second pulse generator and the divider input and output were recorded simultaneously on a Tektronix type 555 double beam oscilloscope. The low voltage side of the divider was made of two 10Ω carbon resistors in parallel and the output was taken through a 75Ω cable to a 75Ω attenuator at the oscilloscope. The divider had a total resistance of 6,415Ω and a division ratio of 1,346 : 1. With the 10X attenuator at the oscilloscope the overall division ratio was 13,920 : 1. This generator was used for the 50 cm gap, both positive and negative, and for preliminary work on the shorter gaps. A schematic diagram of the laboratory layout is shown in Fig. 10.

When the old laboratory had to be vacated the new impulse generator had not been installed so work was continued using the impulse generator, which had 6 stages of 0.03 μF at 50 kV, from the undergraduate teaching laboratory. In order to give sufficient energy to use the 6 kΩ potential divider only three sections of this generator were used as

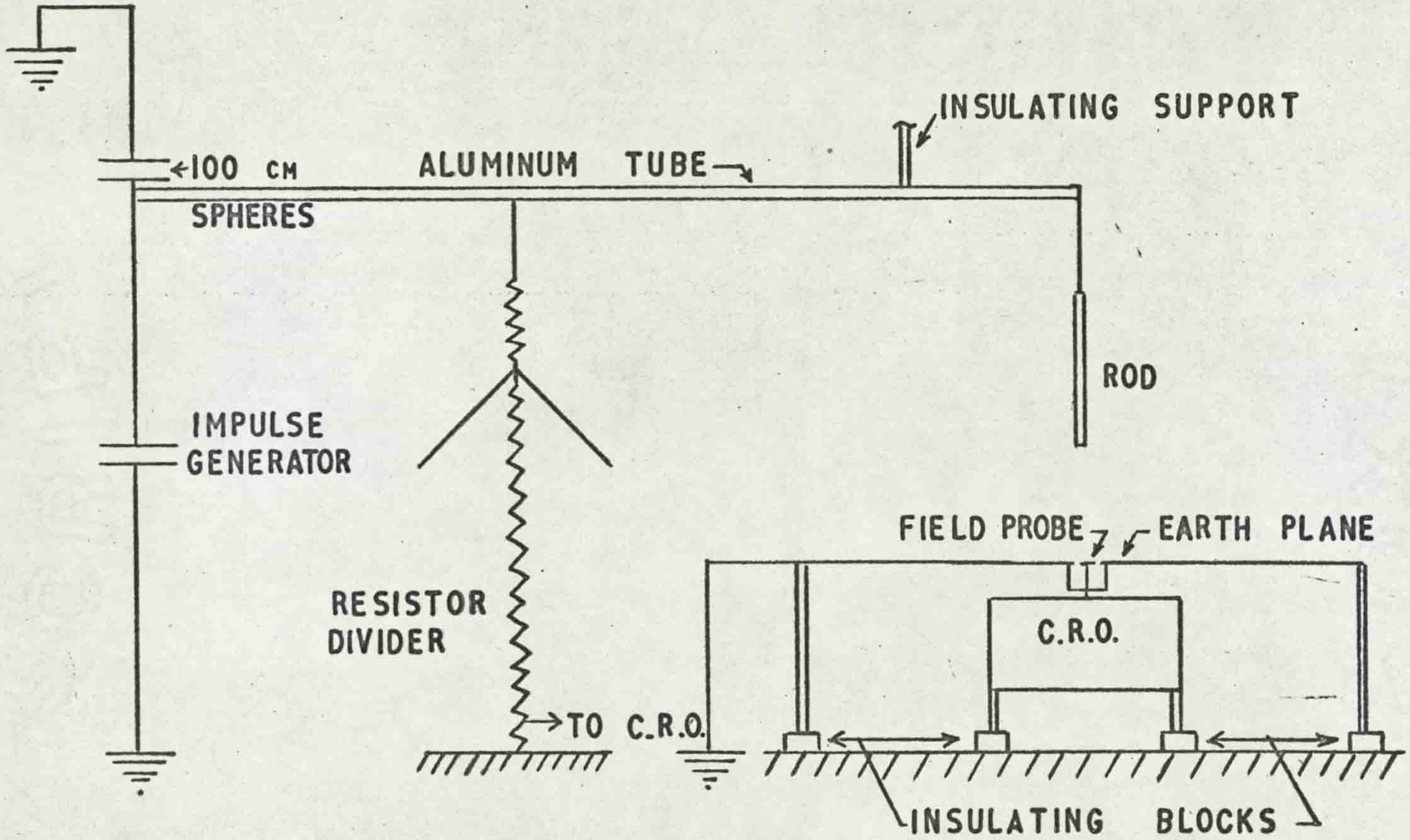

FIG. 10 LABORATORY LAYOUT

shown in Fig. 11. The lowest wave front resistor, 600Ω, was used to give as low a potential division between the wave front resistor and the potential divider as possible. This gave a wave front of approximately 0.4 μsec. This generator was used for the work done on the inverted gap which was reported in a paper presented at the VIIth International Conference on Phenomena in Ionized Gases and which is appended to the thesis.

For the final work on the one and two metre gaps the new impulse generator, 16 stages of 0.14 μF at 100 kV, was used. This generator is shown in Fig. 12. The 6 kΩ resistor divider was no longer used as the wave front capacitor of the new generator was a capacitor divider with a total capacitance of 400 pF. The wave front duration of this generator was approximately 2.0 μsec.

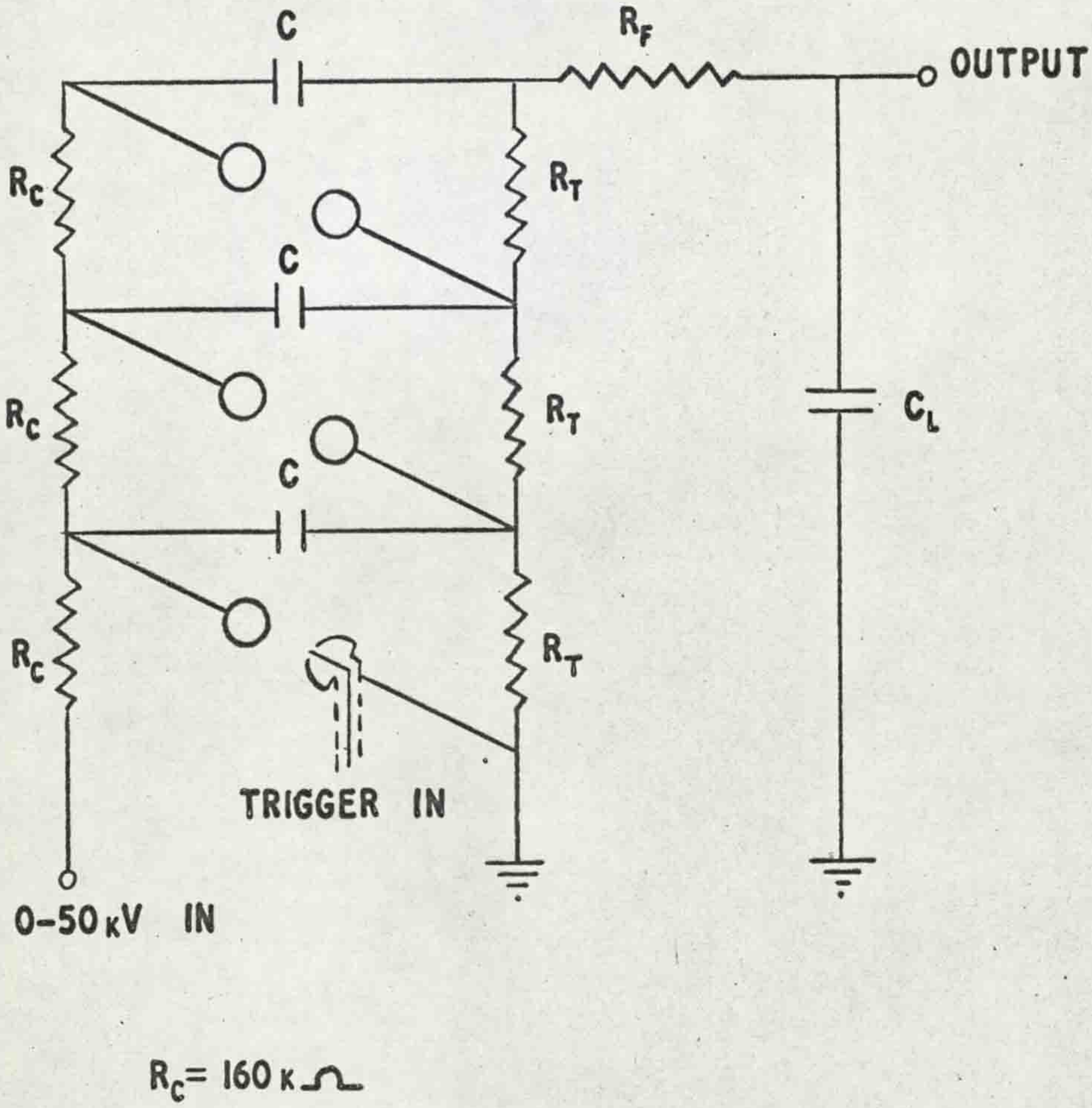

R_C= 160 K

R_T=2.5 K

R_F=600

C =0.03μF, 50KV

C_L=66 PF

FIG. 11 STUDENT GENERATOR

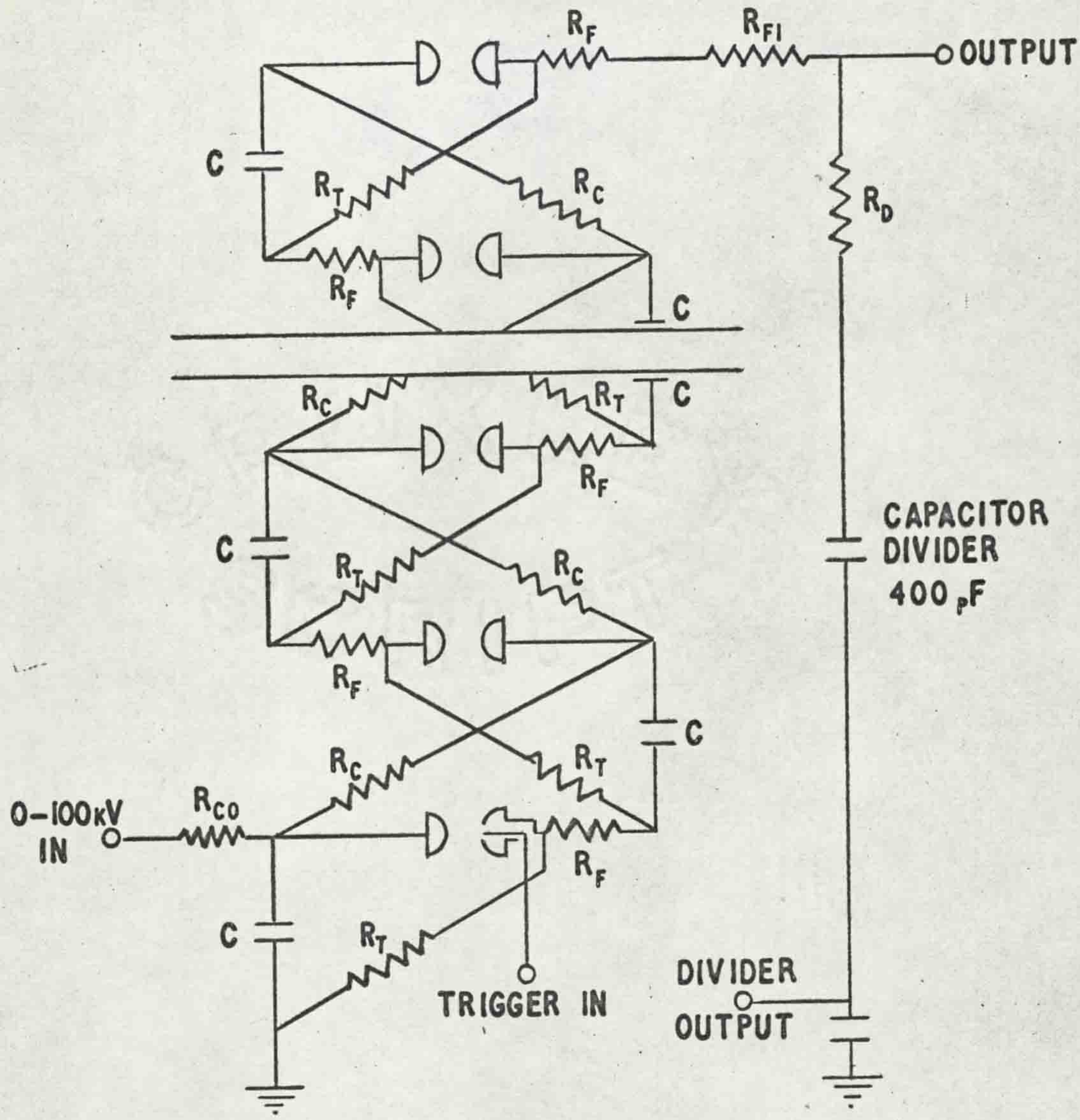

$C = 0.14\,\mu F$, 100kV

$R_C = 25.1$ K Ω

$R_T = 495$ Ω OR 20.3 K Ω

$R_F = 34.2$ Ω

$R_{FI} = 500$ Ω

$R_D = 100$ Ω

$R_{CO} = 538$ K Ω

FIG. 12 16 STAGE IMPULSE GENERATOR

CHAPTER IV

EXPERIMENTAL RESULTS

I. Introduction

When the field measurement technique had been developed it was applied mainly to the study of the field in a positive rod-negative plane gap with results obtained for gap lengths ranging from 5 to 200 cm. In conjunction with the field measurements barriers were used in the gap to limit the growth of the corona filaments which enabled further information to be obtained by observing the change in field due to the effect of the barrier. Lichtenberg figures which formed on the surface of the barrier were observed and yielded information on the number and distribution of the corona filaments. In a final section on the positive rod-negative plane case the charge associated with individual corona filaments is measured by allowing the filaments to terminate on the field probe. This, of course, means that a conduction current occurs to the probe so that the charge measured cannot be equated with the field.

For comparison purposes some work was done on the negative rod-positive plane case using gap lengths of 50 and 100 cm.

Since the results were taken on polaroid film with several different traces on each picture it was decided that the figures in this thesis would be traced from the oscillograms. This has avoided confusion by making it unnecessary to specify a particular trace on a picture and it has made it possible to superimpose traces, thus adding to the ease of comparison.

II. Field Measurements

(i) 15 cm gap

(a) Field on the rod center-line

The field at the plane on the center-line of the rod has been studied and is shown to be made up of two parts. Firstly, the field due to the voltage applied to the high voltage electrode which will be called the geometrical field and secondly the field due to space charge. The geometrical field can be determined up to the point of corona onset only as the space charge introduced into the gap by the corona will change the charge distribution on the high voltage electrode. This means that the field at the earthed electrode due to the applied voltage will be changed and, as a consequence, once corona has started in the gap it is not possible to separate the two fields.

The peak geometrical field is plotted as a function of applied voltage in Fig. 13. This graph is divided into sections which will be discussed along with oscillograms showing the field for each section.

1. Below 32 kV the field is solely the geometrical field with no evidence of corona. The lower trace of Fig. 14A is an example of this field and, as there is no discharge, this field will be identical with the applied voltage wave-shape.

2. In this region the corona occurred occasionally with delays up to about 10 μsec after the voltage crest. The increase in field, above the geometrical field, had an initial steep rise attaining 90% of its value in 0.3 μsec with the final 10% rise occurring in a further 0.2 μsec. The second trace of Fig. 14A shows this field.

3. In this region corona occurred for each impulse although there was still considerable variation in the time delay after the impulse crest. It was noted that in general the shorter the time delay the higher the field rise at the plane with the maximum increase giving a total field about four times that of the geometrical field. Examples of this field are shown in the top two traces of Fig. 14A and the lower trace of Fig. 14B. It should be noted that the delay

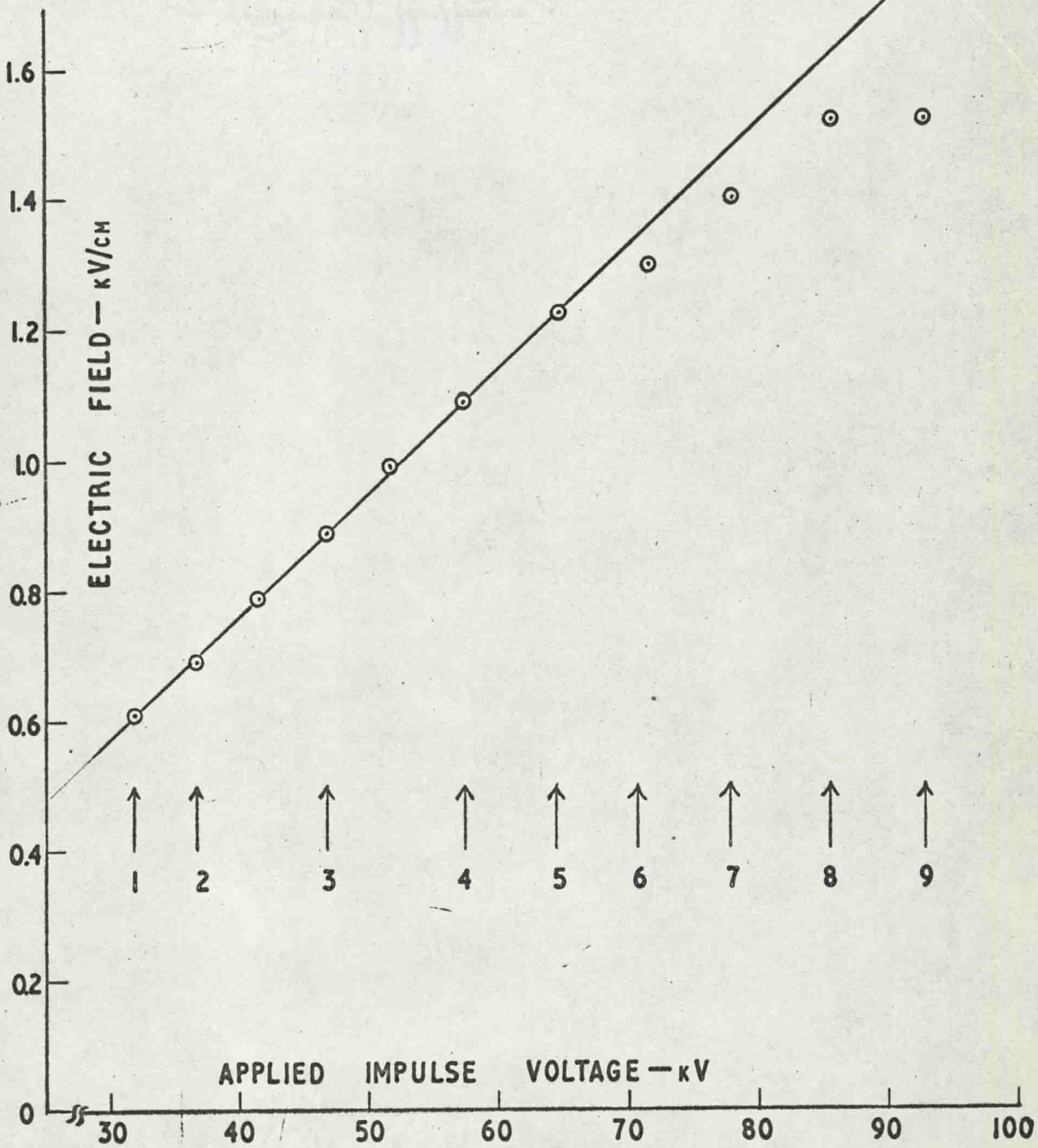

FIG. 13 PEAK GEOMETRICAL FIELD ON THE ROD CENTER-LINE AT THE PLANE IN A 15 cm GAP

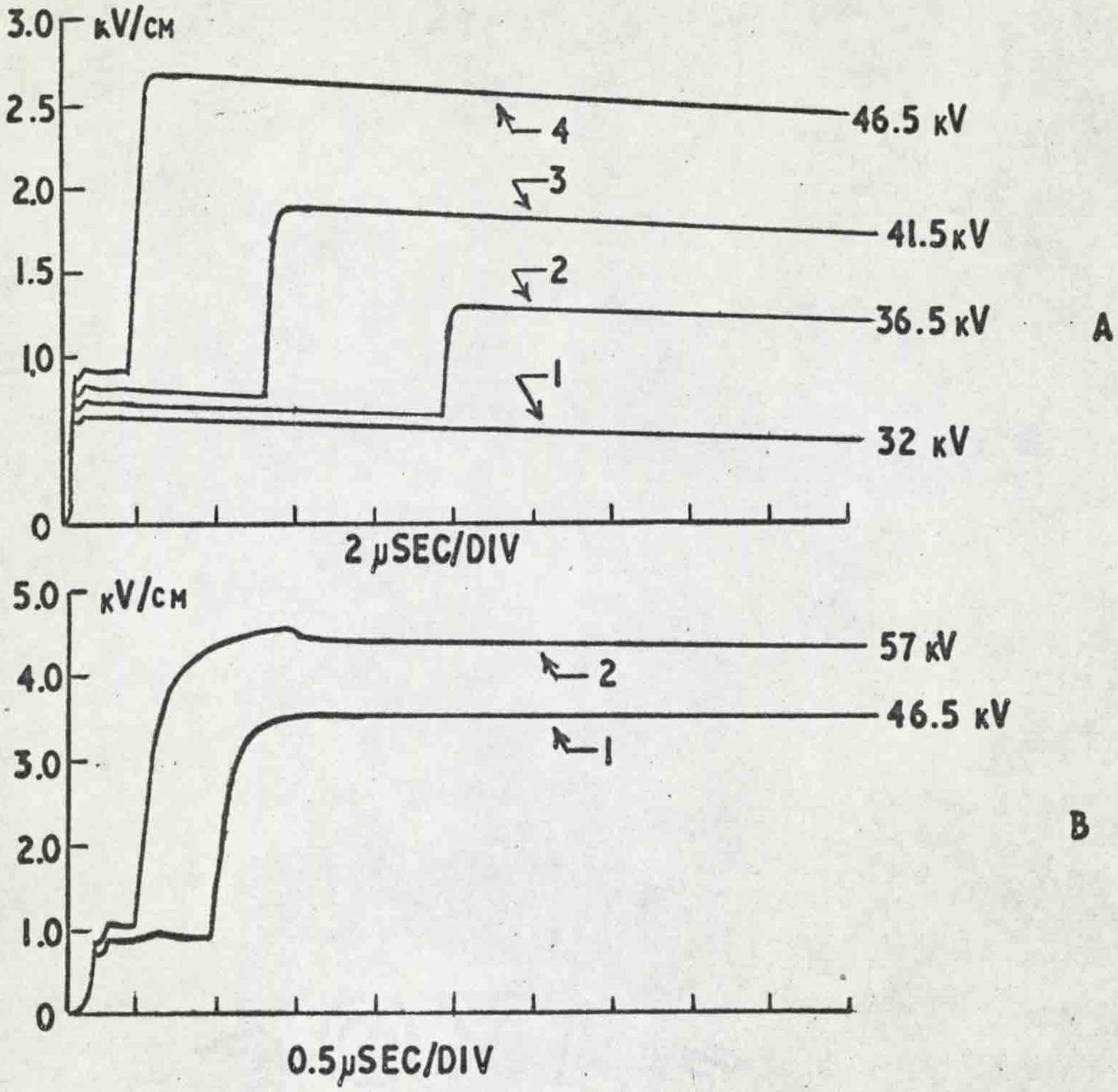

FIG. 14 FIELD OSCILLOGRAMS AT THE PLANE — 15cm GAP

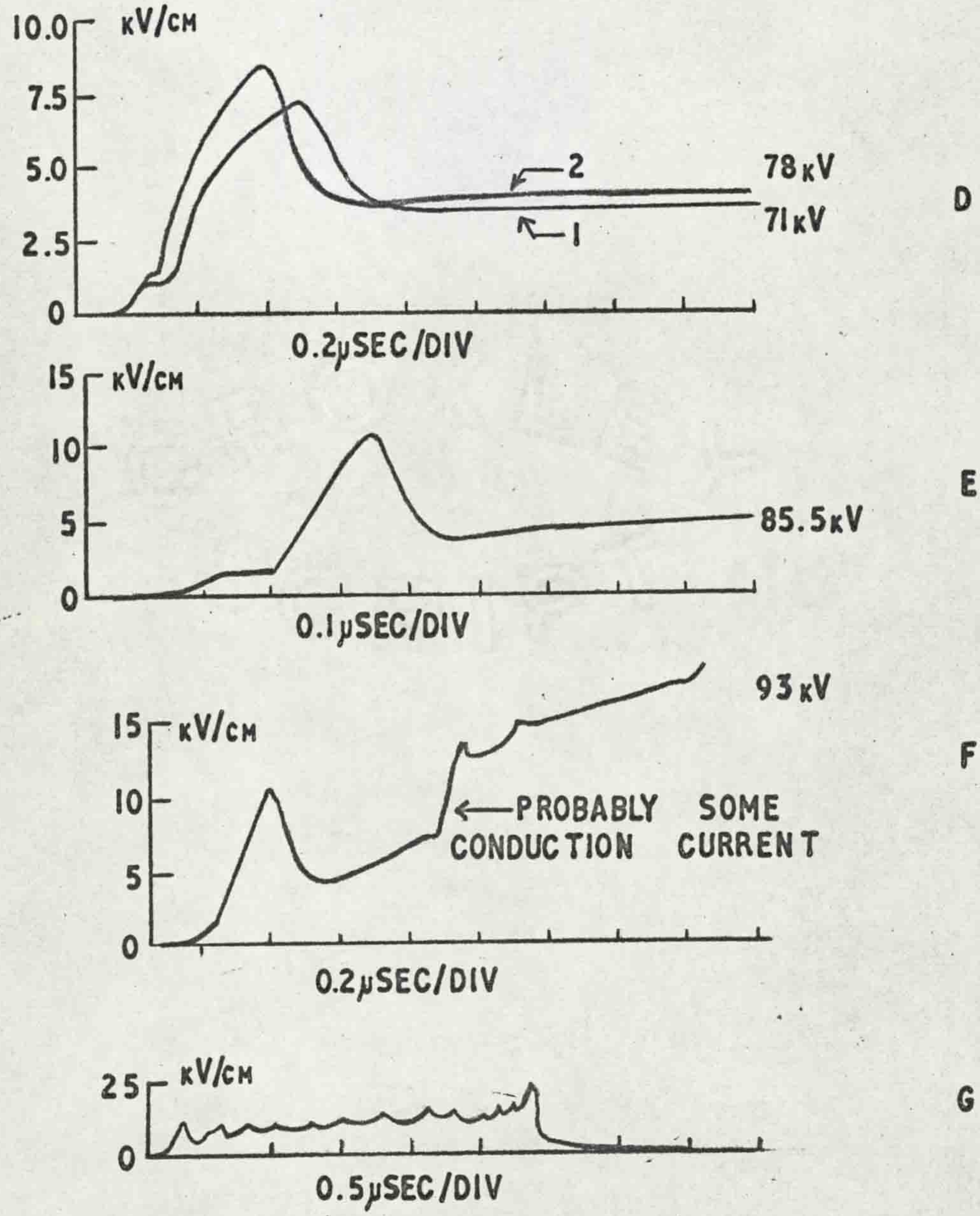

FIG. 14 CONTINUED

times did not necessarily decrease with an increase in voltage as shown in Fig. 14A. The delay time was quite variable but for the Fig. 14A decreasing delay times were chosen so as to avoid confusion in having the traces superimposed.

4. At an applied voltage of 57 kV some of the corona filaments crossed the gap to the plane. This is indicated by a slight falling off of the field due to the corona filaments' associated space charge being neutralized at the plane. The upper trace in Fig. 14B is a sample oscillogram showing this effect.

5. The number of corona filaments reaching the plane is increasing and on some traces a double peak occurs with a peak separation of about 0.4 μsec. This is shown in Fig. 14C and several explanations were considered. It could be that there are two "waves" of corona filaments crossing the gap with different velocities of propagation but if they all started from the rod at the same time the velocity variation would have to be greater than 2 to 1. Observations of primary and secondary streamers by Hudson[35] and Dawson[37] would tie in with this possibility. Secondly it was considered that corona might start from two different points on the rod at different times but field measurements at the rod showed that the initial corona filaments caused

a large decrease in the field at the rod and there was no evidence that a further corona discharge occurred. The most likely explanation of the double peak is that branches in the corona filament are stopped, because their field is opposed by the field of the main part of the filament, and then start again when the space charge of the main filament is neutralized at the plane. This mechanism would also explain the primary and secondary streamers mentioned earlier.

The time lag before initiation of the corona is still quite variable with times being recorded up to about 1.8 μsec after the wave crest.

6 & 7. Above approximately 70 kV the corona starts before the wave crest so the time lag is short. Unfortunately the voltage wave has a small step just before the crest so the corona tends to start on the flat portion of this step which causes some variation in corona onset time. At this point the graph starts to diverge from the straight line which is obtained as long as the corona starts after the wave crest. The field oscillograms in Fig. 14D show examples of this for applied voltages of 71 kV and 78 kV.

8. At this voltage the field is similar to that in the previous section but the peak value is increasing up to

about 14 kV/cm. The field then decreases to about 4 kV/cm and finally increases slightly before reaching a constant value which decreases as the applied voltage decreases. A second peak was not observed at this voltage but the second rise could be due to corona filaments restarting and progressing part way across the gap. A sample oscillogram with an applied voltage of 85.5 kV is shown in Fig. 14E. There is again some variation in corona starting time as the point of initiation is still on the step near the wave crest.

9. At 93 kV the corona is initiated on the steeply rising part of the wave front so its starting time is consistent within a few nanoseconds. The starting field is the same as that for an applied voltage of 85.5 kV which indicates that the field at the rod has reached a value which is sufficient to cause an initiating electron to be readily removed from a negative ion without appreciable time lag. The oscillogram of Fig. 14F shows the field at an applied voltage of 93 kV which rises to a second peak after the initial corona has crossed the gap and been neutralized. Later records taken at the rod electrode show that this second peak occurs before a second discharge has occurred at the rod which indicates that it must be due to corona

initiated in the mid-gap region. This is added evidence in favour of the hypothesis that branches of the corona filaments stop and are restarted when the main corona filaments are neutralized at the plane. The clearing of this second "wave" of space charge from the gap allows the field at the rod to increase to a value sufficient to enable a leader stroke to be initiated.

Fig. 14G shows the field right up to breakdown. This was accomplished by covering the probe with a perspex cap so that no conduction current could occur in the probe. After the two initial peaks in the field, which are caused by the first corona filaments and the filaments which are restarted in mid-gap, a succession of peaks occurs caused by corona filaments which are initiated at the head of the leader stroke. The average field rises slightly as the leader stroke approaches the plane and then drops sharply as the final breakdown occurs. The field does not collapse to zero immediately which indicates the presence of positive space charge in the gap which takes some time to clear.

Fig. 13 is replotted in the lower curve of Fig. 15 to show its relation to the space charge fields which occur in the gap. The upper curve of Fig. 15 shows the peak field at the plane as the corona filaments cross the gap, the

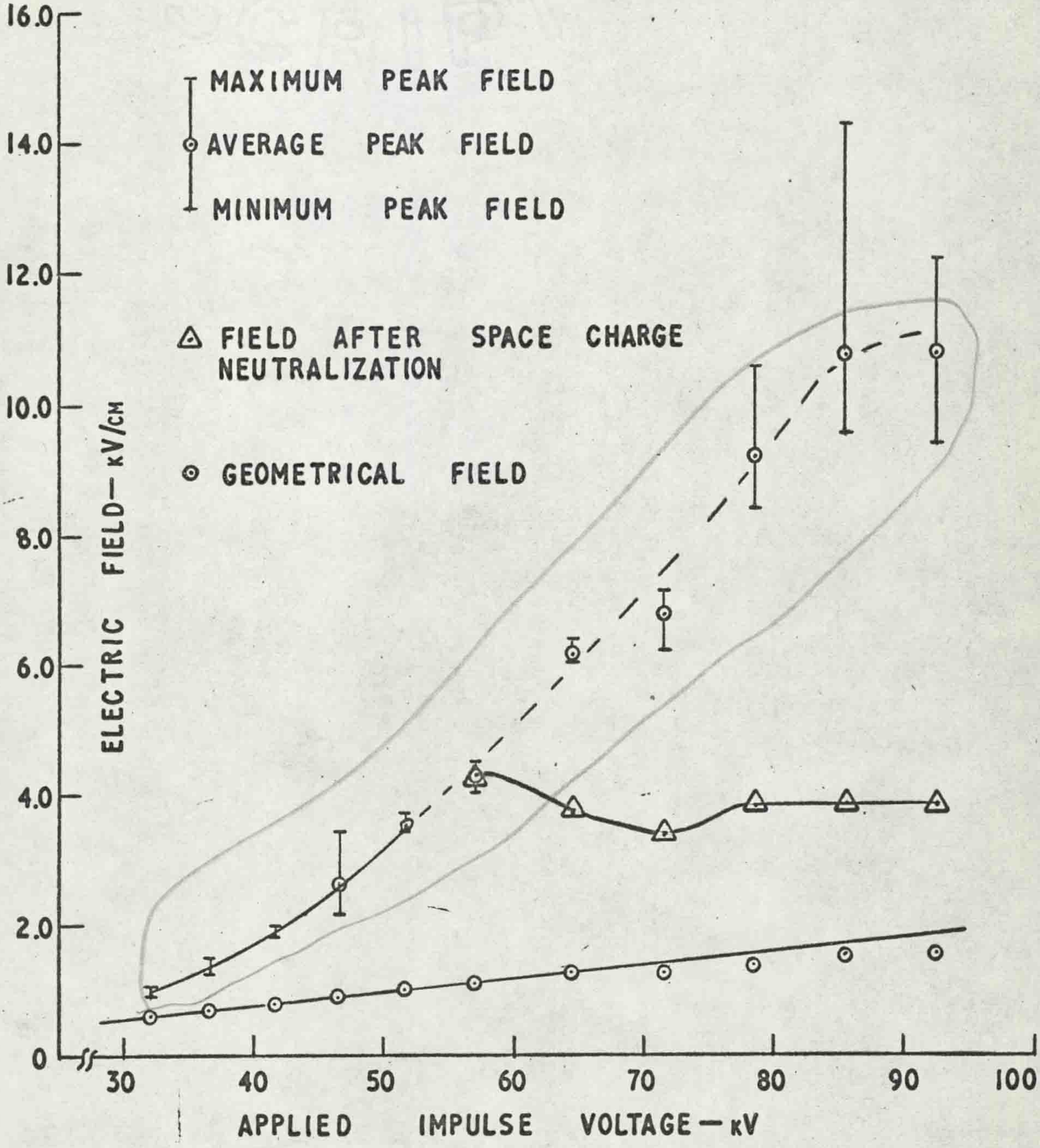

FIG. 15 FIELD ON THE ROD CENTER-LINE AT THE PLANE IN A 15CM GAP

maximum value being approximately 8½ times the geometrical field. The spread in values at the lower voltages is due to the variation of the corona with the time lag after the voltage crest and the spread in values for the points at higher voltages is probably due to the variation of the position of the corona filaments with respect to the probe, that is to say the nearer the corona filaments to the probe the higher the field will be. The middle curve shows the value to which the field drops when the corona filaments have reached the plane and their associated space charge has been neutralized.

(b) Field distribution along the plane

In order to gain more information regarding the spread of space charge in the gap the field distribution along the plane was measured. This work was done using the small impulse generator and the gap shown in Fig. 2 so the absolute values of the fields at the rod center-line will be slightly different from those of the previous section.

Field oscillograms taken at various distances along the plane from the rod center-line with an applied impulse of 89 kV are shown in Fig. 16. Fig. 16A shows the field on the rod center-line and 5 cm from it. These two are very similar but the field decrease at 5 cm is slower and it does

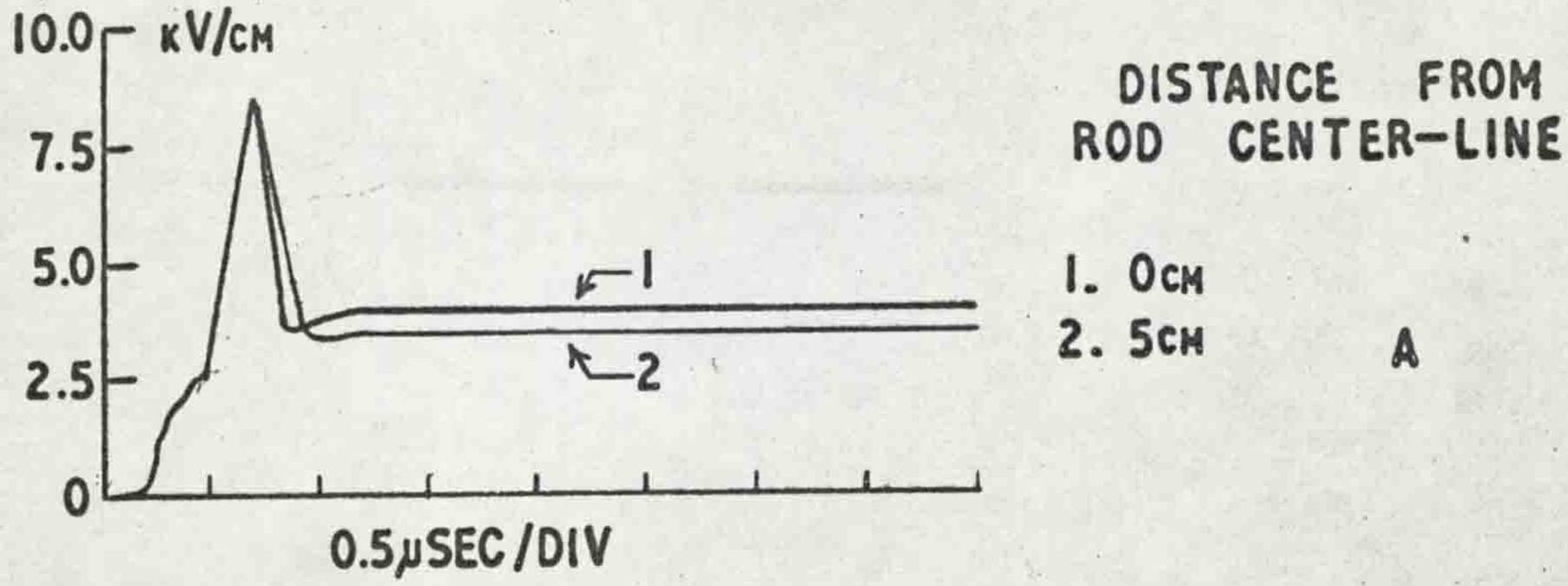

FIG. 16 FIELD AT VARIOUS DISTANCES FROM THE ROD CENTER-LINE 15cm GAP — 89kV IMPULSE

not have as pronounced a second rise. Fig. 16B shows the field at 10, 15 and 20 cm from the rod center-line. The decrease from the peak value is becoming less pronounced and the field after the corona has stopped decreases with the decreasing impulse voltage. Fig. 16C shows the field 25 and 30 cm from the rod center-line and here it can be seen that the space charge field adds very little to the geometrical field. There is still a small decrease in field due to the space charge being neutralized at the plane and then the field decreases due to the decreasing impulse voltage. The fact that the field directly under the rod does not decrease as the impulse voltage decreases indicates that the field is mainly due to space charge.

A similar series of field oscillograms for an applied voltage of 64 kV is shown in Fig. 17. Here again the decreasing effect of the space charge with increasing distance along the plane from the rod center-line can be clearly seen.

The values from these two series of oscillograms have been plotted and Fig. 18 shows the results for an applied voltage of 89 kV. The lower curve is the corona onset field or geometrical field which occurs 0.25 μsec after the start of the impulse. The upper curve shows the peak

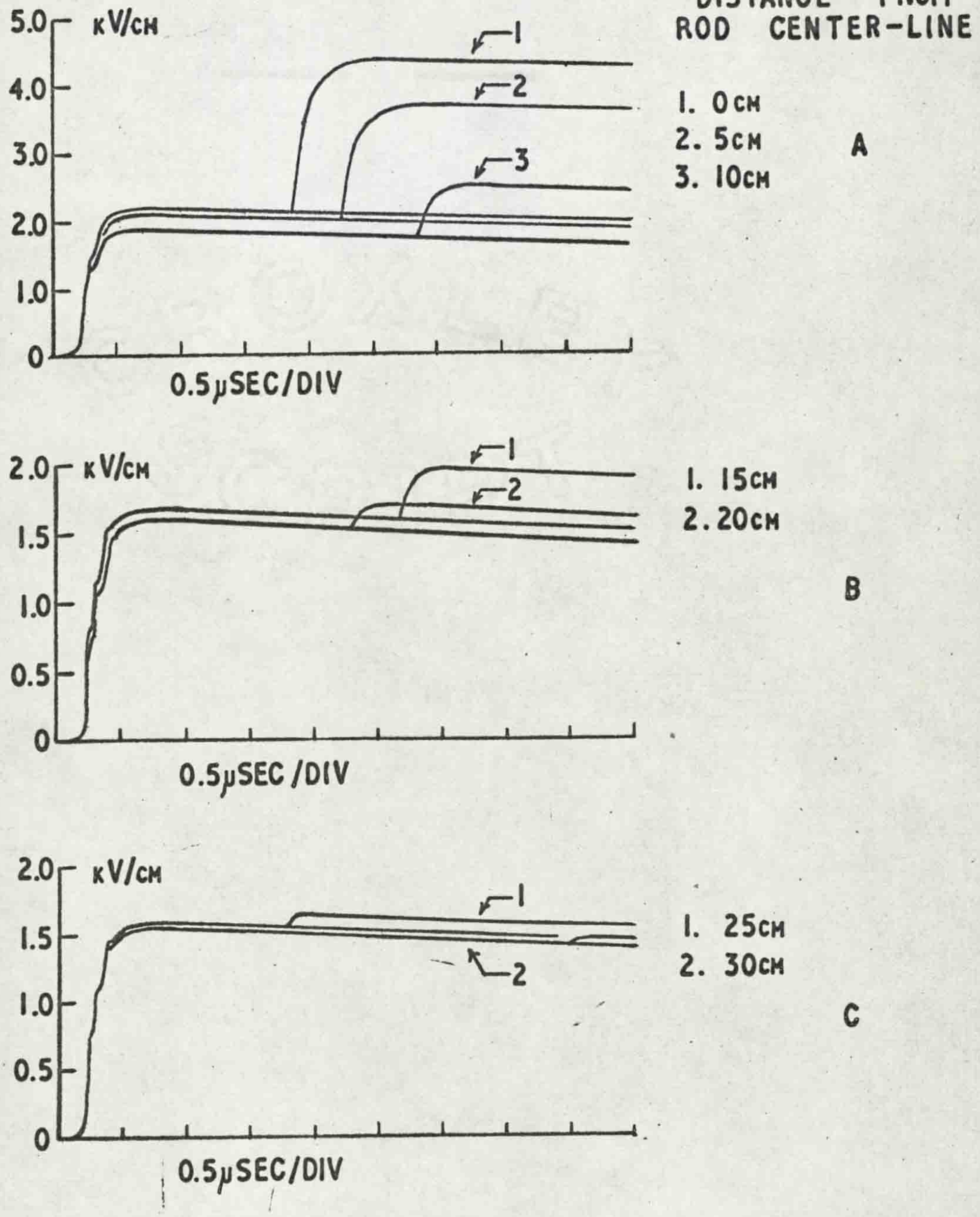

FIG. 17 FIELD AT VARIOUS DISTANCES FROM THE ROD CENTER-LINE 15cm GAP – 64kV IMPULSE

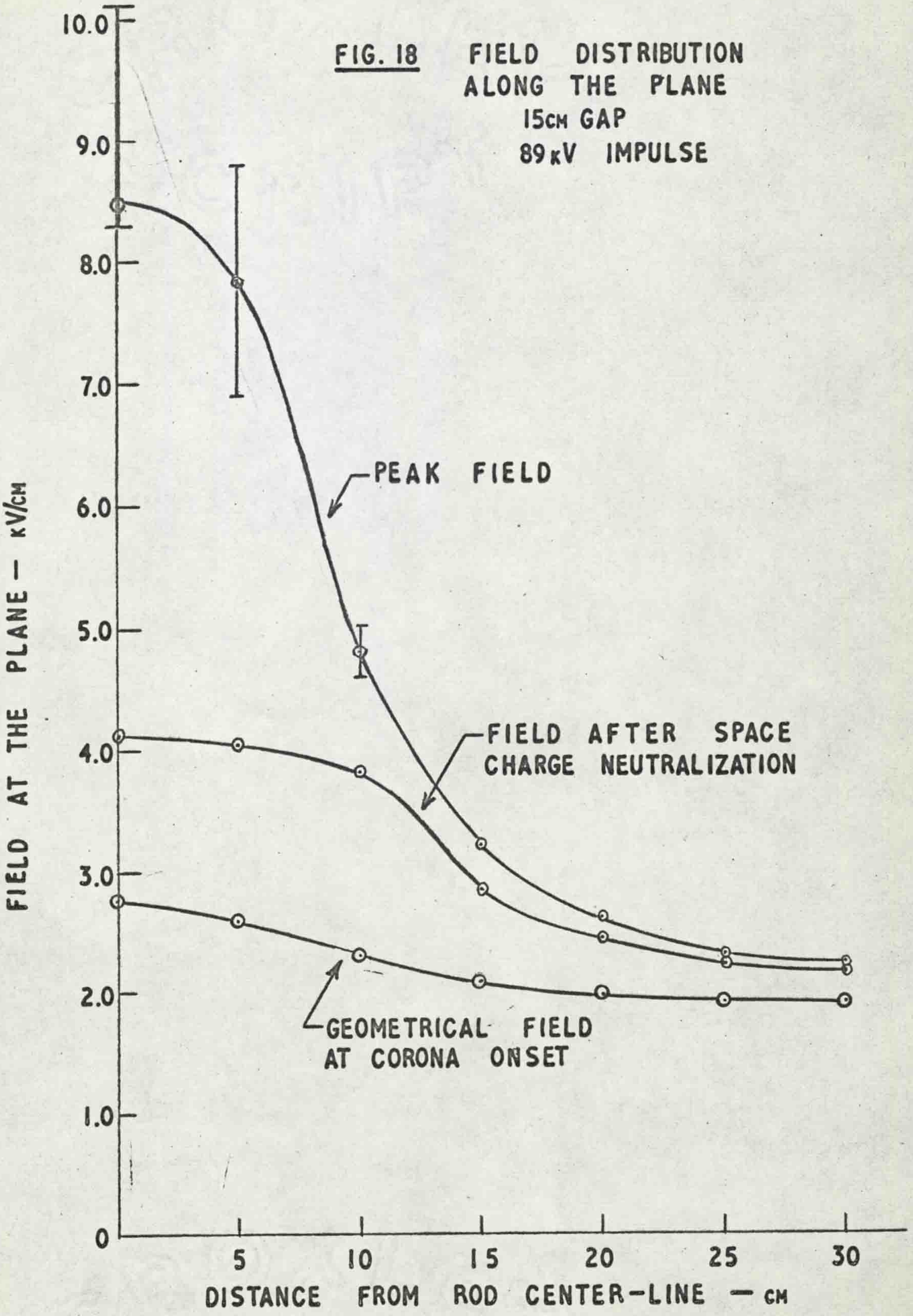

FIG. 18 FIELD DISTRIBUTION ALONG THE PLANE 15cm GAP 89 kV IMPULSE

field which occurs after a further 0.25 μsec. This is the field before the space charge is neutralized on the plane and from the shape of the curve it can be deduced that the charge is near the plane. The middle curve shows the field approximately 1.3 μsec after the start of the impulse. This is after the corona in the gap has ceased and from the broad shape of this curve it appears that the space charge is spread throughout the gap.

The graph of field at the plane vs the distance along the plane from the rod center-line for the second case is shown in Fig. 19. The lower curve in this case shows the field due to the high voltage plane and was obtained by removing the rod. The middle curve then shows the peak geometrical field with the rod in position. This curve is the same shape as the lower curve in the preceding graph but is slightly lower in value. The upper curve shows the peak field due to the corona and again a space charge in the lower part of the gap is indicated by the nature of the curve which is high on the rod center-line and falls rapidly as the distance from the rod center-line increases.

(c) Field at the rod

In order to measure the field at the rod an inverted gap was used as shown in Fig. 2. The Lichtenberg figure,

FIG. 19 FIELD DISTRIBUTION ALONG THE PLANE

15CM GAP
64KV IMPULSE

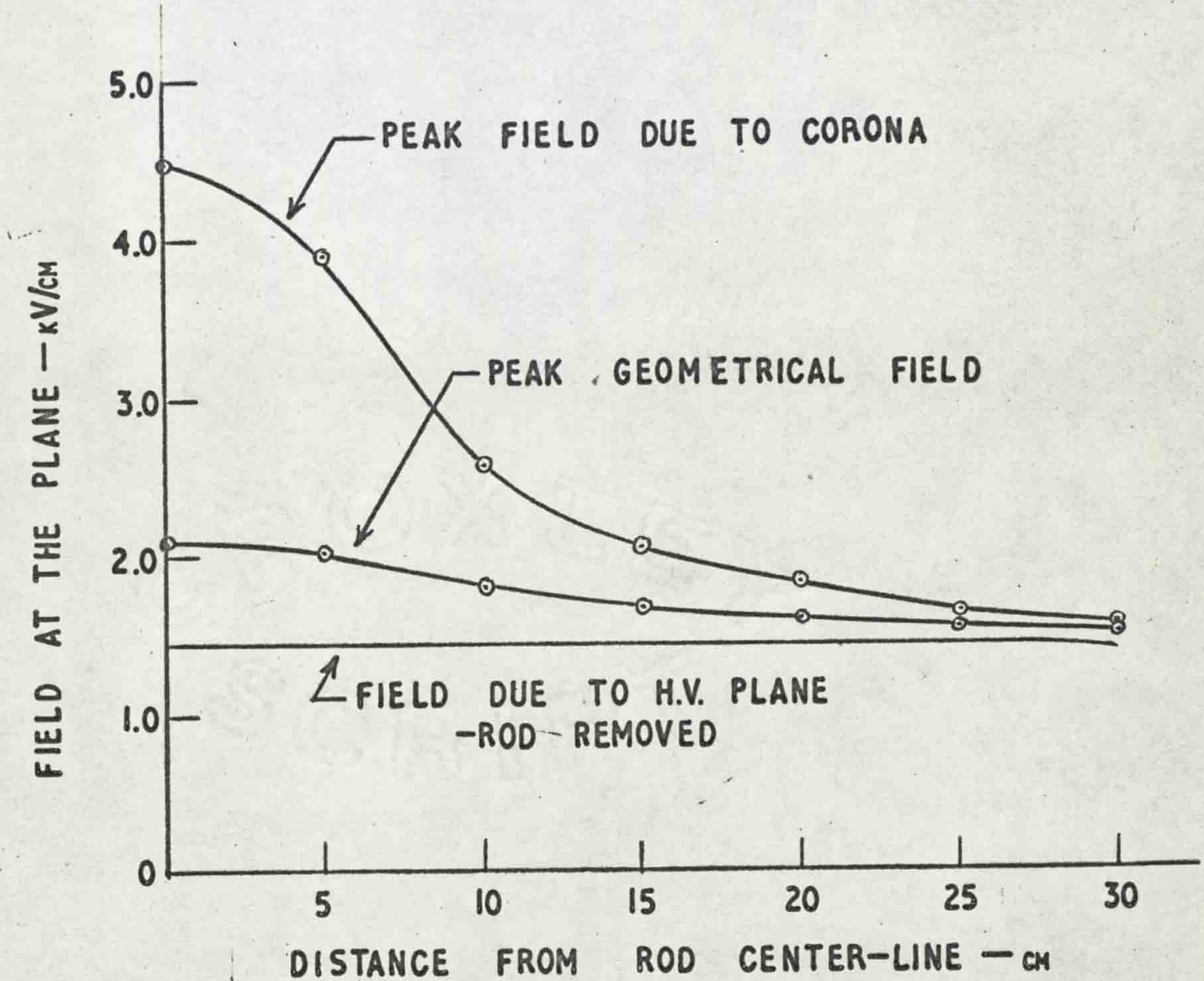

Fig. 7, shows the result of placing the film vertically between the rod and the plane with one edge of the film centred on the rod end. This shows that the corona starts from the edge of the rod only so that the conduction current to the center of the rod would be zero, which enabled the probe to be mounted in the rod end. When the probe had been installed a piece of polythene was placed over it. Since this did not change the measurement it was assumed that there was in fact no conduction current to the probe.

Using the probe situated in the rod end the oscillograms in Fig. 20 were obtained. Fig. 20A, curve 1, shows the field without any corona discharge. This is the geometrical field and is the same shape as the applied voltage wave. Curve 2 shows the field when the corona starts on the wave crest. The corona creates a space charge in the gap which has a field at the rod in opposition to the applied field so that the field drops to a low value which prevents any further discharge from occurring. After the initial collapse of field at corona onset the field rises slightly as the space charge propagates away from the rod. In curve 3 it can be seen that as the voltage is raised the corona starts on the wave front and the rise after the initial field collapse is slightly more pronounced since the space charge propagates farther from the rod.

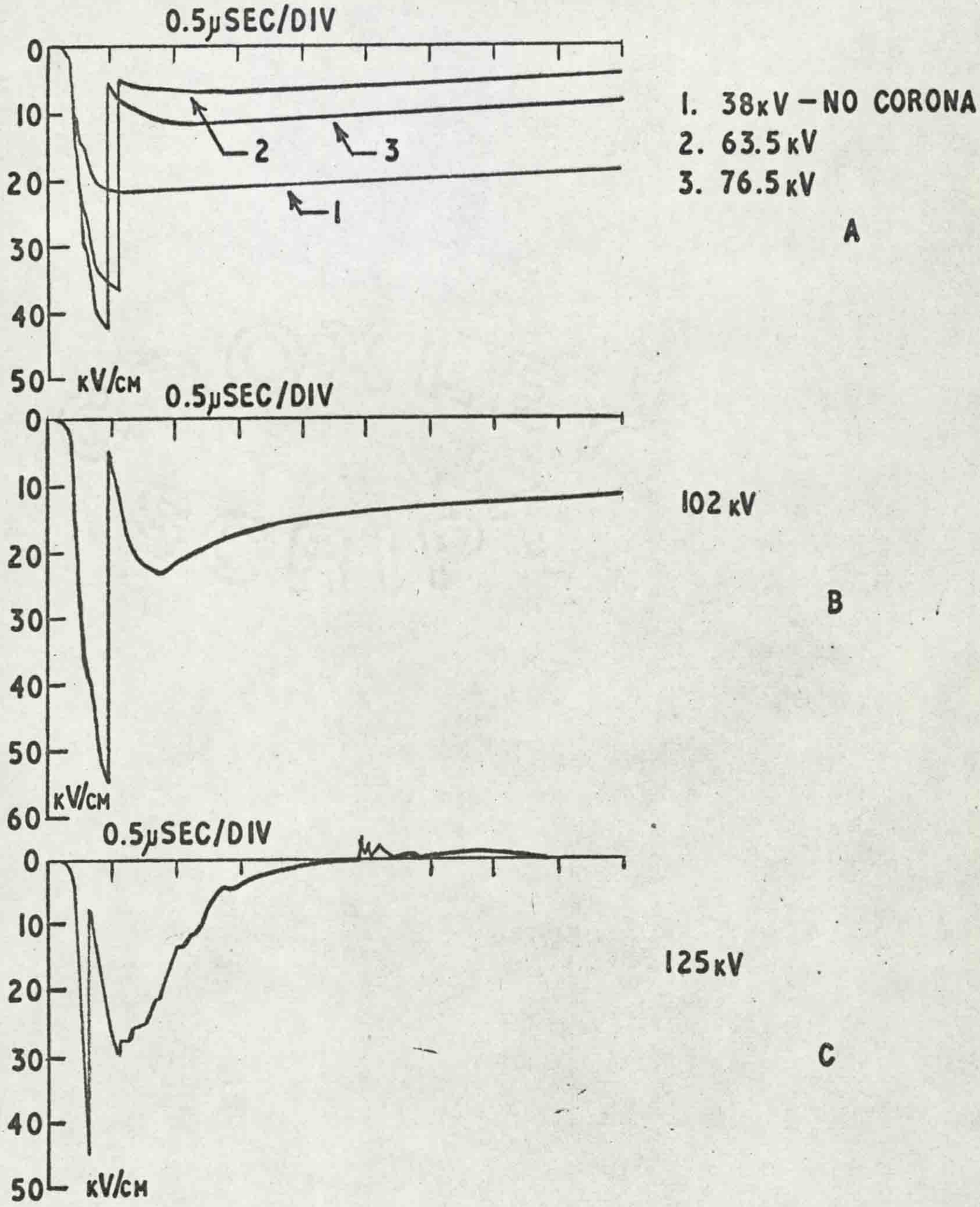

FIG. 20 FIELD AT THE ROD

15cm GAP

The field at a voltage just below the breakdown voltage is shown in Fig. 20B. In this case the field rises to about 25 kV/cm after the initial collapse and then decays quite quickly to about 15 kV/cm. This decay from 25 kV/cm to 15 kV/cm does not appear to be due to further corona discharge but is probably due to any remaining electrons and some of the negative ions being drawn out of the region around the rod leaving a higher net positive space charge which will not disperse as quickly as it is drifting into a region of lower field. Since the field at the edges of the rod will be considerably higher than the 25 kV/cm recorded on the rod end it is possible that some ionization does occur which would aid the clearing of negative charge from the rod region. This possibility has not been investigated.

Finally, the field at the rod under breakdown conditions is shown in Fig. 20C. In this case, after the initial collapse at corona onset the field rises again due to the fact that the voltage is still rising and due to the propagation of space charge away from the rod and the subsequent neutralization of this space charge at the plane. The field rises sufficiently to allow a leader stroke to be initiated which propagates across the gap. This time the field does not collapse as it did when the corona was initiated,

rather it falls slowly as the leader grows across the gap. This can be explained by considering the leader stroke to be a conducting channel growing out from the rod and having very little net space charge so that the opposing field is small. When the final breakdown occurs the field reverses since the applied field is removed when the voltage collapse occurs leaving only the field due to the positive space charge which, as was shown in field measurements at the plane, takes time to clear from the gap.

(d) Effect of a conductor in the gap

In order to establish the effect of a conducting channel starting at the rod edge and projecting into the gap, on the field at the rod center, several tests were made with conductors positioned as shown in Fig. 21A. In the first test, the results of which are shown in Fig. 21B, the field with the rod alone was compared with the field when a piece of 18 gauge wire projected into the gap 2 cm. The field with the rod alone collapses due to corona from the rod and the field with the wire in place decreases due to corona on the wire end, but comparison of the fields before corona occurs shows that the shielding effect of the wire is small compared with the shielding effect of the space charge. It is interesting to note

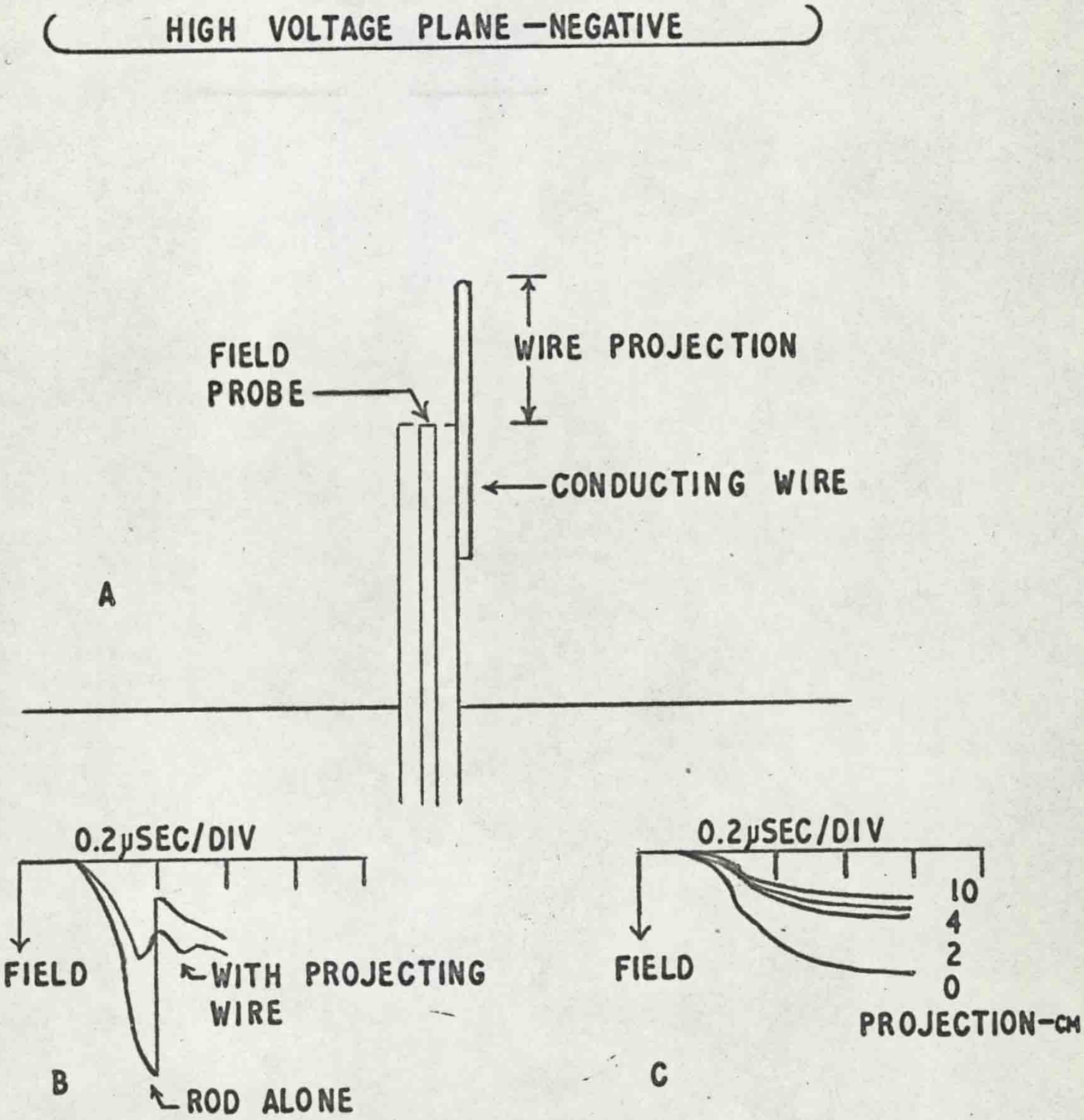

FIG. 21 EFFECT OF A CONDUCTOR PROJECTING INTO THE GAP FROM THE ROD

A. TEST ARRANGEMENT
B. WITH 18 GAUGE WIRE
C. WITH A 1CM DIAMETER ROD

that the corona which occurs at the end of the wire, 2 cm from the probe, does not cause as great or as fast a field decrease as the corona at the rod edge.

In order to eliminate the corona a 1 cm diameter rod with a hemispherical end was used as the projecting conductor. The field was measured with this conductor projecting 0, 2, 4 and 10 cm into the gap and the oscillograms are shown in Fig. 21C. This shows that the projection of the first 2 cm causes the greatest decrease with the effect of each succeeding bit of projection being less than for the previous bit. From a comparison of Fig. 21B and Fig. 21C it is reasonable to assume that the 1 cm rod has a much greater effect than the 18 gauge wire which more nearly represents the size of the leader channel. Although the leader channel cannot be accurately represented by a wire protruding into the gap this experiment does tend to support the interpretation of the second slow decrease of field at the rod, as shown in Fig. 20C, as being due to a conducting leader stroke growing from the rod towards the plane.

A further simple experiment to check the effect of space charge in the gap on the field at the rod end was carried out using the apparatus in Fig. 22 A. An impulse of 110 kV was applied to the plane for three conditions; (a) no sphere,

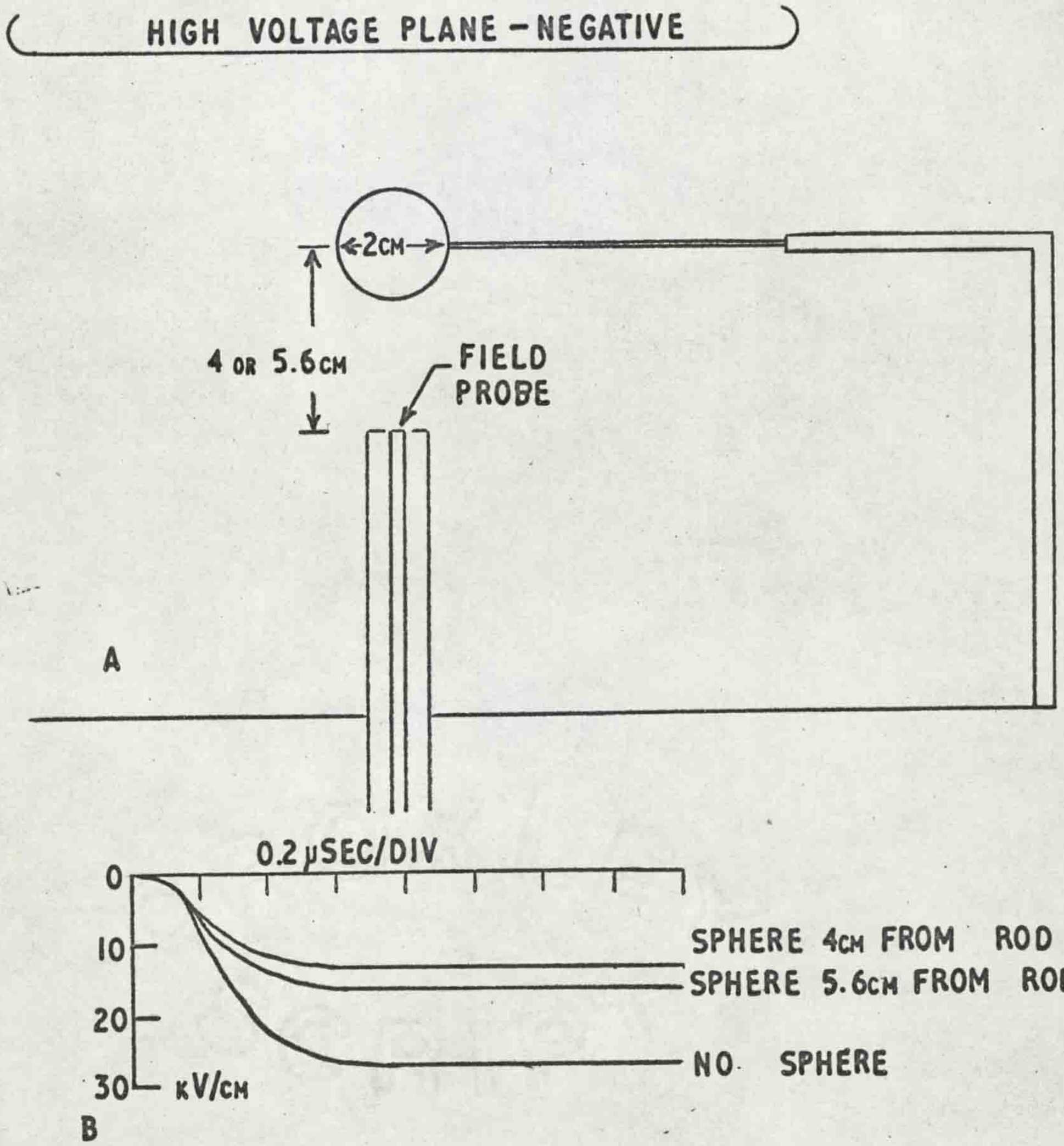

FIG. 22 EFFECT OF SPACE CHARGE ON FIELD AT ROD

A. TEST ARRANGEMENT
B. FIELD OSCILLOGRAMS

(b) sphere center 4 cm from the rod end and (c) sphere center 5.6 cm from the rod end. The resulting field oscillograms are shown in Fig. 22B and the peak fields are 27.5 kV/cm, 13.7 kV/cm and 16.7 kV/cm respectively. Assuming that the sphere has a capacitance of approximately 2 pF to the plane then it will have a charge of 2.2×10^{-7} coulombs. If this charge is assumed to be at the center of the sphere it will create an opposing field at the rod end of 12.4 kV/cm in the first case and 6.3 kV/cm in the second case which when added to the measured fields gives 25.1 kV/cm and 23.0 kV/cm. Considering the assumptions made these figures agree quite well which illustrates experimentally the effect of space charge in the gap.

(e) Effect of the shape of the rod end on the field at the plane

The field at the plane was measured for three different rod endings, (1) square-cut, (2) 30° cone, (3) hemispherical, and the resultant oscillograms are shown in Fig. 23. Trace A is for the square-cut end, trace B for the 30° cone and trace C for the hemispherical end, all for an applied impulse voltage of 78 kV. Ten oscillograms were recorded for each and with the square-cut end corona occurred for each impulse but the corona onset varied from the wave front to 0.3 μsec

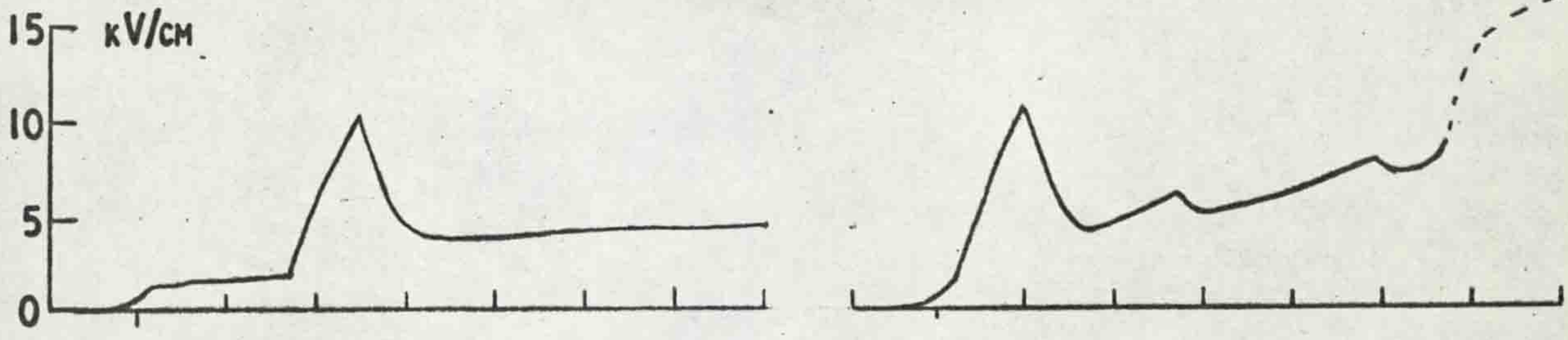

A SQUARE-CUT END D

0.2μSEC/DIV IN EACH

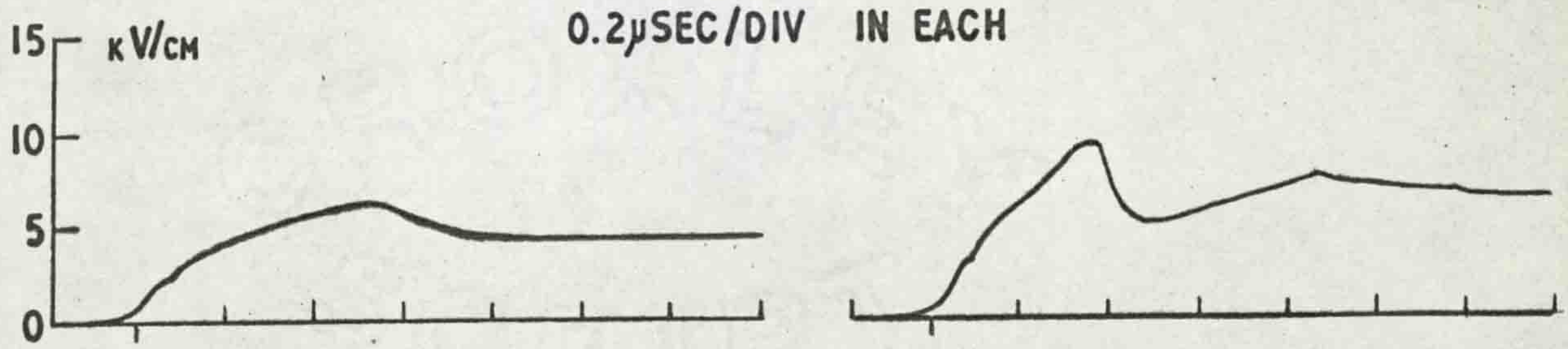

B 30° CONE E

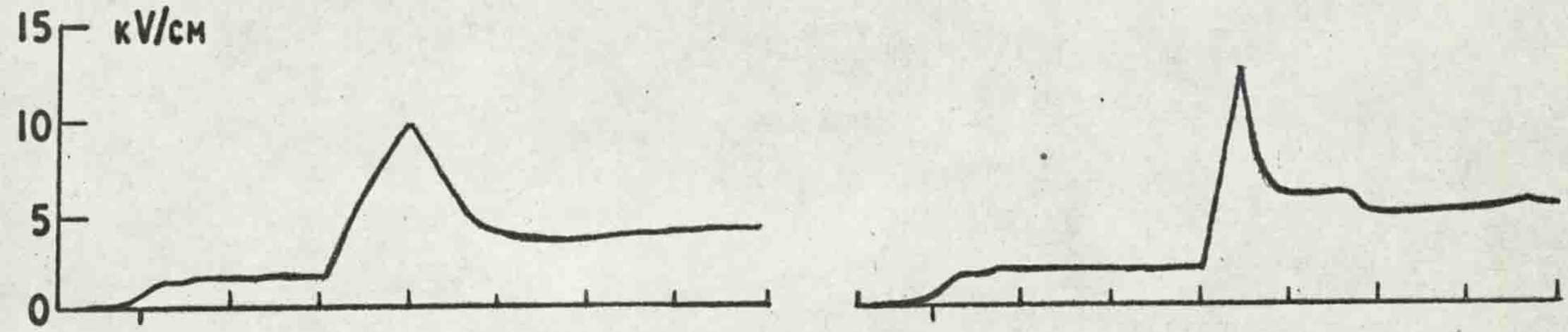

C HEMISPHERICAL END F

FIG. 23 FIELD AT PLANE FOR VARIOUS ROD END SHAPES

15cm GAP
A,B&C — 78kV
D,E&F — 90kV

after the crest. In each case the effect of space charge being neutralized at the plane was observed but for the corona starting on the wave front the peak field was not reached for 0.4 μsec while for the corona starting latest the peak was reached in 0.13 μsec.

With the 30° cone the corona always started on the wave front with the peak value occurring after 0.4 - 0.7 μsec. The peak value of field reached was only about half that for the square-cut end but the final value, after the space charge had been neutralized at the plane, was the same. Using the hemispherical end corona occurred for only two of the ten impulses and in one case the time to peak was 0.32 μsec and for the other 0.19 μsec. The peak values were slightly less than those for the square-cut end with the final value being the same as for the square-cut end and the 30° cones.

With the applied voltage raised to 90 kV another series of 10 impulses was applied to each rod end and the results are shown in trace D for the square-cut end, trace E for the 30° cone and trace F for the hemispherical end. With the square-cut end the corona always started on the wave front and gave consistent results with a time to peak value of 0.13 μsec. The peak field recorded was similar to that for the applied voltage of 78 kV as was the minimum field after

the corona had reached the plane. A second rise was then recorded which generally led to the probe being "hit" by a corona filament as shown in the dashed line of the figure.

For the 30° cone the corona again started on the wave front with the time to peak value varying from approximately 0.2 - 0.3 μ sec. In this case the peak values recorded were similar to those obtained with the square-cut end as were the succeeding values. Even though the fields were similar four breakdowns occurred with the 30° cone whereas there were no breakdowns recorded for the other two rod ends.

Using the hemispherical end at 90 kV applied voltage, corona occurs on every impulse but it always occurred on the wave crest or on the tail up to 1.1 μ sec after the start of the wave. After the initiation of corona there appears to be little difference in the time to reach the peak value which was 0.08 μ sec. The peak field values are slightly higher than those for the other two rod ends but when the field has fallen due to the neutralization of space charge at the plane the value does not rise as it did for the other two cases.

Further information and discussion on the differences between the rod ends will be given in the section on Lichtenberg figures.

(ii) Gap length variable, 5 - 20 cm

An example of the field at the plane in a 5 cm gap is shown in Fig. 24A for an applied impulse voltage of 37 kV. It is noted that the corona filaments cross the gap even though the applied voltage is only sufficient to cause corona on the wave tail. This is explained by the fact that the field is more uniform since the size of the rod was kept constant while the length of the gap was shortened. The same effect occurred for the 15 cm gap when the field was made more uniform by using a hemispherically ended rod instead of the square-cut rod. The field rose to a peak value of approximately 16.5 kV/cm in 0.06 μsec and then fell to 5.5 kV/cm. A second peak in the field then occurs similar to those observed in the 15 cm gap. The final field is only 50% greater than the geometrical field which indicates that there is very little space charge remaining in the gap after the corona discharge has finished. The oscillation on the wave crest exists on the voltage wave and is due to insufficient damping when only one stage of the generator was used.

The field at the plane in a 10 cm gap is shown in Fig. 24B for an applied impulse voltage of 43 kV in trace 1 and 52 kV in trace 2. Again if corona occurs some of the

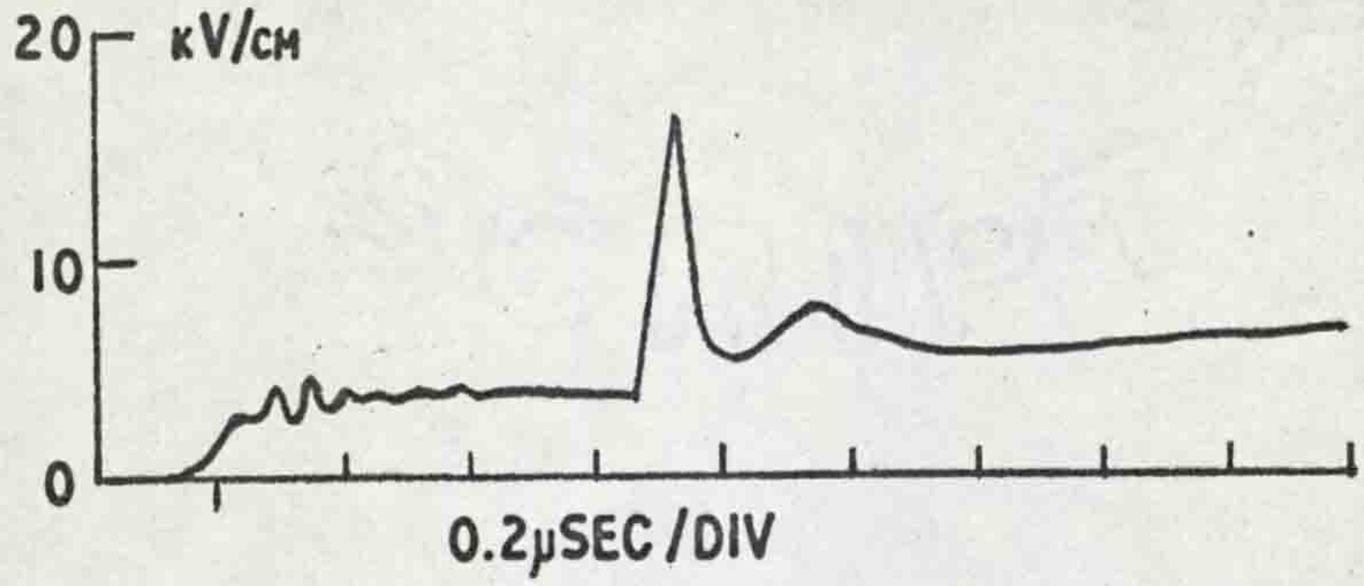

A

5cm GAP
37kV

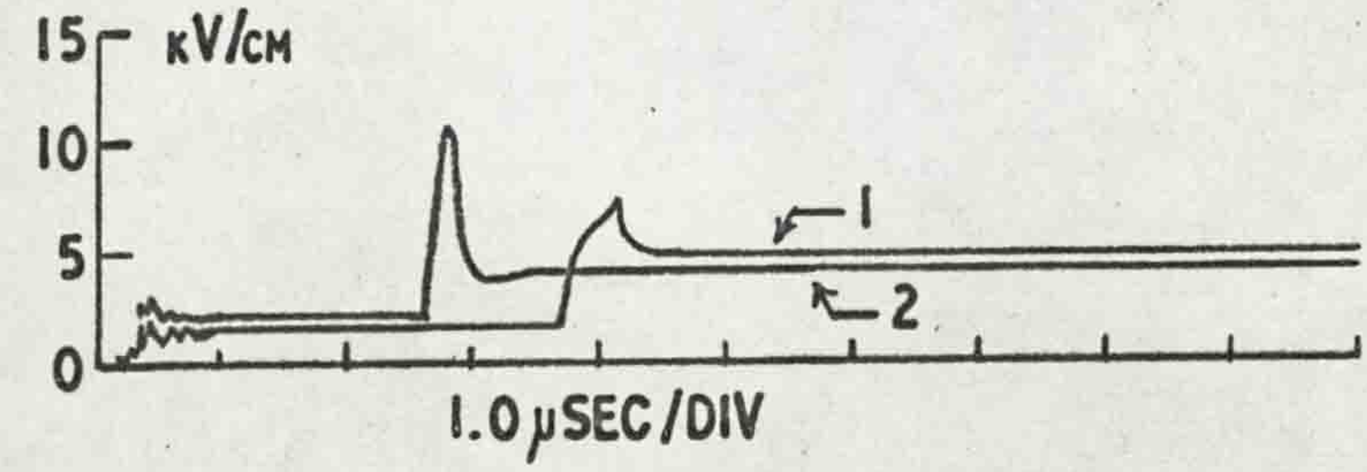

B

10cm GAP
1. 43kV
2. 52kV

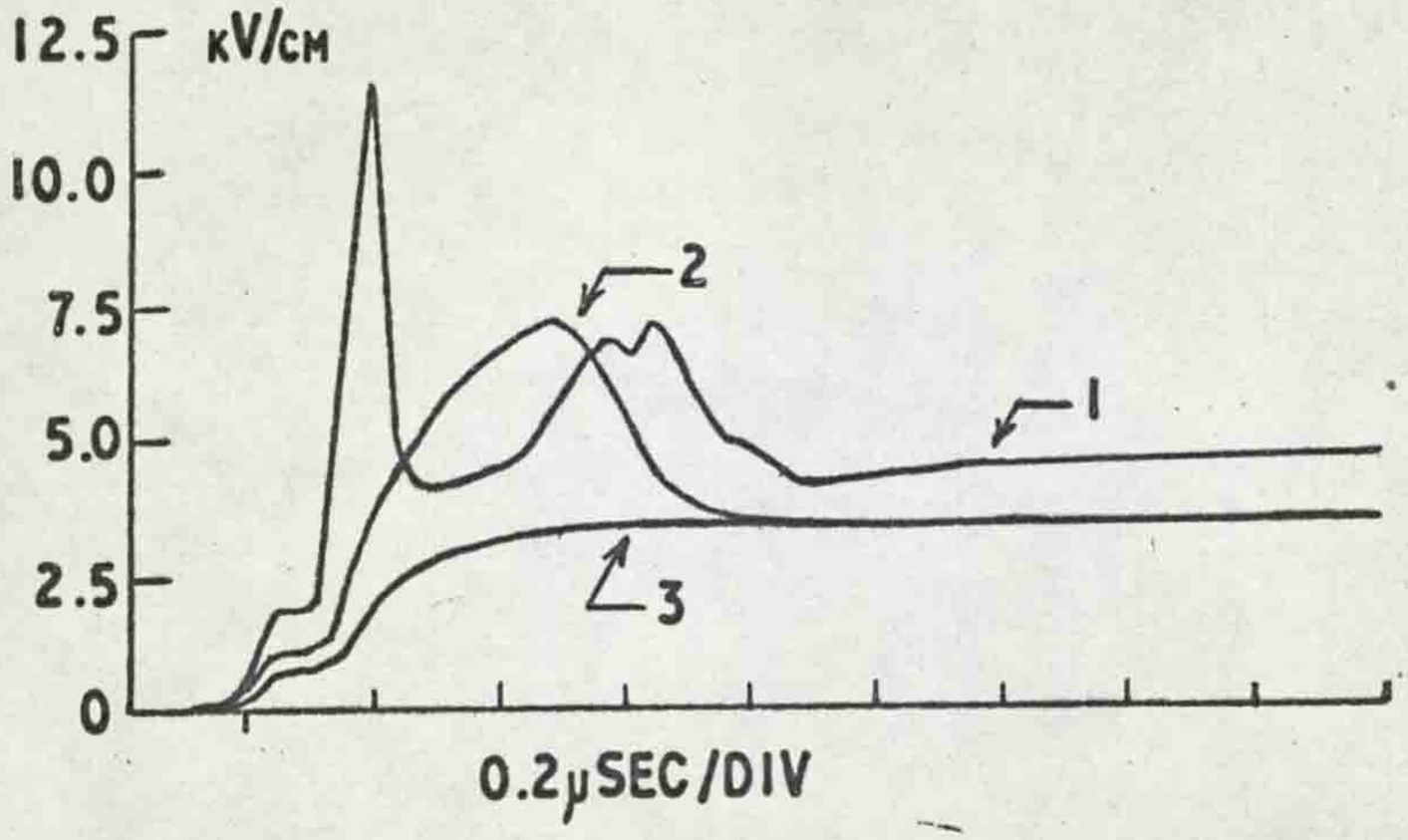

C

72kV
1. 10cm GAP
2. 15cm GAP
3. 20cm GAP

FIG. 24 FIELD AT THE PLANE WITH GAP LENGTH 5–20cm

filaments cross the complete gap but considerable space charge remains in the gap, especially with the lower voltage where the final field is about 3½ times the geometrical field. In the first case a peak field of 8 kV/cm is reached after 0.4μ sec and in the second case the peak field is 11 kV/cm reached after 0.2μ sec. Trace 1 of Fig. 24C shows the field in a 10 cm gap for an applied impulse voltage of 72 kV which is sufficient to cause breakdown occasionally. In this case the field reaches a peak value of 11.5 kV/cm in 0.08μ sec.

The gap was then lengthened and a 72 kV impulse applied to a 15 cm gap and to a 20 cm gap, the results of which are shown in Fig. 24C, trace 2 and trace 3 respectively. In the 15 cm gap the corona crosses the gap causing a peak field of 7 kV/cm to occur after 0.36μ sec. The field then falls to 3.5 kV/cm as the space charge is neutralized. With the 20 cm gap the corona does not cross the gap but it does increase the field to 3.5 kV/cm. The fact that this is the same as the final field for the 15 cm gap is probably coincidental.

As the gap length is increased the geometrical field decreases, the peak field due to the corona discharge decreases and the time to corona onset increases. That

these trends should occur is quite obvious but the decrease in time during which there is corona activity in the gap, as evidenced by the change in field at the plane, bears consideration. In the 10 cm gap the initial corona crosses the gap to the plane where the space charge is neutralized. This permits a second discharge to start within the remaining space charge which also crosses the gap and has its associated space charge neutralized leading to a third discharge. The third discharge does not cross the gap but it produces the slight increase in field at about 1 μsec. In the 15 cm gap only one discharge occurs and when the space charge associated with the initial corona filaments is neutralized no more corona is initiated. Finally, for the 20 cm gap the corona does not cross the gap. It ceases to grow when less than 20 cm in length so that there is no neutralization of charge at the plane.

(iii) 50 cm gap

(a) Field at the plane

As in the case of the 15 cm gap a complete study of the field at the plane for a 50 cm positive rod-negative plane gap has been made. Fig. 25 shows the field at the rod center-line as a function of voltage with the lower straight line showing the geometrical field extrapolated

FIG. 25 FIELD AT THE PLANE ON THE ROD CENTER-LINE

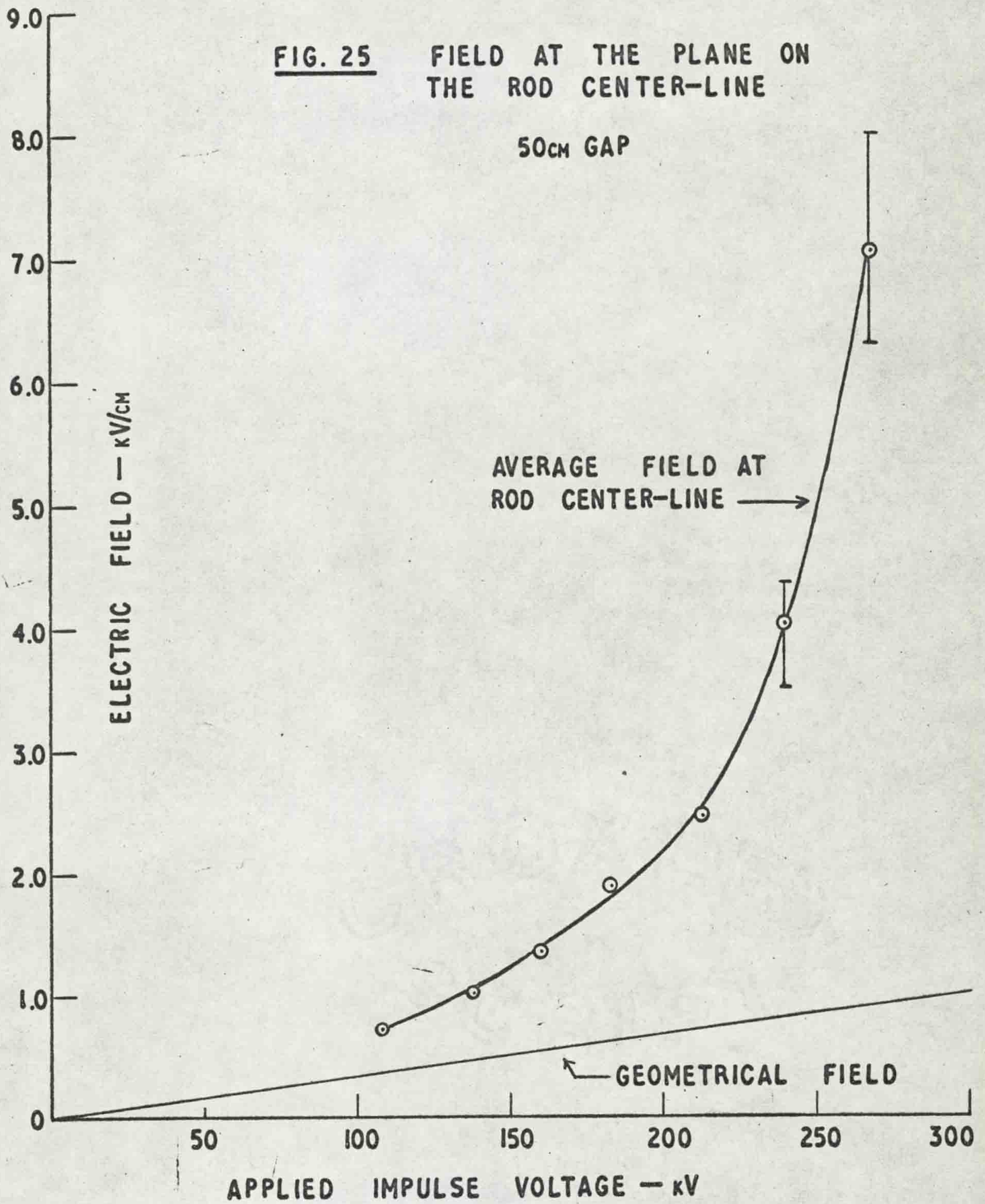

from low voltage measurements. The sudden large spread in field values which occurs at 240 kV in the upper curve is caused by corona filaments crossing the gap at that voltage so that the peak field is dependent on the relative position of the filaments with respect to the probe. Breakdown occurred about 50% of the time for an applied voltage of 268 kV at which voltage the peak field measured was 8 kV/cm.

Examples of the field oscillograms are shown in Fig. 26. It is not possible to detect the corona onset point since it occurs on the steeply rising front and does not give a discontinuity as was the case in the 15 cm gap. Another factor which tends to obscure the corona onset point is that the effect of the initial corona on the field at the plane will be much less for a 50 cm gap than for a 15 cm gap since the field is an inverse function of the square of the distance. Fig. 26A shows the field for applied voltages of 108 kV in trace 1, 138 kV in trace 2 and 160 kV in trace 3. At 160 kV the field rises to a crest and then there is another rise starting after about 0.3 μsec. This also occurs at 183 kV and 213 kV as shown in Fig. 26B, traces 1 and 2, but the time delay decreases as the voltage is raised so that at 213 kV the first crest is just discernible. This effect can be explained in the same manner

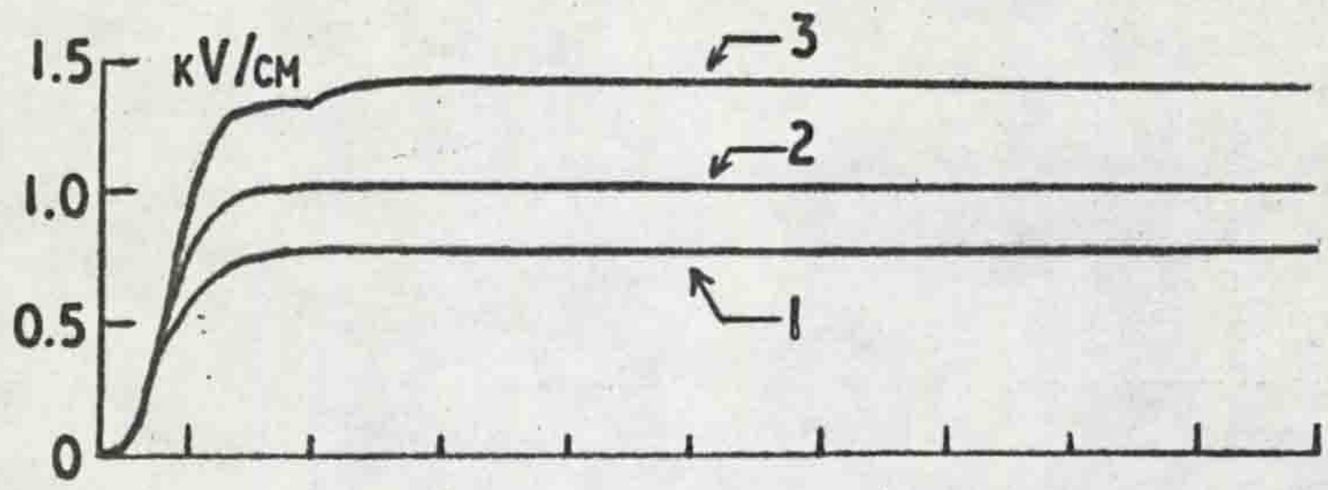

A
1. 108 kV
2. 138 kV
3. 160 kV

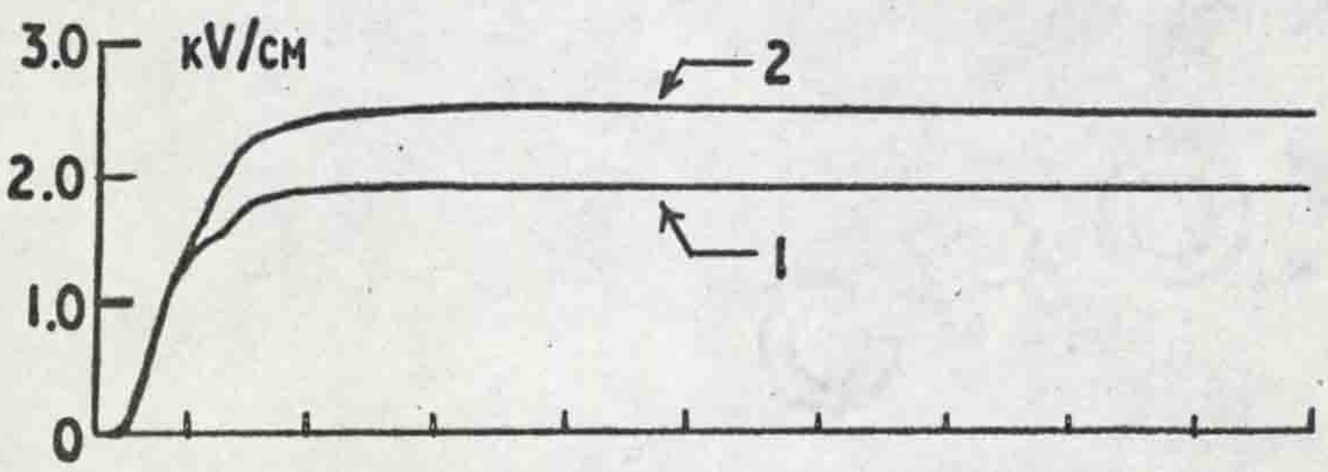

B
1. 183 kV
2. 213 kV

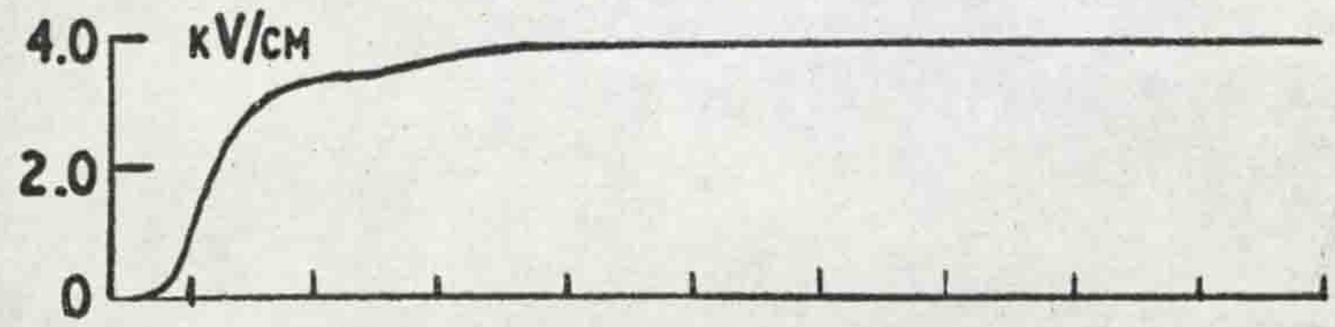

C

240 kV

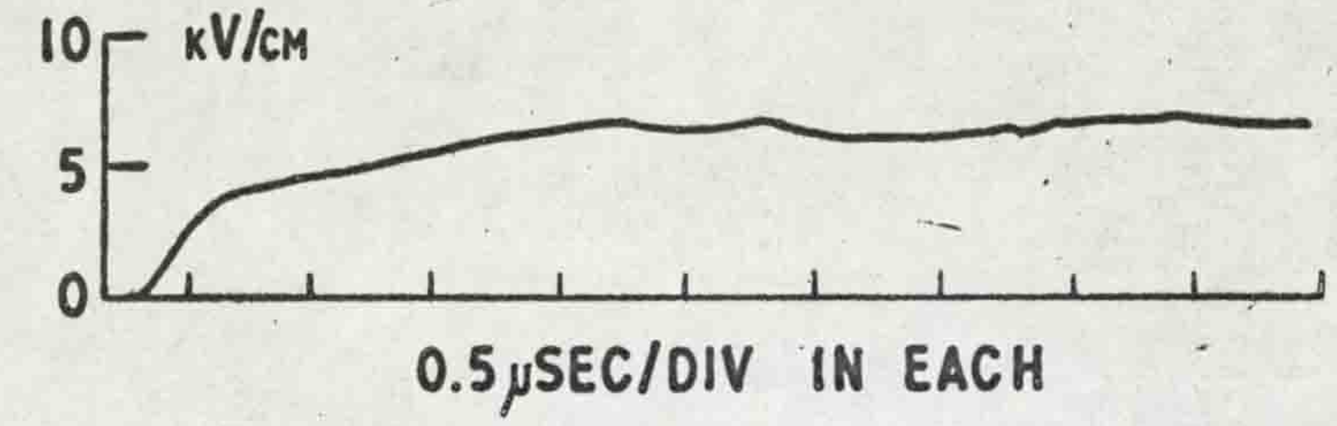

D

268 kV

0.5 μSEC/DIV IN EACH

FIG. 26 FIELD AT THE PLANE ON THE ROD CENTER-LINE

50 cm GAP

as the double peaks observed in the 15 cm gap, but in this case the mid gap corona starts not because the space charge of the main corona filaments has been neutralized at the plane but because the space charge of the main filaments has propagated a sufficient distance from the space charge which has been left behind to enable the mid gap corona to start. Fig. 26C shows the field at an applied impulse voltage of 240 kV. At this voltage the initial crest occurs slightly later than for the lower voltages and then the second rise starts about 0.3μsec later. In some cases the second rise continued until the corona reached the plane in approximately 2μsec. This can be explained in the same way as the lower voltage cases but since the corona actually reaches the plane it may be that the main corona filaments stop and then start again due to the approach of space charge from higher up in the gap. The field for an applied voltage of 268 kV is shown in Fig. 26D. This is similar to the field at 240 kV except that the pronounced break does not occur. Instead the field reaches a crest and then continues to rise gradually.

The field distribution along the plane was measured for an applied voltage of 240 kV with the results shown in the graph of Fig. 27. The lower curve is the field at the

FIG. 27 FIELD DISTRIBUTION ALONG THE PLANE

50 CM GAP
240 kV

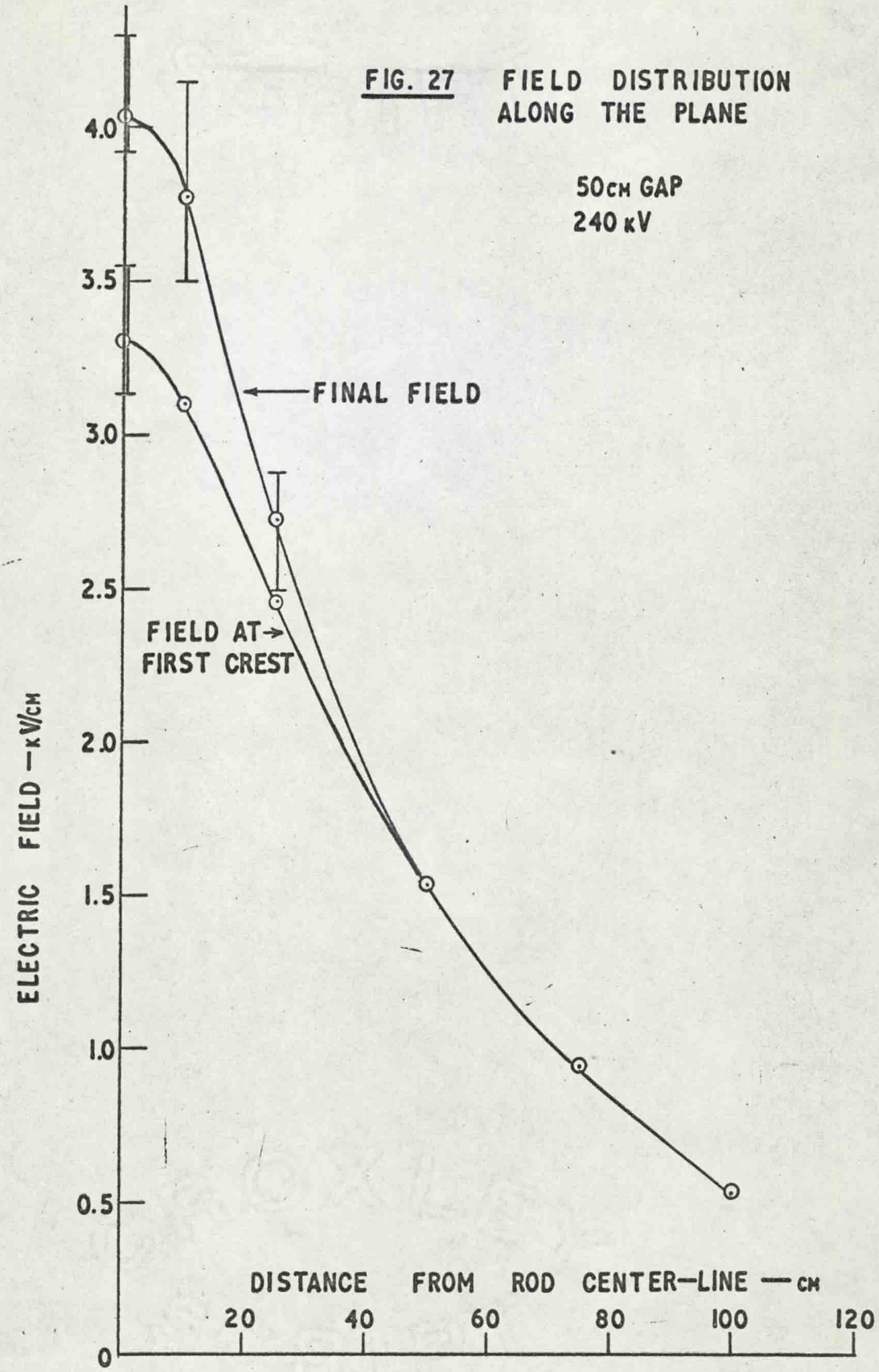

first crest while the upper curve is the final field after the second rise has occurred. The second rise has a much greater effect near the axis of the gap which is reasonable since the space charge is propagating directly towards a point on the axis but is moving at an angle to a point off the axis. This means that the cos θ term will be decreasing so that the field increase is less.

Oscillograms showing the field at various distances from the rod center-line are shown in Fig. 28. Fig. 28A, trace 1 is the field on the center-line, trace 2 is 10 cm from the center-line and trace 3 is 25 cm from the center-line. Fig. 28B shows the field 50 cm from the rod center-line and Fig. 28C, trace 1 shows the field 75 cm and trace 2 the field 100 cm from the rod center-line. The second rise is still apparent even 100 cm from the axis but the increase is very small.

(b) Field at the rod

The field at the rod was measured using the same arrangement as was used for the 15 cm gap. The breakdown voltage with the rod at the earthed end was found to be about 10% higher than for the case with the rod the high voltage electrode but it was assumed that this was close enough to permit comparison between the two cases. The

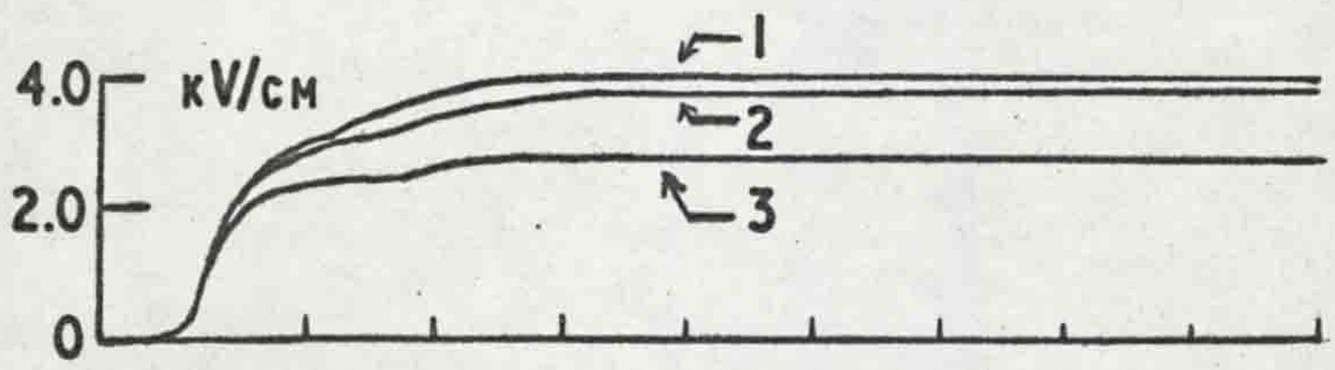

DISTANCE FROM ROD CENTER-LINE

1. 0cm
2. 10cm

A

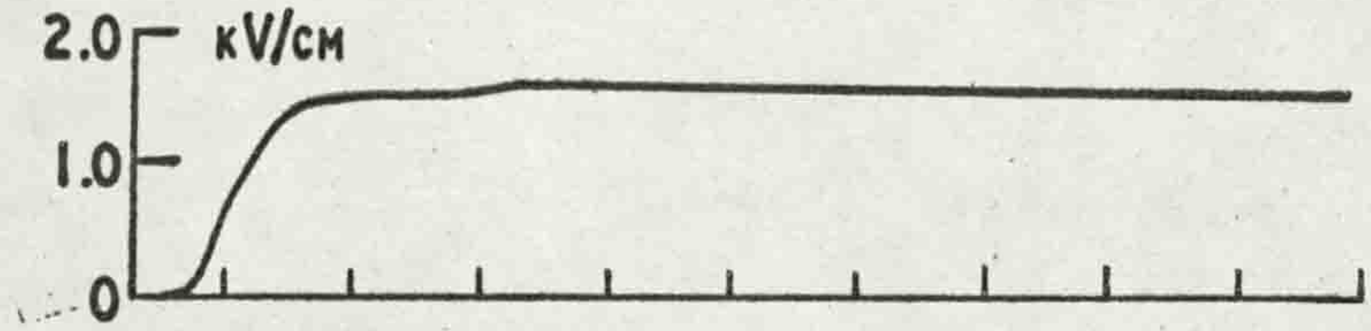

50cm

B

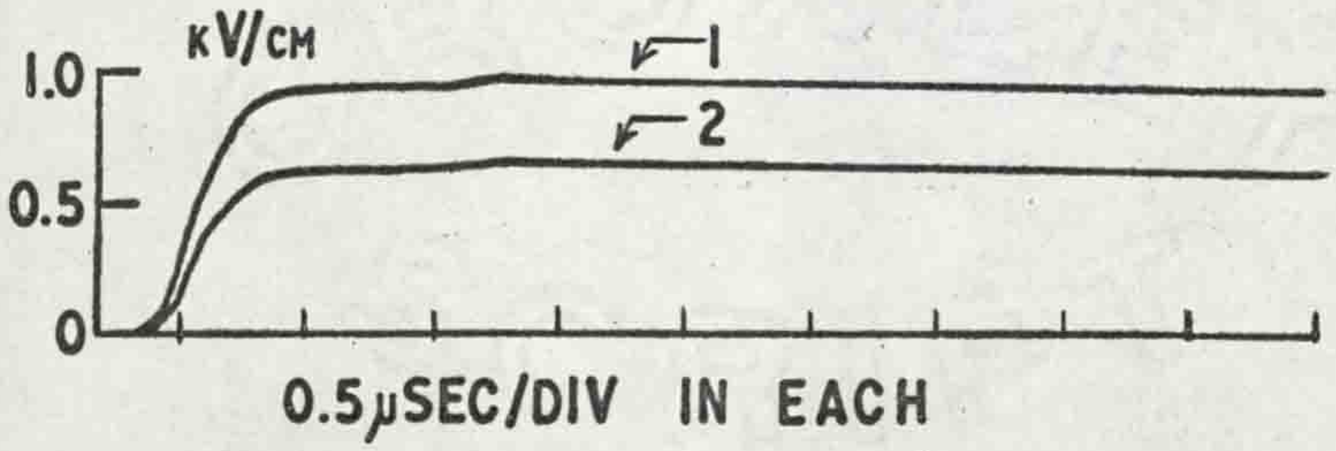

1. 75cm
2. 100cm

C

FIG. 28 FIELD AT VARIOUS DISTANCES FROM THE ROD CENTER-LINE

50cm GAP
240 kV

corona appears to start later with the rod earthed so that the field at 213 kV as shown in trace 1 of Fig. 29A follows the geometrical field almost to the crest before the corona is initiated causing the field to collapse to a low value as for the 15 cm gap. The field for an applied voltage of 240 kV, as shown in trace 2 of Fig. 29A, is similar except that the corona starts earlier on the wave front. In both cases after the initial collapse the field rises slightly as the space charge propagates away from the rod towards the plane. This rise levels off and then the field increases again which is added evidence indicating corona starting in the mid gap region. If corona started again at the rod one would expect a decrease in the field rather than the increase which occurs. After the second small rise a gradual decline in the field is observed. This decline is greater than could be caused by the voltage falling so it must be due to a gradual build-up of the positive space charge near the rod due to a clearing of electrons and negative ions into the rod. Fig. 29B shows the field with 268 kV applied in trace 1 and 293 kV in trace 2. At 268 kV the field is again similar to that at the lower voltage but it rises higher as the space charge propagates farther into the gap and the break in

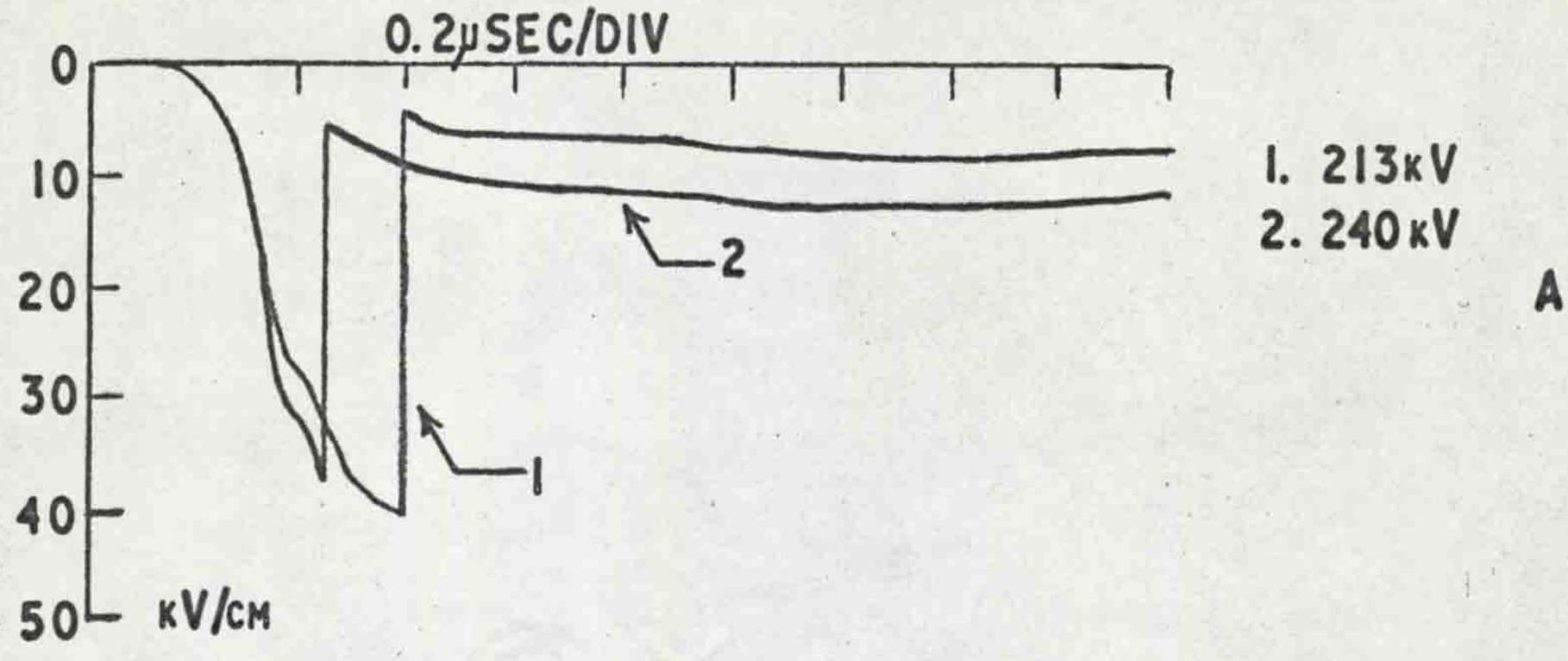

FIG. 29 FIELD AT THE ROD IN A 50cm GAP

the rise is not as pronounced. This is probably due to the mid-gap corona starting before the initial corona has stopped. At 293 kV the field, after the initial corona, rises to a value such that the leader stroke starts from the rod. This causes a slow decrease in the field and leads to breakdown which occurs beyond the edge of the oscillogram in time.

The breakdown field is shown in Fig. 29C, trace 1, on a different time scale so that the final breakdown is shown. The field goes positive before breakdown because the prebreakdown current causes a considerable decrease in the applied voltage. When the final breakdown occurs the field takes a step positive because the applied voltage collapses so that the only field is due to the positive space charge. Some of the positive space charge will produce a sufficiently high local field to cause streamers to propagate to the discharge channel or to the rod which accounts for the fact that the positive field pulse is only of very brief duration. The remainder of the positive space charge disperses more slowly as can be seen by the gradual return of the field to zero. Trace 2 of Fig. 29C shows the field when breakdown is interrupted by chopping the voltage with a sphere gap. As the field

is decreasing due to the growth of the leader stroke the voltage is chopped which causes a large positive swing in the field since the applied field is removed leaving only the space charge field. A reverse discharge (see Gorin and Stekolnikov[18]) occurs which reduces the positive field until the discharge ceases allowing the field to rise again positively. Subsequent reverse discharges reduce the field to a value at which the remaining space charge is no longer sufficient to initiate further discharges. The time constant of the field probe was too low to measure the rate of decay of this remaining field which caused a field of approximately 5 kV/cm at the rod.

(iv) <u>100 cm gap</u>

A thorough investigation of the 100 cm gap was not carried out in the low voltage region but a comprehensive study of the field on the plane at the rod center-line was made for the voltage range from 473 kV at which voltage corona occasionally crossed the gap to 510 kV at which voltage the gap broke down in most cases. The field at the rod was not measured as a sufficiently large plane high voltage electrode was not available.

Fig. 30A shows the field at the rod center-line with trace 1 corresponding to 473 kV when corona does not cross

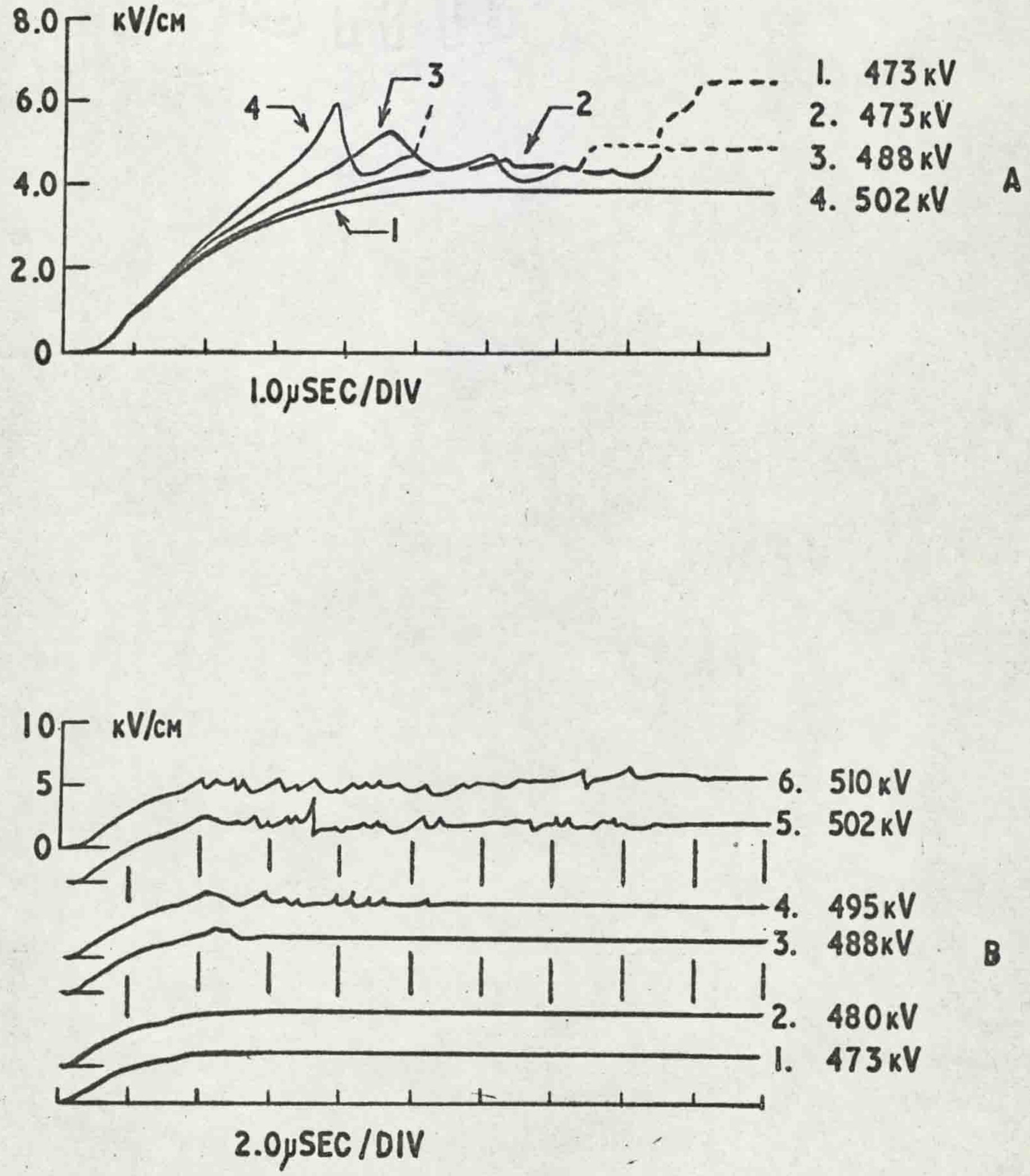

FIG. 30 FIELD AT THE PLANE ON THE ROD CENTER-LINE

100cm GAP

the gap and trace 2 corresponding to 473 kV when corona does cross the gap. Trace 3 shows the field for an applied voltage of 488 kV and trace 4 for an applied voltage of 502 kV. The dashed lines at the ends of the traces indicate that a conduction current has probably occurred to the probe so that the field measurement ceases to be accurate. This is deduced from the sudden step which indicates that the charge of a corona filament has hit the probe. At 473 kV the time to the maximum field is about 5.5 μsec when corona does not cross the gap while the peak field when corona does cross the gap occurs at about 5 μsec. The voltage wave reaches a crest in slightly less than 2 μsec from the start of the wave so that the corona continues for some time after the wave crest. With an applied voltage of 480 kV the corona filaments crossed the gap in most cases and with an applied voltage of 488 kV the filaments crossed the gap in every case with a time to peak value of from 4.0 to 4.4 μsec. For an applied voltage of 495 kV the peak value of field occurred at 3.9 μsec and for 502 kV, at which voltage breakdown occurred occasionally, the time to peak value varied from 3.3 to 3.8 μsec. With an applied voltage of 510 kV breakdown occurred in most cases and the peak value of field occurred in approximately 3.3 μsec.

Using a different time scale the field at the rod center-line is shown in Fig. 30B for applied voltages of 473, 480, 488, 495, 502 and 510 kV in traces 1 to 6 respectively. Here it can be seen that at 495 kV and higher voltages the corona filaments continue to hit the plane for a considerable period of time after the arrival of the initial filaments. Although the average field remains quite constant this can be deduced from the short, sharp spikes on the field oscillogram which are caused by the space charge of a filament increasing the field as it approaches the plane. When the filament hits the plane the space charge is neutralized and the field returns to its former value. The fact that the field does not decrease appreciably (except for the first corona filaments to cross the gap) below the average value when the corona filaments hit the plane indicates that the space charge neutralized is small relative to the total space charge in the gap. In some cases there is a brief dip below the average as the space charge is being neutralized and it is possible that this is due to the corona filament producing a short conducting filament at the plane which gives some shielding effect on the nearby probe.

From previous workers'[33] photographic results it appears likely that the long succession of corona filaments hitting the plane indicates that a leader stroke has started from the rod but that it dies out before causing a complete breakdown of the gap.

Fig. 31 shows the field at the plane as a function of the applied voltage for voltages approaching the breakdown value. The upper curve represents the crest value of field as the corona filaments approach the plane and it is drawn through the lower points as these represent a better average value, the higher ones being due to the space charge of an individual filament coming very close to the probe. The lower curve shows the average value after a short time interval when the field has reached a relatively steady average which does not increase unless breakdown occurs. For the lowest two points the corona did not cross the gap so no space charge was neutralized and there was therefore no drop in field. The dashed line represents the average field in the gap at the peak voltage and it can be seen that the initial peak field goes above this average while the final field does not. In order for the peak field at the plane to exceed the average, the field in the gap must decrease if the integral of the field over the gap length

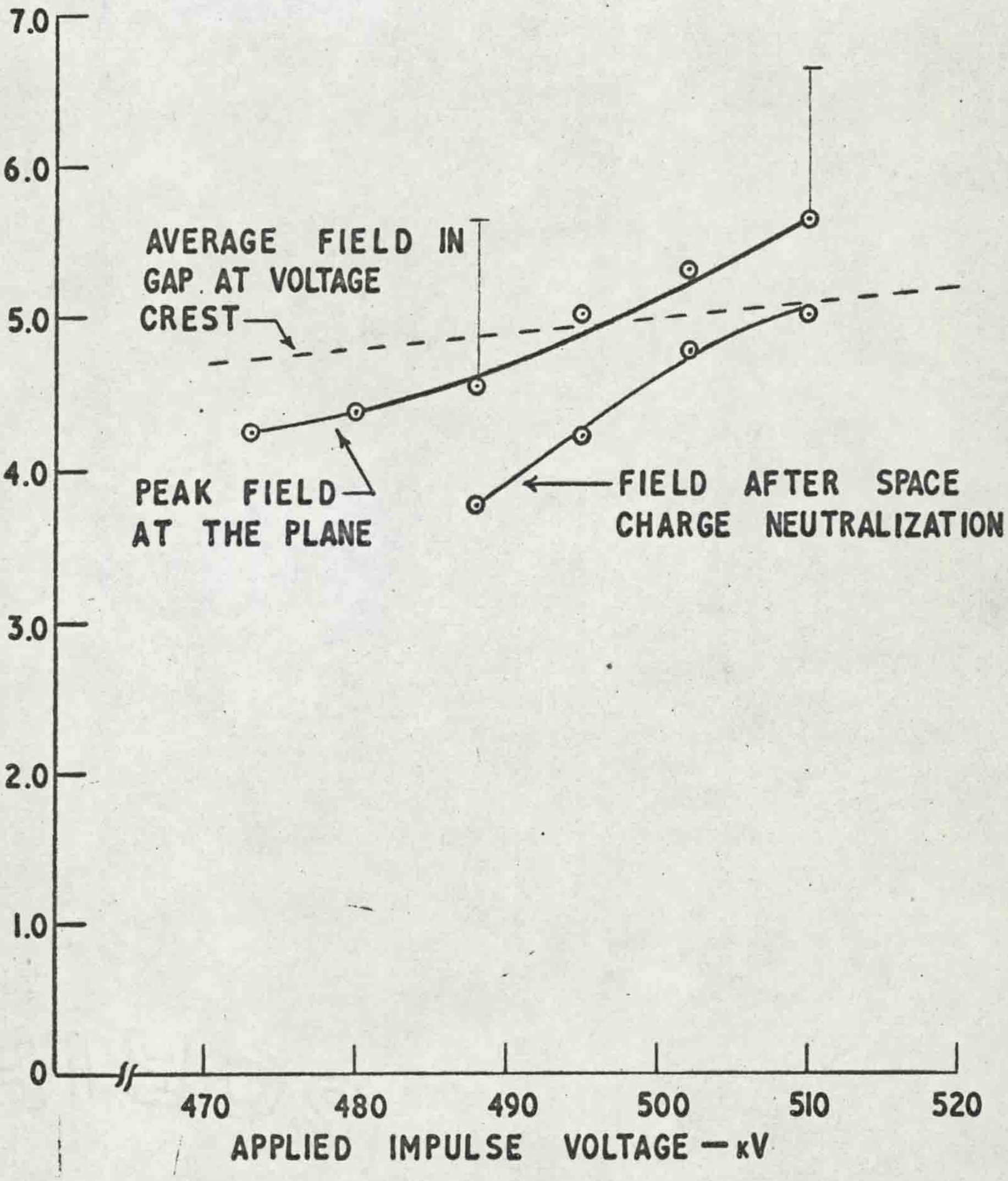

FIG. 31 FIELD AT THE PLANE IN A 100cm GAP

is to equal the voltage. This is in agreement with the theory that the initial corona tips form a "wave" of high space charge density behind which the field will be considerably lowered and in front of which the field will be enhanced. The fact that the field at the plane tends to remain constant as the applied voltage wave tail decreases indicates that either the field in the gap is decreasing or the leader stroke is effectively extending the high voltage electrode so that the field in the remainder of the gap stays constant at the average value. As long as corona activity continues in the gap the latter case must be true otherwise a very low field would be created at the rod.

(v) 200 cm gap

For the 200 cm gap the field was measured as a function of voltage and as a function of distance from the rod center-line. The graph, Fig. 32, shows the field variation with voltage for a point on the plane directly under the rod. The curve, similar in shape to those for shorter gaps, rises with increasing slope up to the breakdown voltage. The corona initiation point was not determined as corona was seen on the rod at the minimum applied voltage of 148 kV. The field measured at this voltage was extrapolated linearly in the lower dashed curve to give

FIG. 32 FIELD AT THE PLANE IN A 200CM GAP

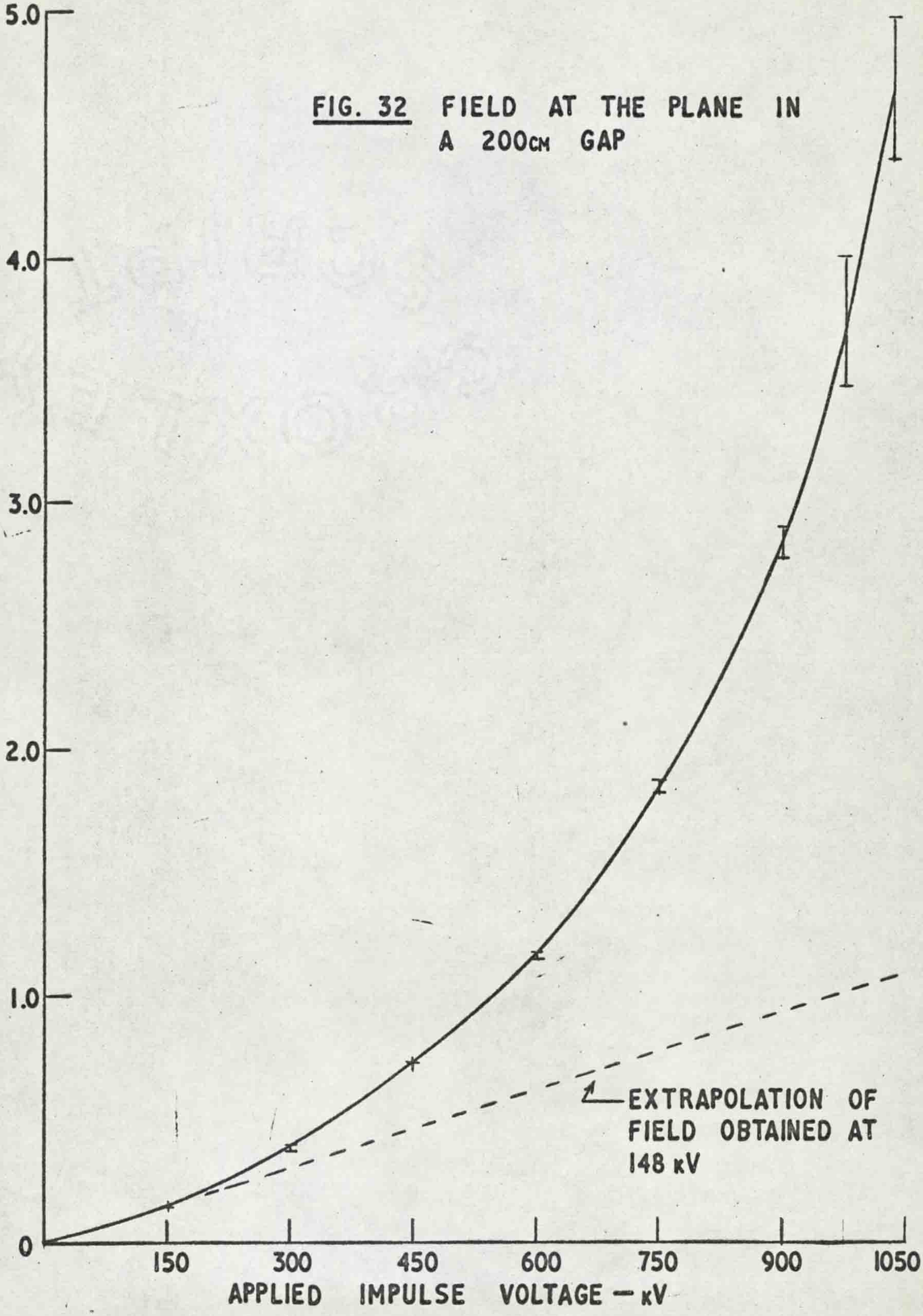

a comparison with the higher voltage fields and it can be seen that the final field is about five times this linear extrapolation. As the voltage is increased the spread in the measured field increases indicating irregularities in the space charge growth. This effect was noted previously and when the filaments actually cross the gap the variation is largest as it is due to the varying distance of the corona filaments from the probe.

Fig. 33 shows the field oscillograms for various applied voltages ranging from 148 kV in Fig. 33A, trace 1 to 1020 kV in Fig. 33D, trace 2. At the lowest voltage the shape of the field oscillogram is very close to that of the applied voltage wave with the crest occurring approximately 1½ - 2 μsec after the start of the wave. It was not ascertained whether the step on trace 1, Fig. 33A was due to the corona initiation or whether it was due to a slight oscillation on the voltage wave. The latter is the more likely. As the voltage is raised the field oscillograms show that the field increases more slowly so that the crest occurs after the voltage crest with a maximum time to the crest of about 8½ μsec as shown in Fig. 33D, trace 1. The delay in the crest is caused by the time required for the corona filaments to propagate across the

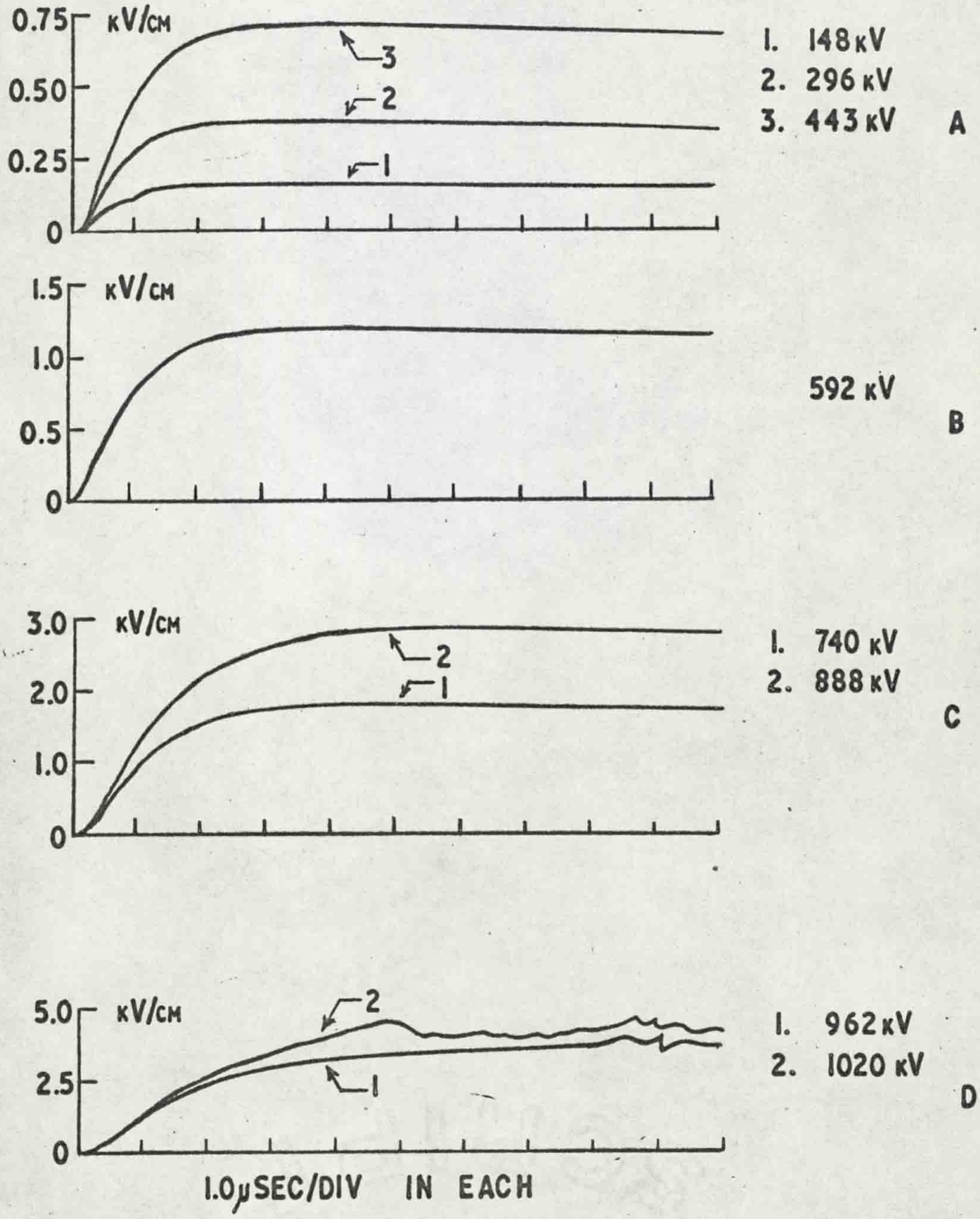

FIG. 33 FIELD AT THE PLANE IN A 200CM GAP

gap. Fig. 33D, trace 2 shows the field decreasing after the peak as some of the filaments cross the gap and the space charge is neutralized at the plane. The time to peak value has decreased to between 4 and 5μ sec indicating that the average velocity of the corona filaments has increased.

The field distribution along the plane was measured for an applied voltage of 990 kV and the results plotted in Fig. 34. Up to about 50 cm from the rod center-line the filaments reach the plane and thus cause considerable variation in the peak field depending on the proximity of a corona filament to the probe. This can be seen in the upper curve which is the peak field distribution. The field distribution after 10μ sec is shown in the lower curve which apart from the value at 25 cm from the rod center-line gives a smoother curve.

For this length of gap the transit time of the corona filaments across the gap is sufficient to enable the field distribution to be plotted at various times as the corona crosses the gap. This has been done in Fig. 35 where the field distribution is shown for 1μ sec intervals starting 0.8μ sec after the start of the impulse wave. For comparison purposes the field distribution with an applied

FIG. 34 FIELD DISTRIBUTION ALONG THE PLANE

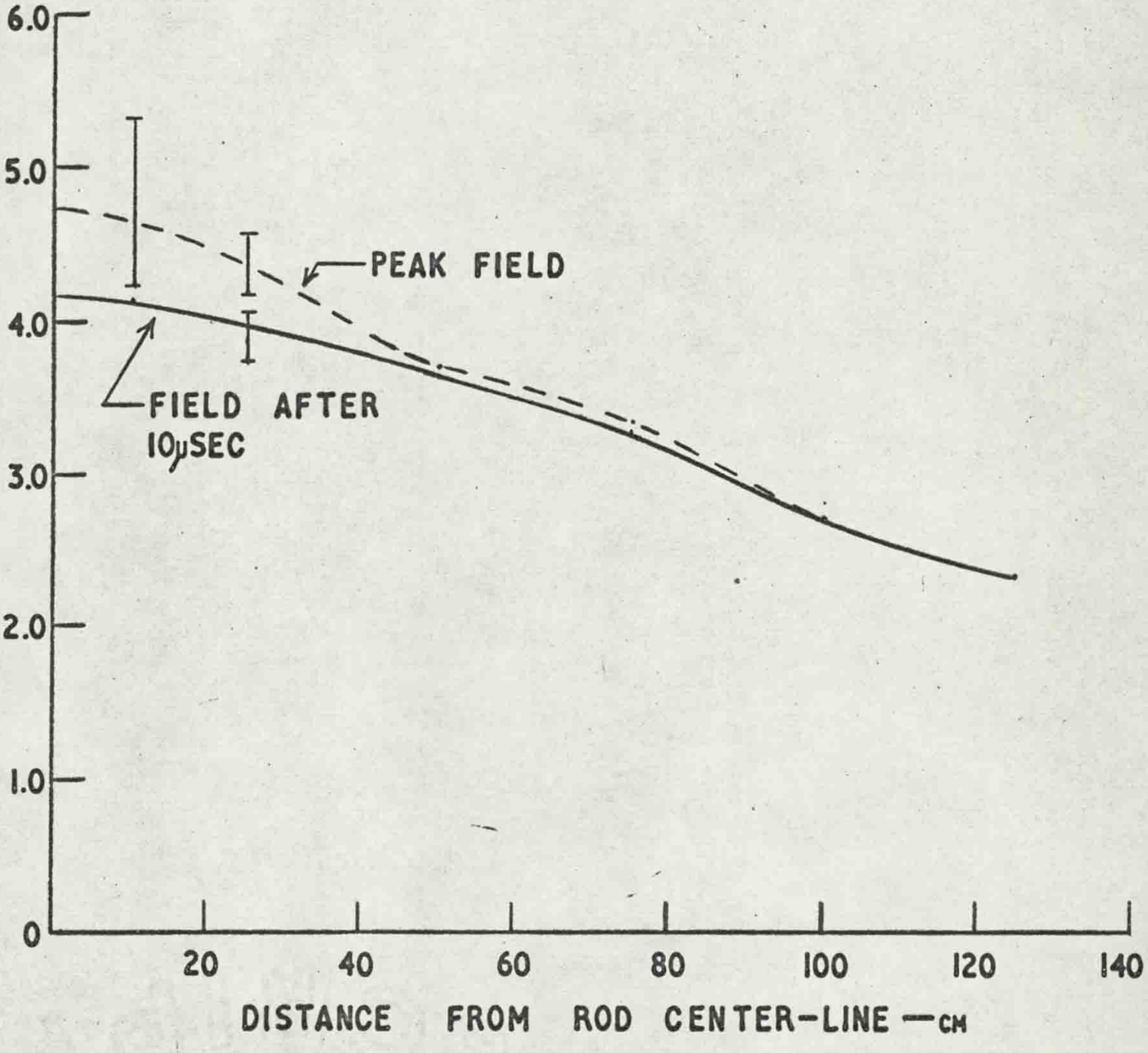

FIG. 35 FIELD DISTRIBUTION ALONG THE PLANE AT 1μSEC INTERVALS

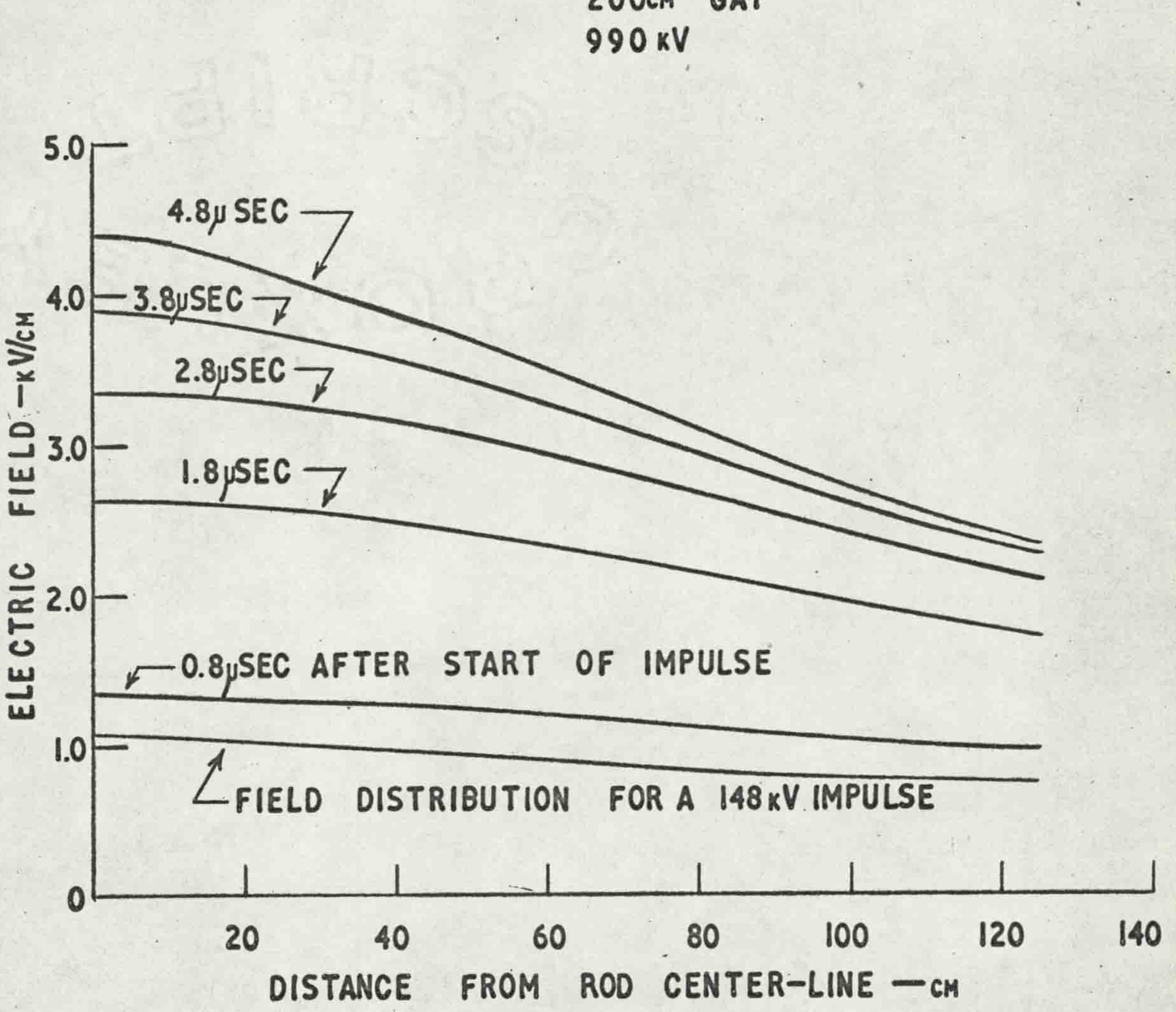

impulse voltage of 148 kV, which is the lowest curve, is shown. It is quite similar in shape to the field distribution at 0.8 μsec with 990 kV applied. As the corona grows into the gap the field at the center increases more than the field away from the rod center-line which, as mentioned earlier, is due to the fact that the space charge of the corona filament tips is approaching the center directly while it is moving at an angle to the more distant points on the plane.

In order to emphasize the change in distribution as the corona grows the curves of Fig. 35 have been replotted in Fig. 36 on the basis of a constant amplitude at 125 cm from the rod center-line with the remaining points on the curves changed proportionally. This shows more clearly the relatively greater increase in field on the rod center-line. The field distribution after 10 μsec has been included and is the dashed curve. It is slightly flatter than the field at 4.8 μsec indicating a slight spreading out of the space charge.

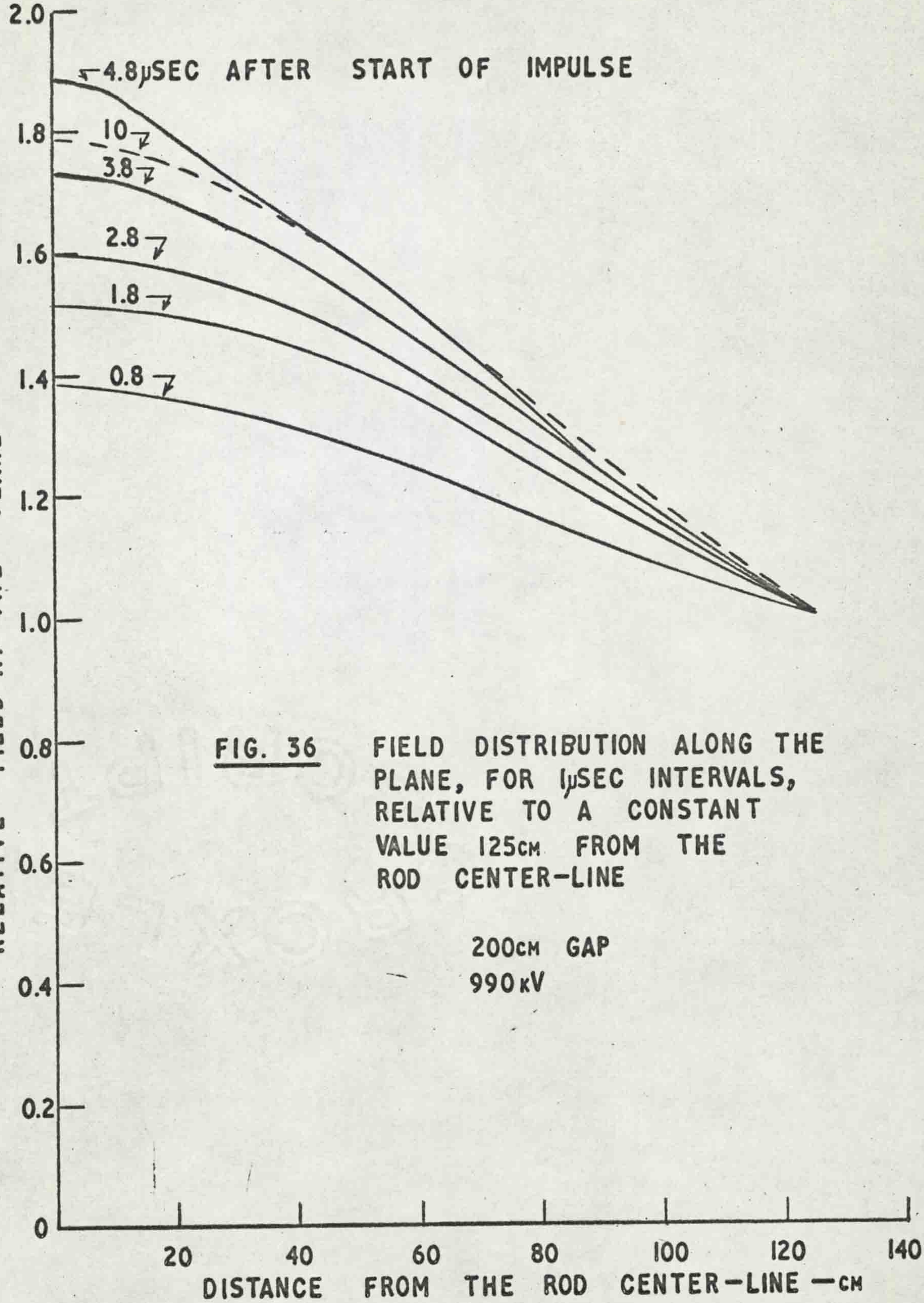

FIG. 36 FIELD DISTRIBUTION ALONG THE PLANE, FOR 1μSEC INTERVALS, RELATIVE TO A CONSTANT VALUE 125CM FROM THE ROD CENTER-LINE

III. Results Using Barriers

(i) Introduction

From previous work[28] it was known that in a positive point-plane gap a barrier placed in the gap stopped the corona filaments from reaching the plane and increased the breakdown voltage. Since the space charge is associated with the advancing corona filaments this means that the space charge position can, to a certain extent, be controlled by a barrier in the gap. The following work makes use of this by measuring the field with and without a barrier in the gap and comparing the results.

(ii) 15 cm gap

(a) Field on rod center-line

The effect on the field at the rod and at the plane of placing a barrier in the gap is shown in Fig. 37. The field with no barrier in the gap is shown in Fig. 37A with the upper trace being the field at the plane and the lower trace being the field at the rod. The field at the plane increases as the corona filaments cross the gap and then decreases as the space charge is neutralized at the plane. A second rise then occurs as either electrons and negative ions are cleared from around the rod or a combination of that and the propagation of mid-gap corona filaments occurs.

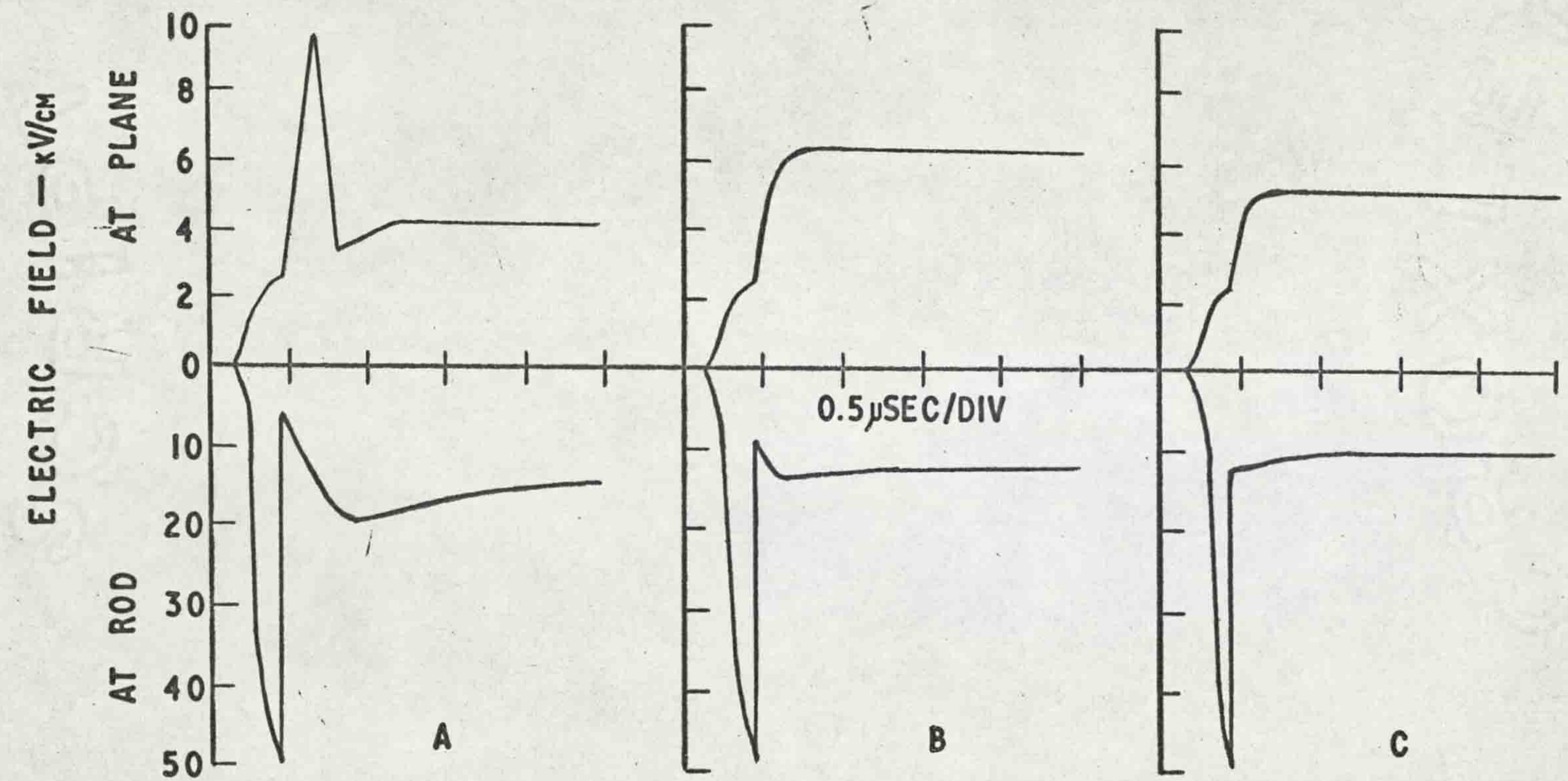

FIG. 37 EFFECT ON THE FIELD OF AN INSULATING BARRIER IN THE GAP

A. NO BARRIER
B. BARRIER 5cm FROM THE PLANE
C. BARRIER 10cm FROM THE PLANE

At the rod the field decreases sharply when corona occurs and then rises as the corona propagates to the plane and the space charge is neutralized. The field at the rod continues to rise for a short period of time after the second rise at the plane has started which definitely indicates that corona filaments have started within the remaining space charge. The field at the rod then falls off while the field at the plane remains constant which indicates a very localized effect of electrons and negative ions being drawn into the rod.

A barrier was then placed 5 cm from the plane and the resultant fields are shown in Fig. 37B. At the plane the field rises until the corona reaches the barrier when the field value levels off. There is no decrease in field as the space charge is prevented from reaching the plane so that it is not neutralized. At the rod the field again decreases sharply as the corona is initiated but the rise afterwards is limited as the space charge can only move 10 cm from the rod. Again a slight decrease in the field at the rod occurs while the field at the plane is constant which again indicates a localized clearing of electrons and negative ions into the rod.

Fig. 37C shows the fields with a barrier 10 cm from the plane. The field at the plane is similar but the maximum

field is lower since the space charge is stopped farther from the plane. The field at the rod however is different in that the initial collapse of field due to corona onset is not as great. From this one can conclude that the initial sharp decrease in field is due to corona which exceeds 5 cm in length. After the first drop in field a gradual decrease occurs similar to that which occurred in the other cases which again indicates a localized clearing of electrons and negative ions. This also indicates that with a barrier 5 cm from the rod there is no appreciable propagation of space charge away from the rod.

(b) Field off rod center-line

Lichtenberg figures, which will be discussed in a later section, indicated that the corona spread horizontally along the barrier and in order to check the effect of space charge spreading along the barrier the probe was positioned 20 cm from the rod center-line while two impulses were fired, one with a barrier 2 cm above the plane and one with no barrier. The results are shown in Fig. 38 where the lower trace shows the field with no barrier and the upper trace the field with the barrier. The first arrow shows the corona onset point while the second shows where the field enhancement due to space charge propagating along the barrier begins.

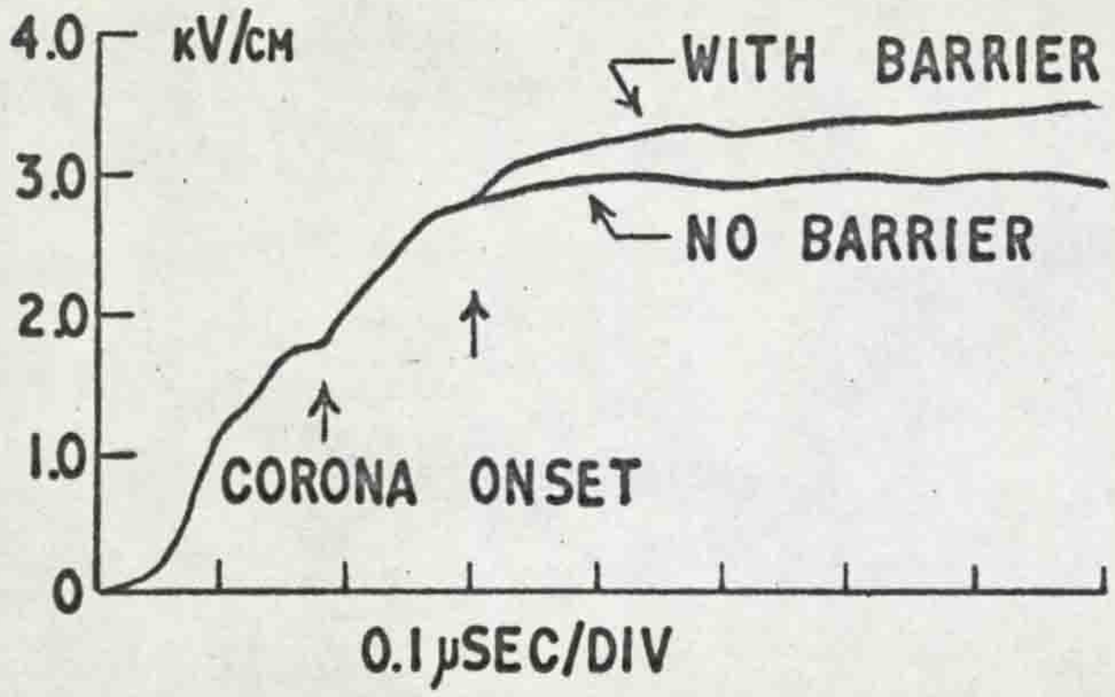

FIG. 38 EFFECT OF CORONA SPREADING ALONG A BARRIER NEAR THE PLANE

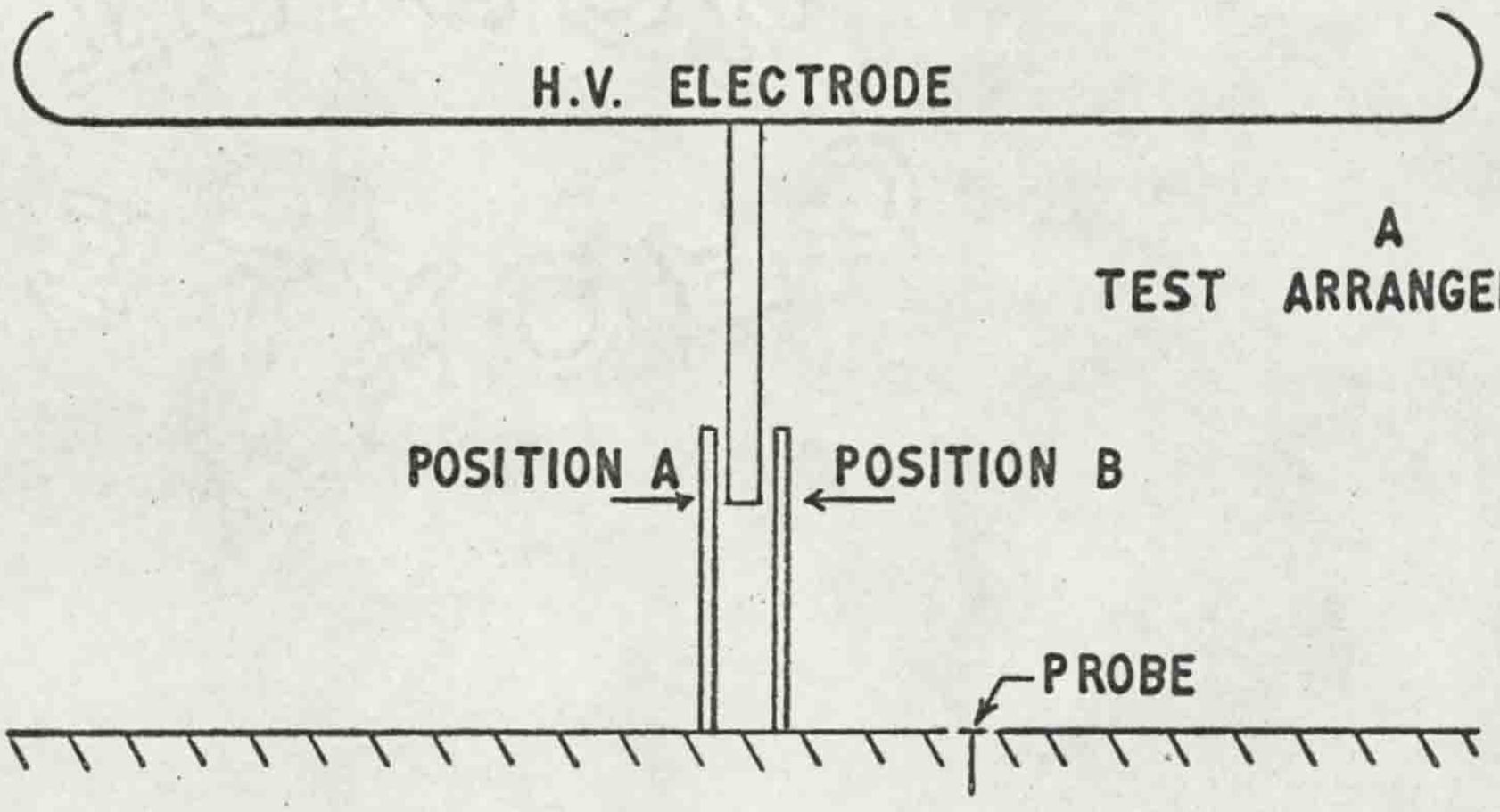

A
TEST ARRANGEMENT

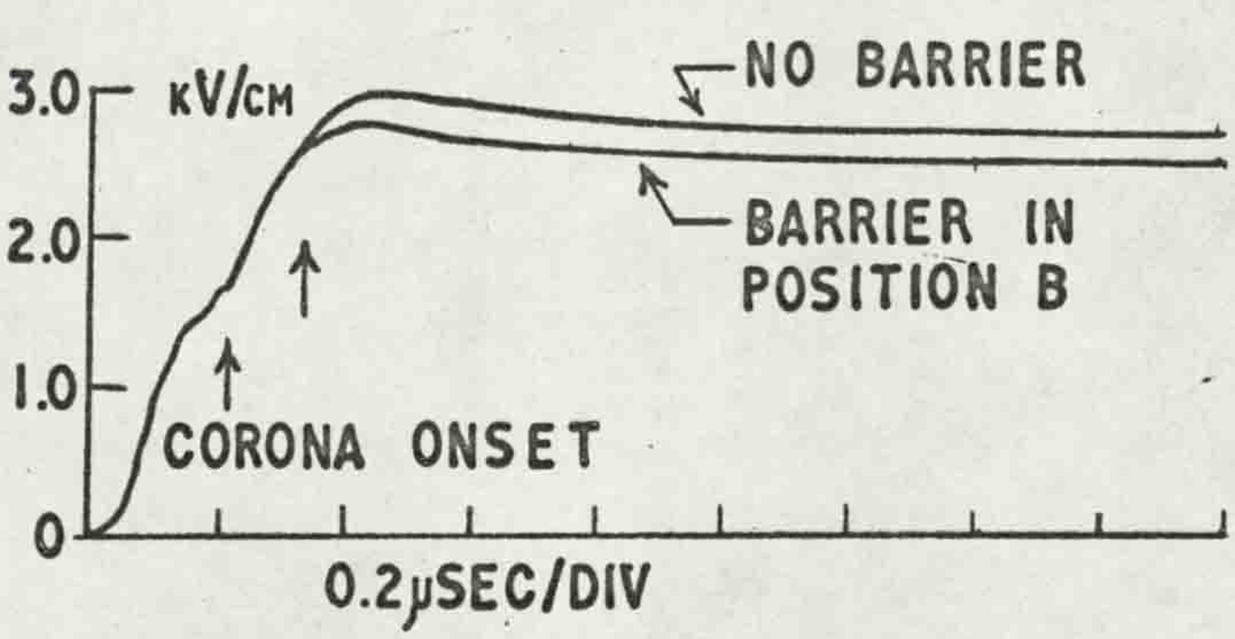

B
FIELD OSCILLOGRAMS

FIG. 39 EFFECT OF LIMITING HORIZONTAL GROWTH OF CORONA

The experiment confirms that the space charge does spread out along the barrier.

A further experiment to show the effect of corona, with an horizontal component of growth, on the field off the rod center-line was performed using the arrangement shown in Fig. 39A. The probe was situated 15 cm from the rod center-line and field oscillograms shown in Fig. 39B were obtained with the barrier in position A, with the barrier in position B and with no barrier. Again the first arrow shows the corona onset point and the second arrow shows the point of divergence of the two traces. The upper trace shows the field with no barrier and with the barrier in position A. Since the two were identical it was assumed that the decrease in the field with the barrier in position B, as shown in the lower trace, was due to the barrier stopping the horizontal development of the corona and not due to some other effect of the barrier. This shows that the space charge associated with the horizontal component of the corona contributes an appreciable amount to the field at a distance of 15 cm from the rod center-line.

(c) <u>Velocity measurement using barriers</u>

Since the barrier halts the forward growth of the corona filaments it was considered that this might provide

a method of measuring the velocity of the corona filaments. The technique used was to superimpose several oscillograms taken with barriers at various levels in the gap on an oscillogram taken with no barrier in the gap. The time interval between the start of corona and the point of deviation of the trace with a barrier from the trace without a barrier would then represent the time taken for the corona to travel from the rod to the barrier. This was done and sample oscillograms are shown in Fig. 40 taken with a barrier 5 cm below the rod, 11 cm below the rod and with no barrier. The oscillogram taken with no barrier went off scale since the sensitivity used was high. It was found that the time resolution was not sufficiently high to enable changes of velocity in the gap to be measured but the average value of 8.5×10^7 cm/sec $\pm$ 10% which was obtained is in general agreement with previously obtained results.[37,53] It is also in agreement with the value obtained by taking the time to cross the whole gap as the time from corona onset to the time of the peak field. This is a valid assumption since there was no evidence of a conduction current in the probe (which indicates the arrival of a corona filament at the plane) prior to the peak field. For the case illustrated above this gave an average velocity of 8.6×10^7 cm/sec $\pm$ 5%.

FIG. 40 USE OF BARRIERS TO DETERMINE CORONA FILAMENT VELOCITY

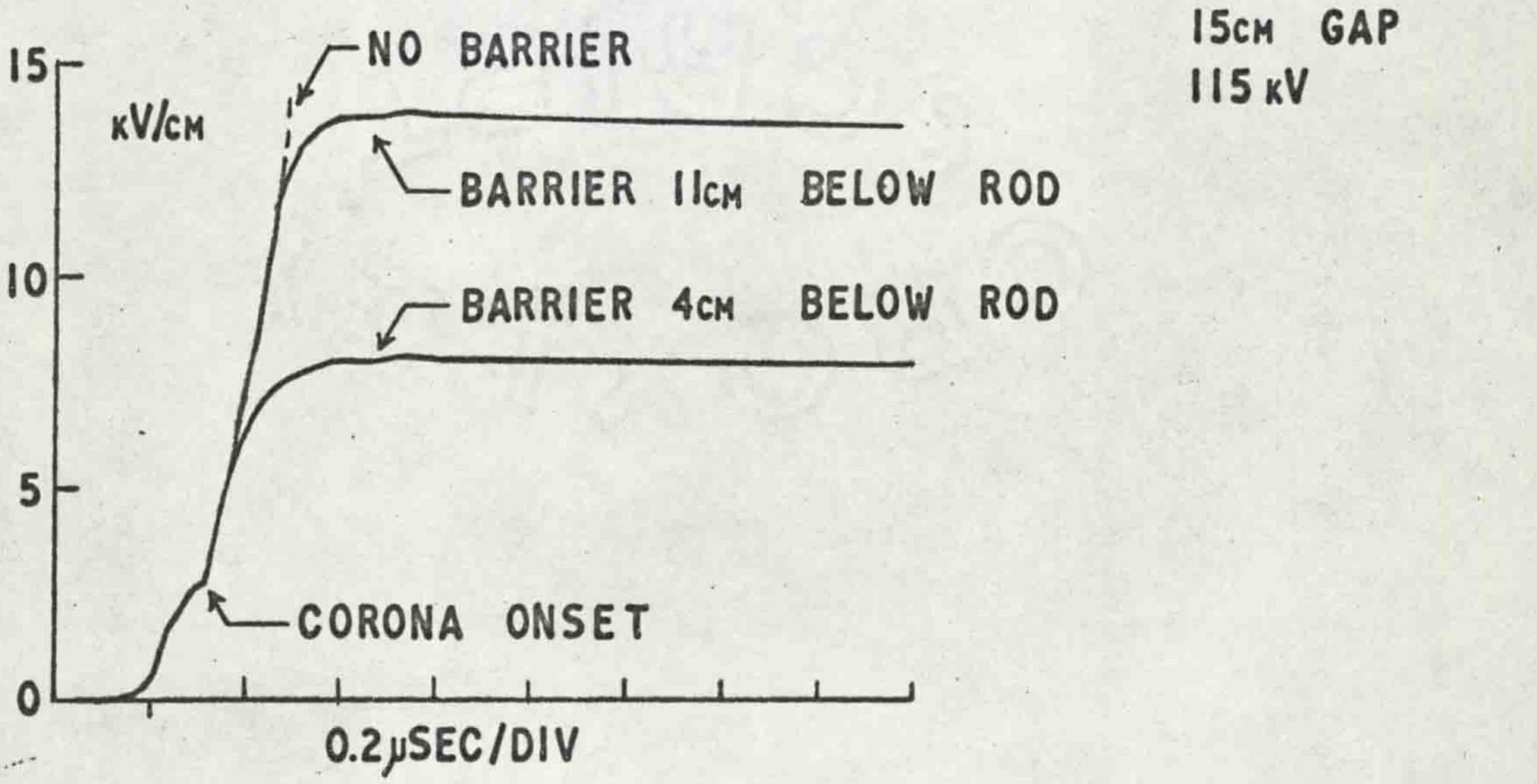

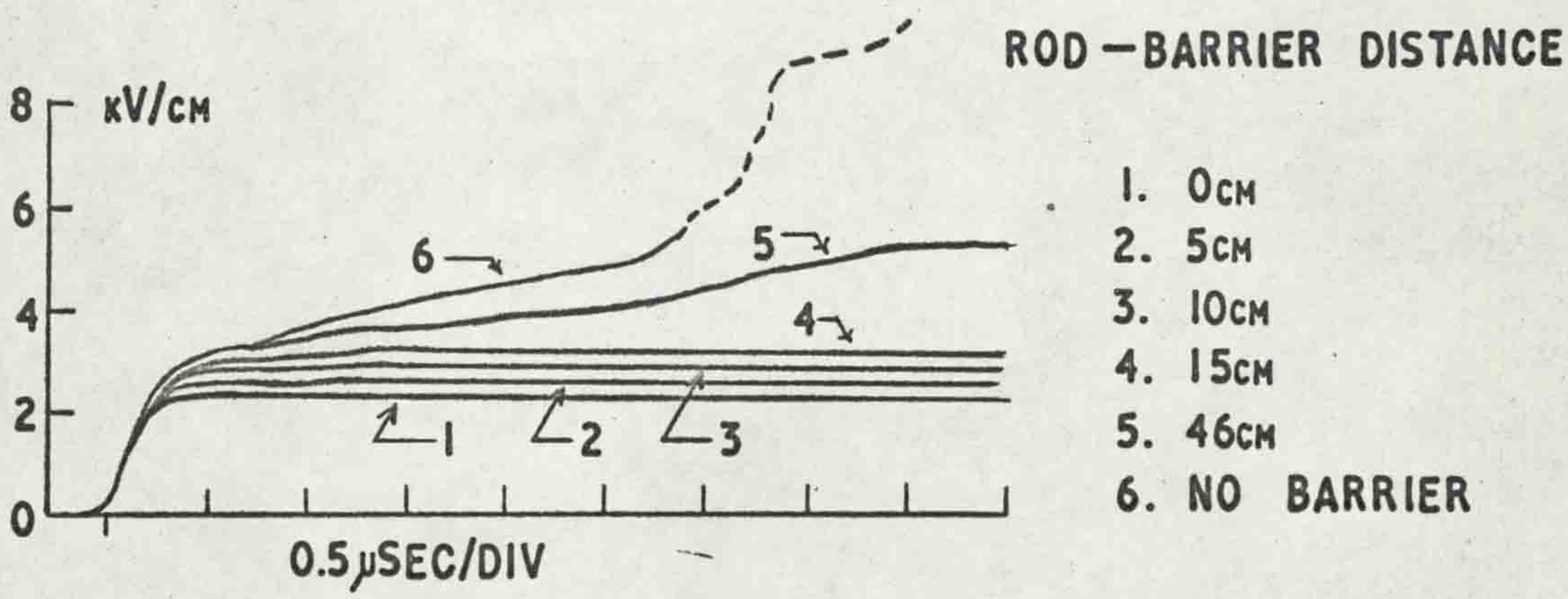

FIG. 41 FIELD AT THE PLANE WITH BARRIERS VARIOUS DISTANCES BELOW THE ROD

50cm GAP
240 kV

(iii) 50 cm gap

(a) Constant voltage, variable barrier height

Placing a barrier in a 50 cm gap affected the field by limiting the corona filament growth as it had done in the 15 cm gap. With an applied impulse voltage of 240 kV oscillograms were taken with a barrier at various distances below the rod with the results for a barrier 0, 5, 10, 15 and 46 cm below the rod and with no barrier shown in Fig. 41, traces 1 to 6 respectively. Field values obtained for these oscillograms are plotted in Fig. 42. The field exhibits an initial rise in the first $\frac{1}{2}\mu$sec followed by a more gradual rise to a peak value. When the barrier was at the rod the second rise did not occur and when the barrier was 20 cm or more from the rod the first rise was not affected which indicates that the first rise is due to space charge within 20 cm of the rod. The second rise was quite variable when the barrier was more than 20 cm from the rod so two points, one at 40 cm and the other at 46 cm from the rod, are included in the graph as examples where it can be seen that the second rise was either the same as it would have been with a barrier 20 cm from the rod or it was quite a high value which had a wide spread. From these results it is concluded that the initial corona propagates approximately 20 cm into the gap

FIG. 42 FIELD AT THE PLANE
-VS-
ROD-BARRIER DISTANCE

50CM GAP
240 KV

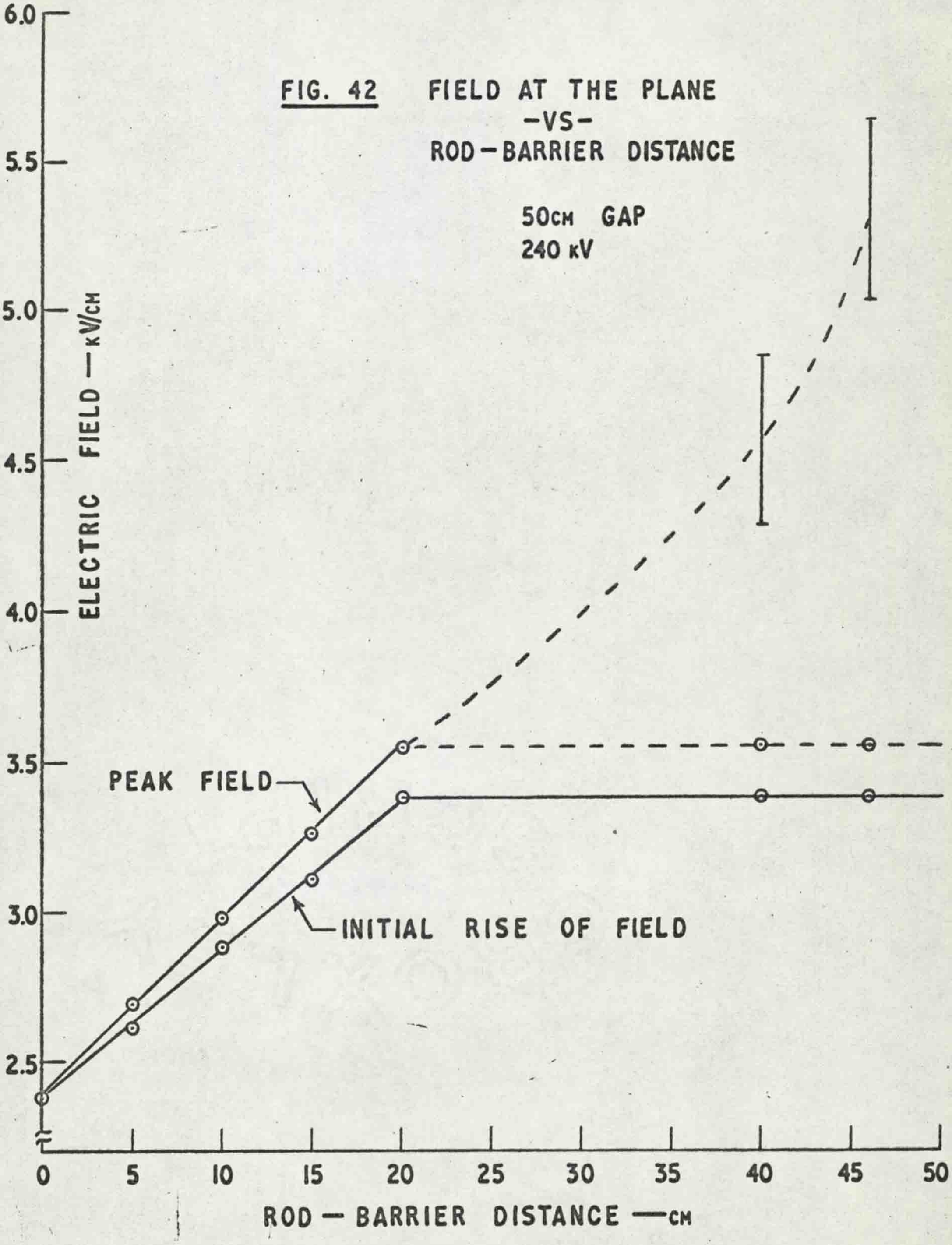

and stops while a slight redistribution of charge occurs. The redistribution of charge is probably caused by mid gap corona starting behind the leading corona filament tips. This may or may not increase the field sufficiently to enable the leading corona filament tips to begin further propagation into the gap but if it does the second discharge continues until it is stopped by the barrier. If a further discharge does not occur the field remains relatively constant after a small second rise.

(b) Variable voltage

In order to show the effect of a barrier on the field at the plane for various applied voltages the field was obtained as a function of applied voltage with a barrier at the rod and with a barrier 15 cm below the rod. These results are plotted in Fig. 43 along with the curve of Fig. 25 which shows the field with no barrier as a function of applied voltage. As before the lower straight line, curve 1, is the geometrical field extrapolated from low voltage measurements. Curve 2 is the field with a barrier at the rod which severely limits the corona growth, thus limiting the field at the plane. The field still rises considerably above the geometrical field because of the space charge which spreads out along the barrier. Curve 3 shows

FIG. 43 FIELD AT THE PLANE WITH BARRIERS

50CM GAP

1. GEOMETRICAL FIELD
2. BARRIER AT ROD
3. BARRIER 15CM BELOW ROD
4. NO BARRIER

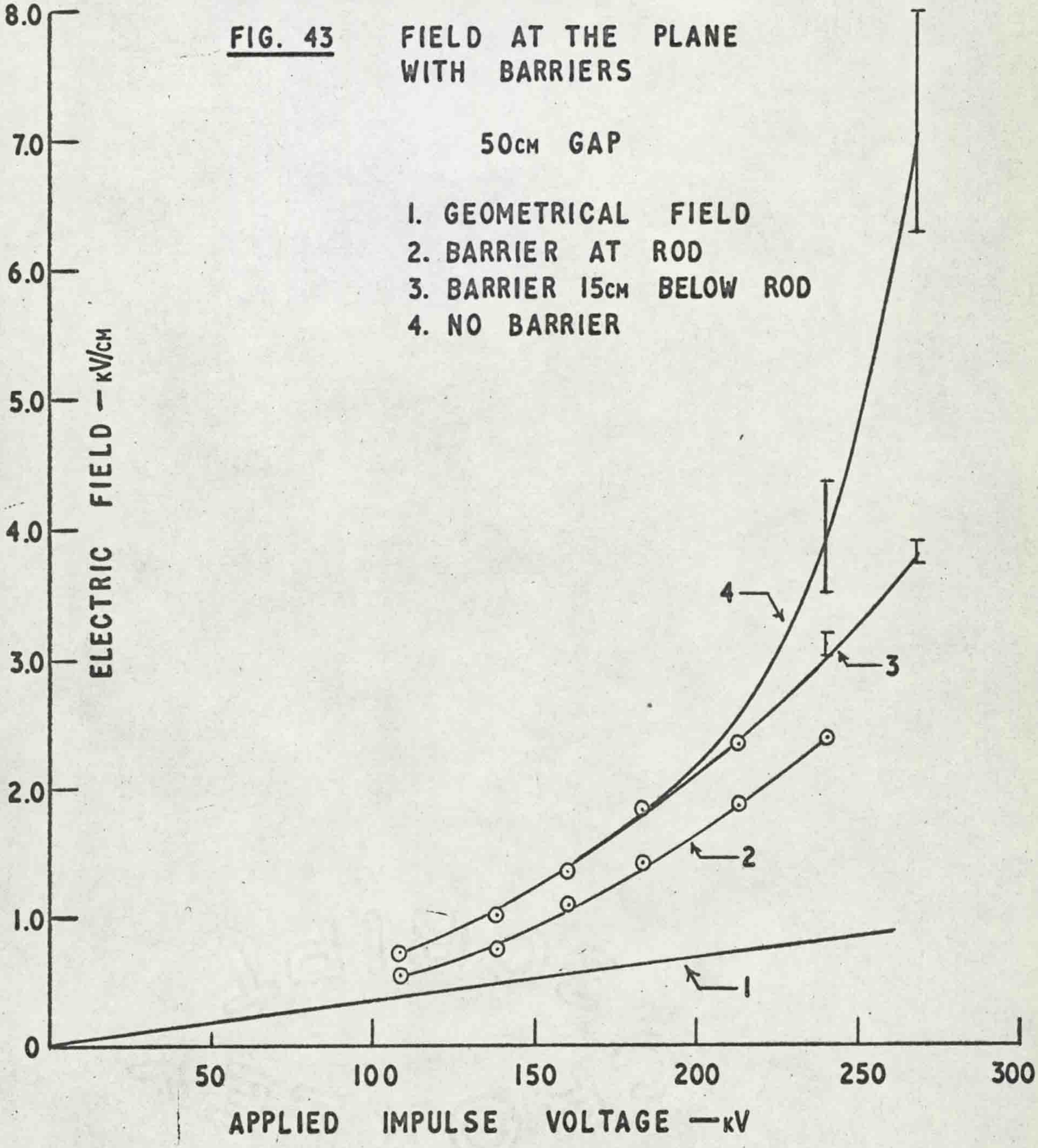

the field with a barrier 15 cm below the rod and curve 4 the field with no barrier. With the barrier 15 cm below the rod the field starts to be limited with an applied voltage of approximately 180 kV indicating that the corona at this voltage propagates about 15 cm into the gap.

(c) Barrier near the plane

With a barrier in the upper part of the gap the effect is to contain the space charge near to the rod which keeps the field at the rod low and prevents a further discharge from occurring. With a barrier in the lower part of the gap the space charge is able to propagate away from the rod so that even though the space charge is not neutralized at the plane the field at the rod rises sufficiently to initiate a further discharge. In this case the field between the barrier and the plane may reach a value sufficient to cause a spark between the plane and the bottom of the barrier or a spark may occur from the top of the barrier over the edge to the plane.

Fig. 44A shows the field under the rod for an applied impulse of 272 kV with a 0.64 cm thick bakelite barrier 1¼ cm above the plane. The field rises to a peak value of 30.2 kV/cm in 5.4 μsec and then collapses to 2.5 kV/cm

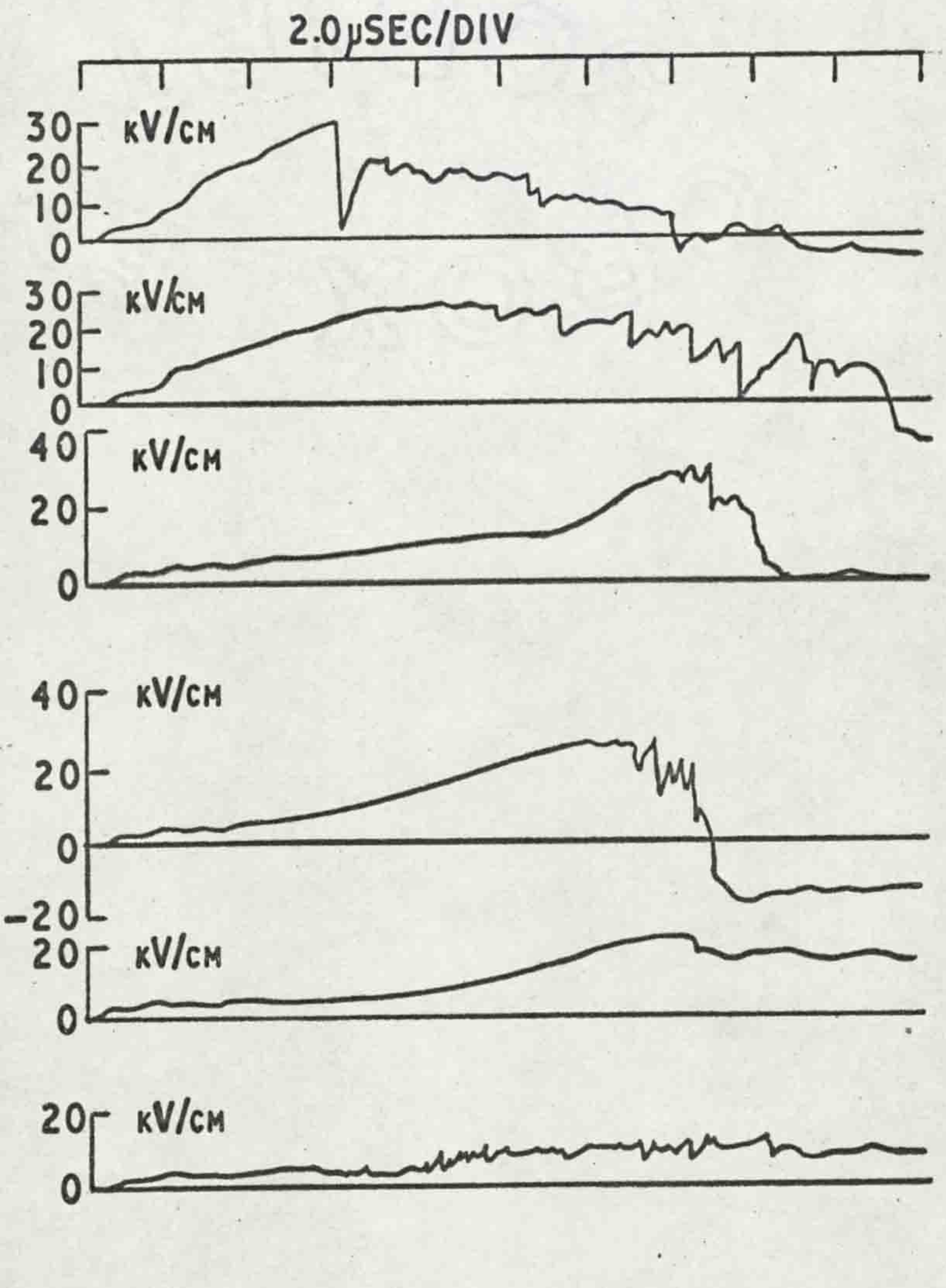

DISTANCE FROM ROD CENTER-LINE

A 0cm

B 10cm

C 25cm

D 25cm

E 25cm

F PROBE 1.5cm BEYOND EDGE OF BARRIER

FIG. 44 FIELD AT VARIOUS DISTANCES FROM THE ROD CENTER-LINE WITH A BARRIER 1.5cm ABOVE THE PLANE

50cm GAP
272 kV

when a discharge occurs between the barrier and the plane. This discharge is extinguished almost instantaneously (the time being too short to measure on the oscillogram) and the field recovers to 20.6 kV/cm. Further brief discharges occur away from the first discharge as a region of high positive space charge builds up away from the rod center-line. The build up of space charge is shown in Fig. 44B where the field 10 cm from the rod center-line rises to a crest of 26.0 kV/cm in 7.7 μsec and Fig. 44C where the field 25 cm from the rod center-line rises gradually to 12.3 kV/cm in 10.2 μsec and then more sharply to a crest of 28.5 kV/cm in a further 3 μsec. In each case the field falls after the crest is reached due to local discharges occurring between the plane and the barrier. In Fig. 44C the field falls to zero when the final breakdown occurs but this is not always the case. Fig. 44D shows the field at the same location but this time the field went negative after the final breakdown indicating an excess of negative charge had accumulated on the bottom of the barrier. If, on the other hand, the number of discharges is small in the region of the probe then the final field collapse leaves a positive value as shown in Fig. 44E due to the positive charge on the upper surface of the barrier. The

probe was then moved 1½ cm beyond the edge of the barrier and the result is shown in Fig. 44F. The field did not rise appreciably since there was no barrier above the probe on which the positive space charge could accumulate. The short sharp rises in field are due to corona filaments growing over the edge of the barrier and then being neutralized on the plane. The frequency of these filaments was such that more often than not the probe was struck by a filament so that a conduction current occurred making the remainder of the field oscillogram meaningless.

With the barrier 4¾ cm above the plane and an applied voltage of 298 kV, Fig. 45A was obtained. In this case only a few discharges occurred from the plane to the bottom of the barrier before the final breakdown occurred over the edge of the barrier. The field at the plane on the rod center-line reached a maximum value of 25.7 kV/cm in approximately 9.6 μsec and then as the final breakdown occurred it fell to a small negative value indicating the presence of some negative charge on the bottom of the barrier.

When the barrier was placed 10½ cm above the plane the field at the plane reached a value of only 13.5 kV/cm as shown in Fig. 45B. In this case there was no evidence of

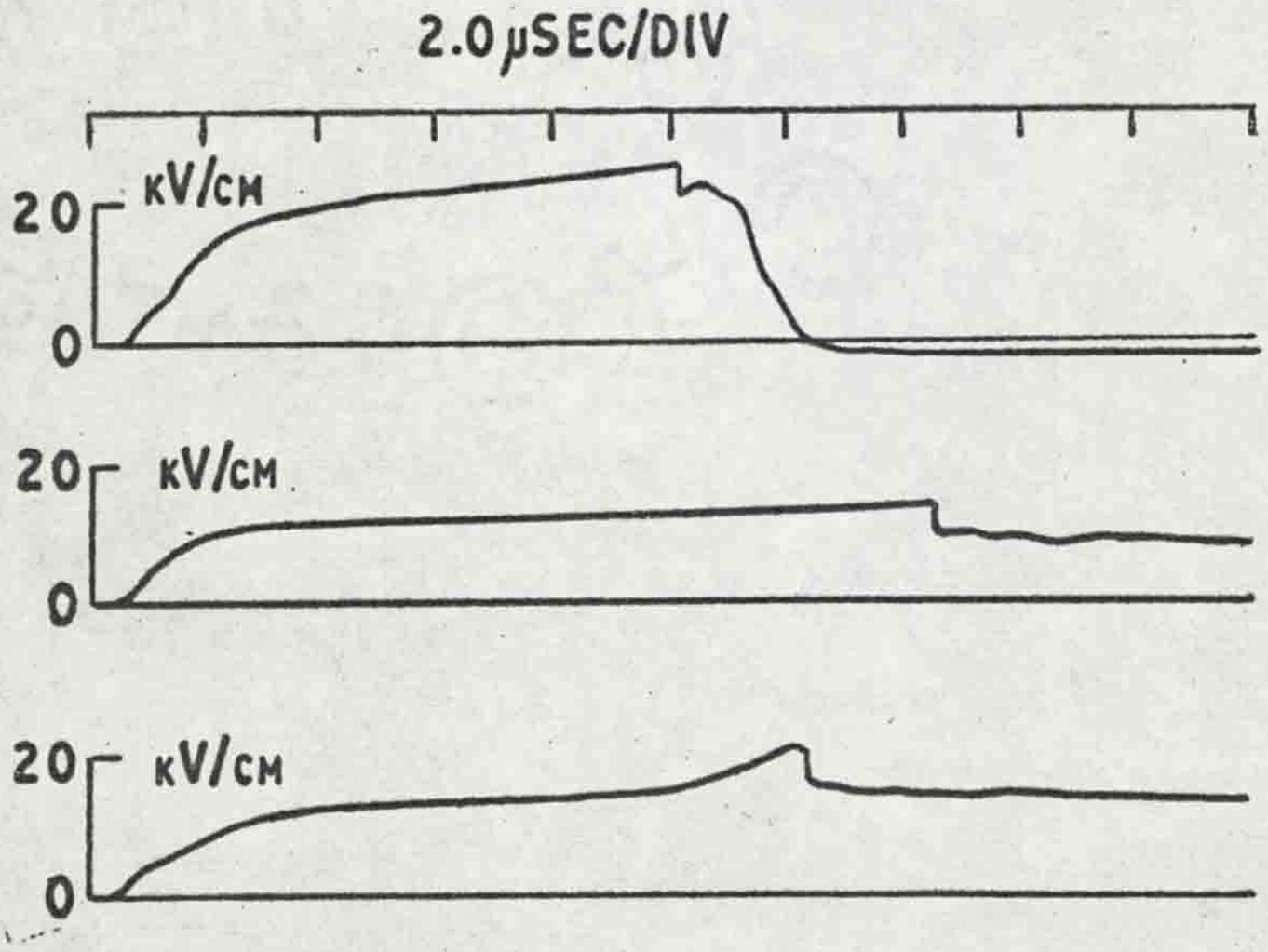

FIG. 45 FIELD ON THE ROD CENTER–LINE WITH VARIABLE BARRIER–PLANE DISTANCE

50 cm GAP

a discharge between the barrier and the plane. After approximately 16 μsec the final breakdown occurred and the field fell to 9 kV/cm which indicated that a considerable space charge remained on the barrier. This is explained by the fact that the discharge goes directly from the rod to the edge of the barrier and then to the plane instead of going from the rod to the center of the barrier, along the barrier to the edge and then to the plane. In the latter case the discharge along the barrier would remove a considerable amount of the space charge whereas in the former case the space charge would remain on the barrier. Applying a lower voltage to the gap with the barrier 4 cm from the plane also causes breakdown from the rod directly to the edge of the barrier. Fig. 45C shows the result with an applied voltage of 285 kV where the field rises to a crest of 20.3 kV/cm in 15.6 μsec and then falls to 14.7 kV/cm at breakdown.

IV. Lichtenberg Figures

(i) 15 cm gap

A further comparison of the three types of rod endings was made using Lichtenberg figures produced on X-ray film. For an applied impulse voltage of 78 kV, Fig. 46, 47 and 48

FIG. 46 LICHTENBERG FIGURE AT PLANE WITH THE ROD END A 30° CONE

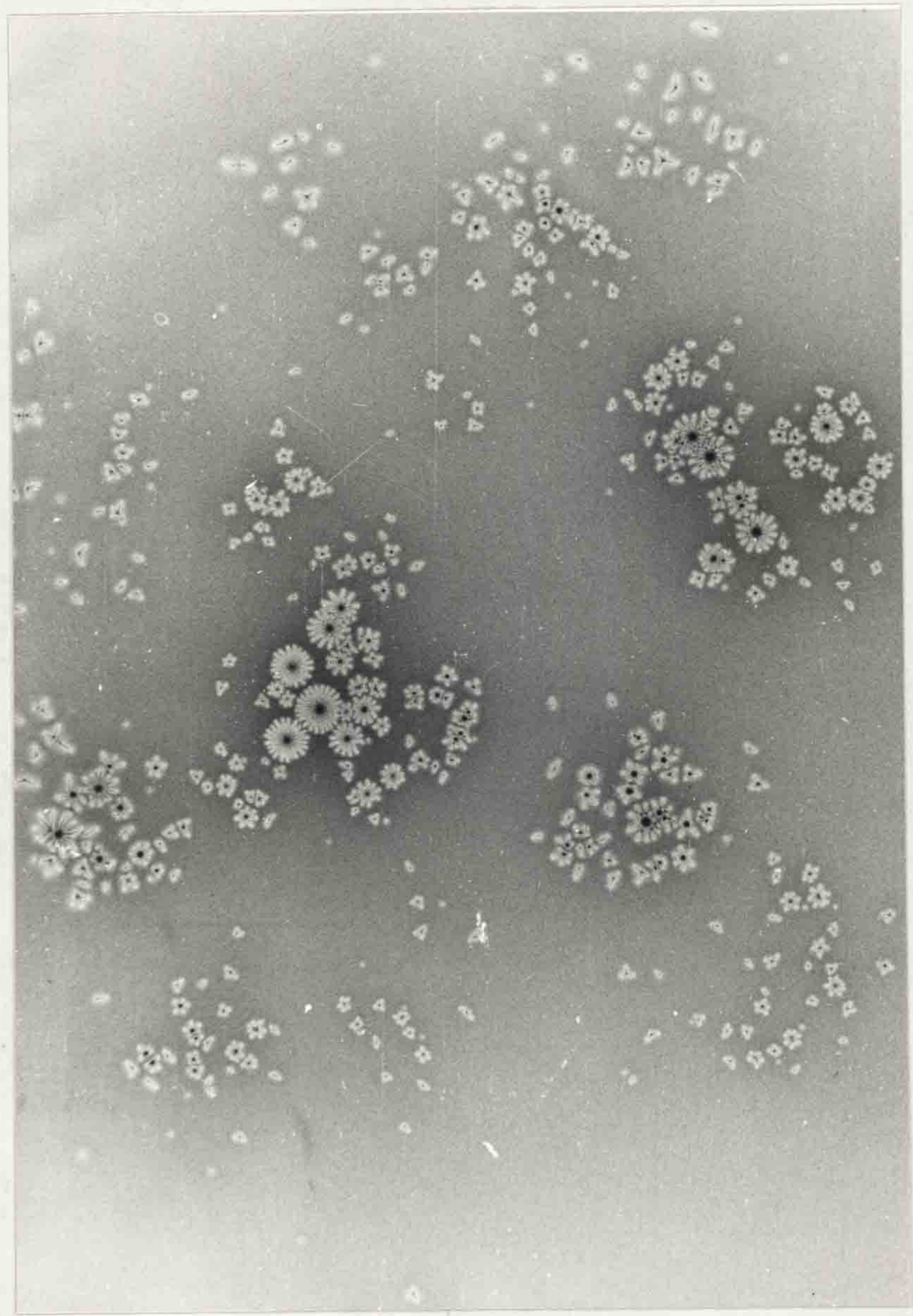

FIG. 47 LICHTENBERG FIGURE AT THE PLANE WITH THE ROD END SQUARE-CUT

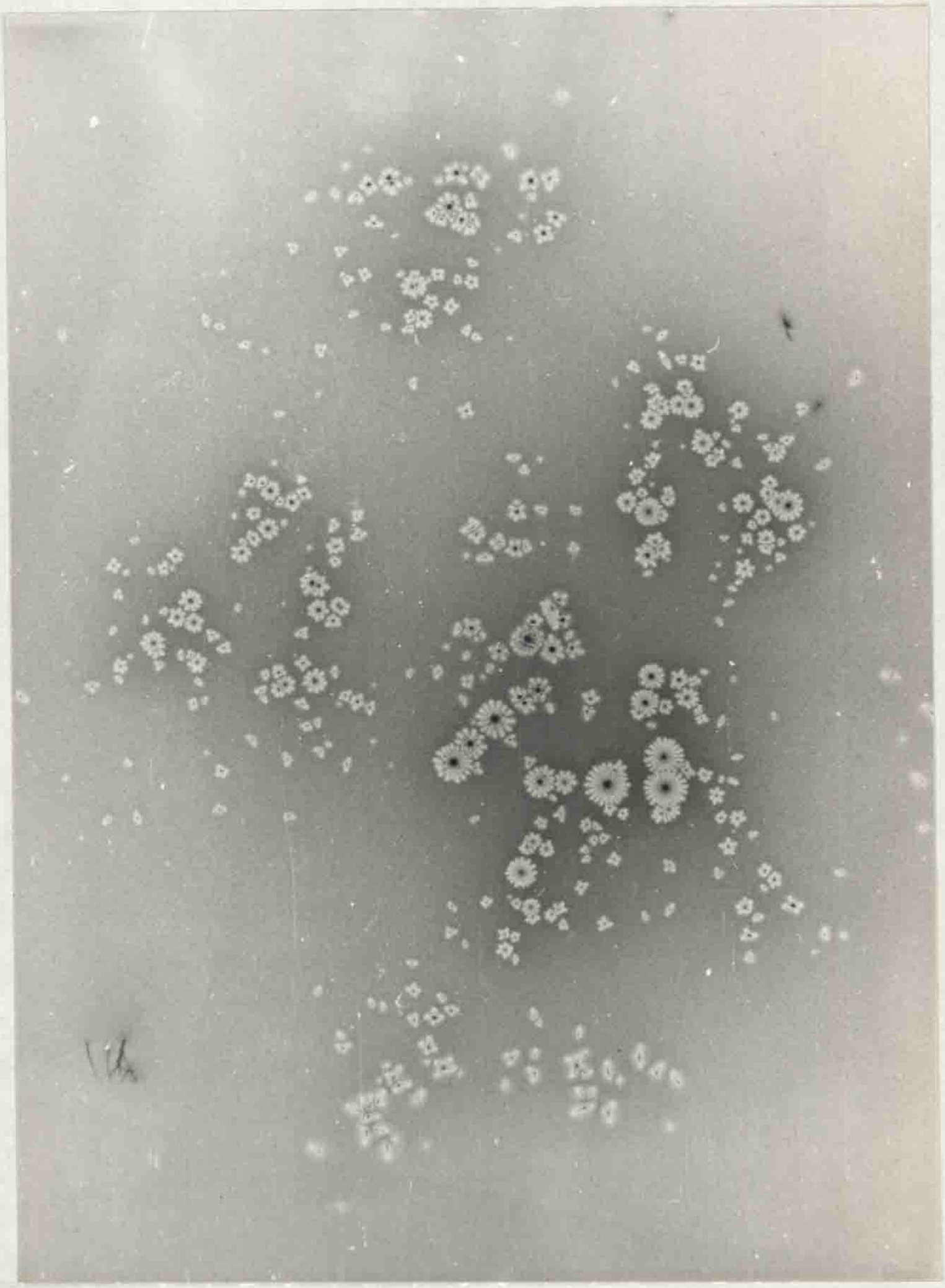

FIG. 48 LICHTENBERG FIGURE AT THE PLANE WITH THE ROD END HEMISPHERICAL

show the Lichtenberg figures at the plane for the 30° cone, the square-cut rod and the hemispherically ended rod respectively. The latter two are quite similar with between 400 and 500 individual figures which vary from dots less than ½ mm in diameter to dots of approximately 1 mm in diameter with up to 25 radial arms giving an overall diameter of up to 9 mm. For the 30° cone the number of figures was between 70 and 100 with a maximum size of 8 radial arms giving an overall diameter of 4.5 mm. This shows that the higher field obtained with the square-cut and hemispherically ended rods was due to a larger number of filaments approaching the plane.

Fig. 49 and 50 show Lichtenberg figures obtained 6 cm above the plane for the square-cut and hemispherical ends respectively. Again the two are similar but they differ from those obtained at the plane in that there are a number of individual figures with long branches up to 5½ cm in length. These long branching figures are produced by the filaments that would have produced figures at the plane had they not been deflected by the barrier. At this level the number of individual figures was again between 400 and 500 which indicated that the number of branches forming was approximately the same as the number

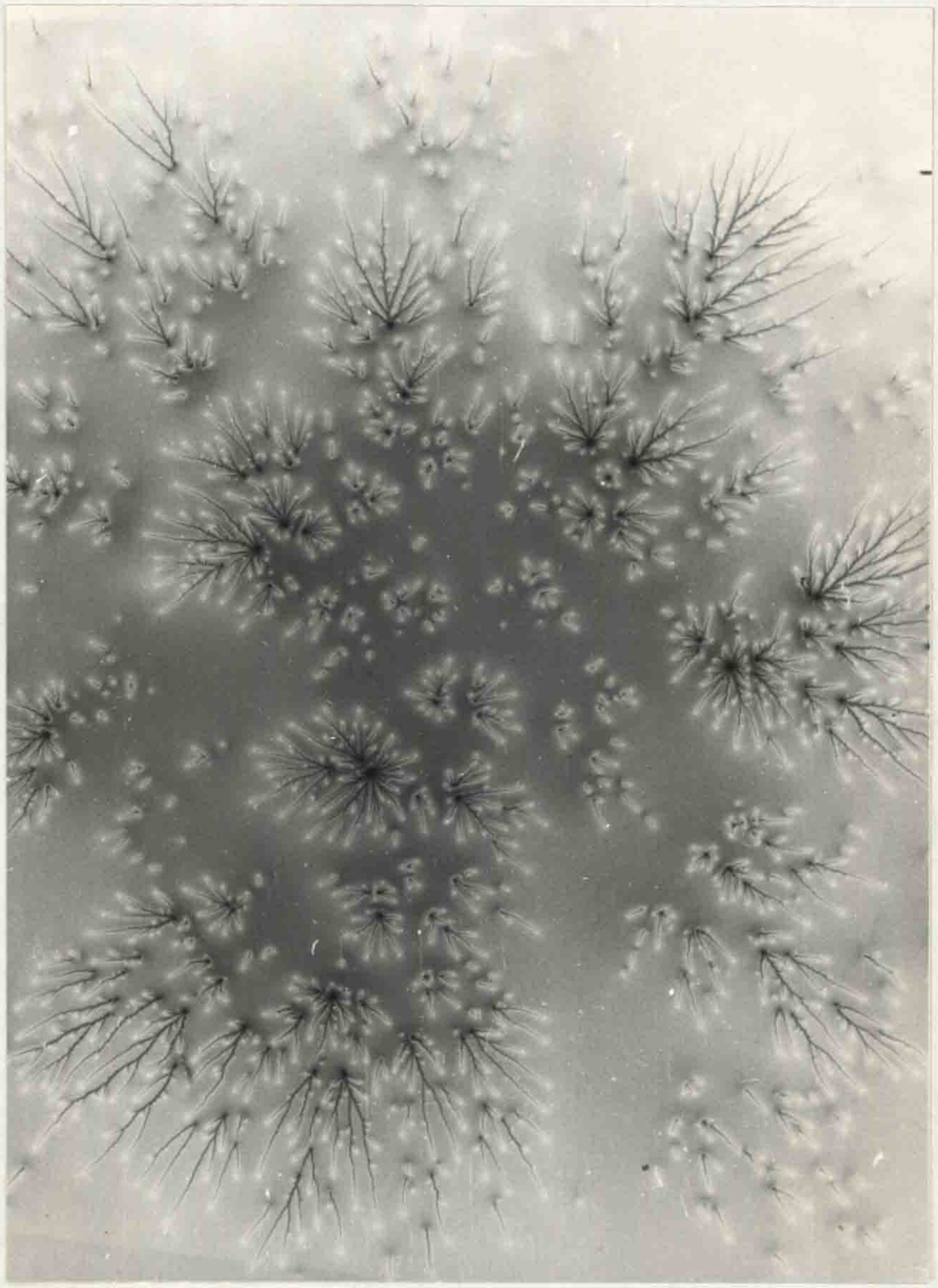

FIG. 49 LICHTENBERG FIGURE 6 cm ABOVE THE PLANE WITH THE ROD END SQUARE-CUT

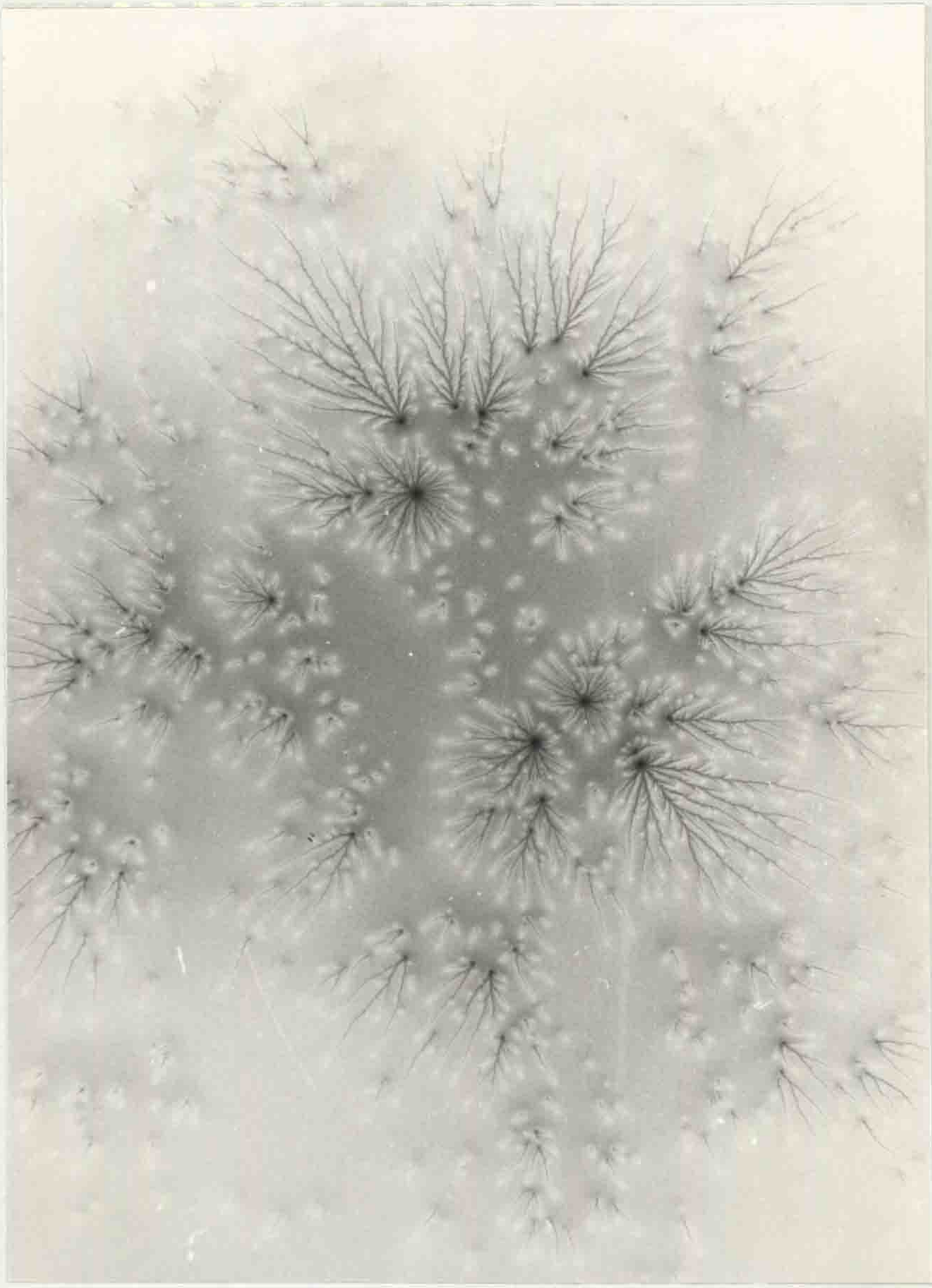

FIG. 50 LICHTENBERG FIGURE 6 cm ABOVE THE PLANE WITH THE ROD END HEMISPHERICAL

of branches which were dying out. The fact that filament branches were dying out 6 cm above the plane was confirmed by the occurrence of the very small individual figures at that level.

Lichtenberg figures were obtained with the film 12 cm above the plane in Fig. 51, 52 and 53 for the square-cut end, the hemispherical end and the 30^{o} cone respectively. All three show the tendency to have several strong figures at the center with branching towards the edges extending for over 12 cm in the first two cases and up to 10 cm in the third case. There are also a few of the very small point figures which indicate the presence of very weak filament branches which are dying out at this level.

In the central region of the Lichtenberg figures a distinct difference is seen between the square-cut end and the hemispherical end. For the square-cut end the filaments start at several points on the edge and due to their mutual repulsion tend to leave a clear space in the center. With the hemispherical end the highest field is in the center so the corona starts there and branches from a central filament which does not leave a clear area in the center. In this respect the 30^{o} cone is similar to the hemispherical end.

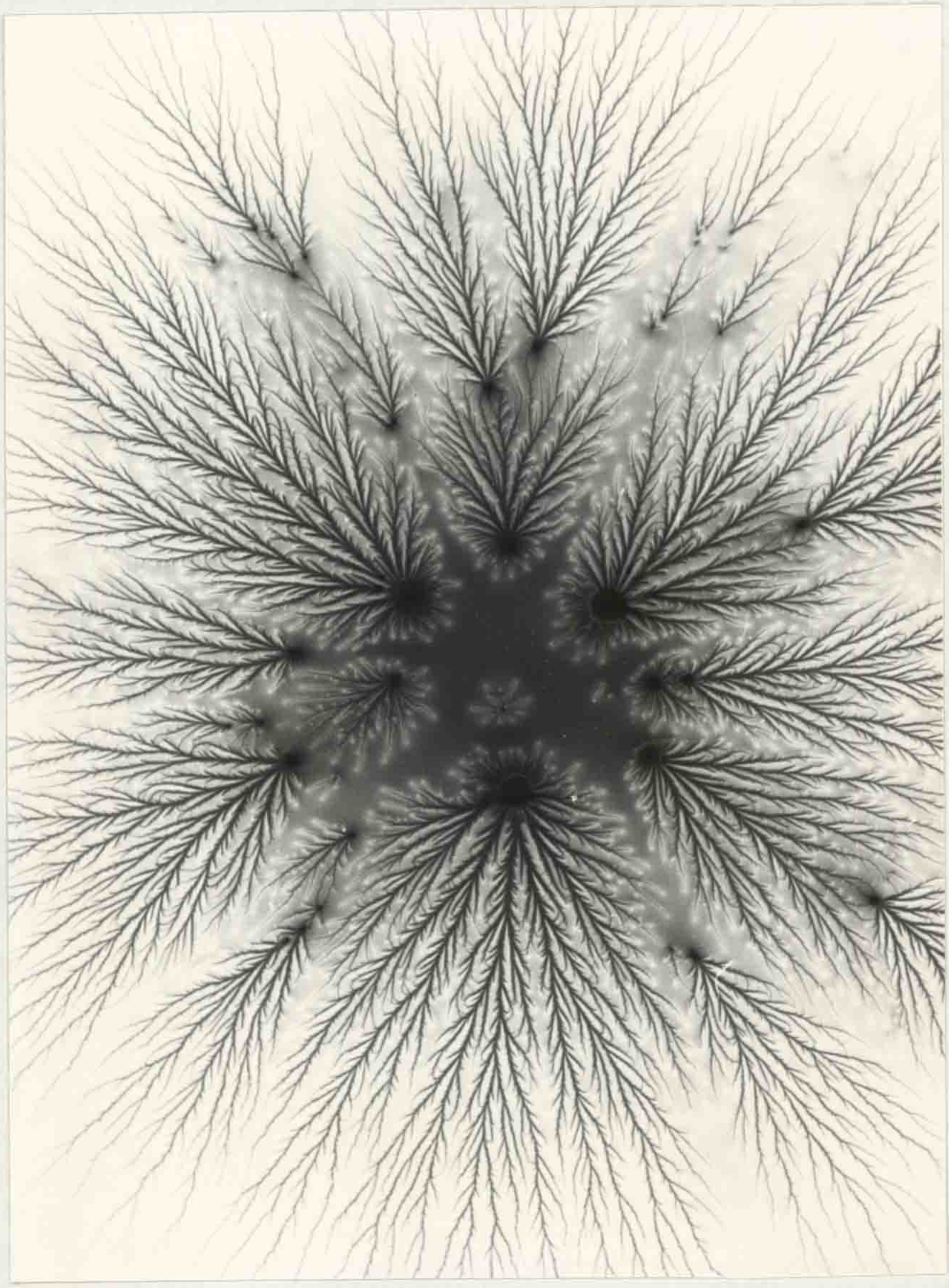

FIG. 51 LICHTENBERG FIGURE 12 cm ABOVE THE PLANE WITH THE ROD END SQUARE-CUT

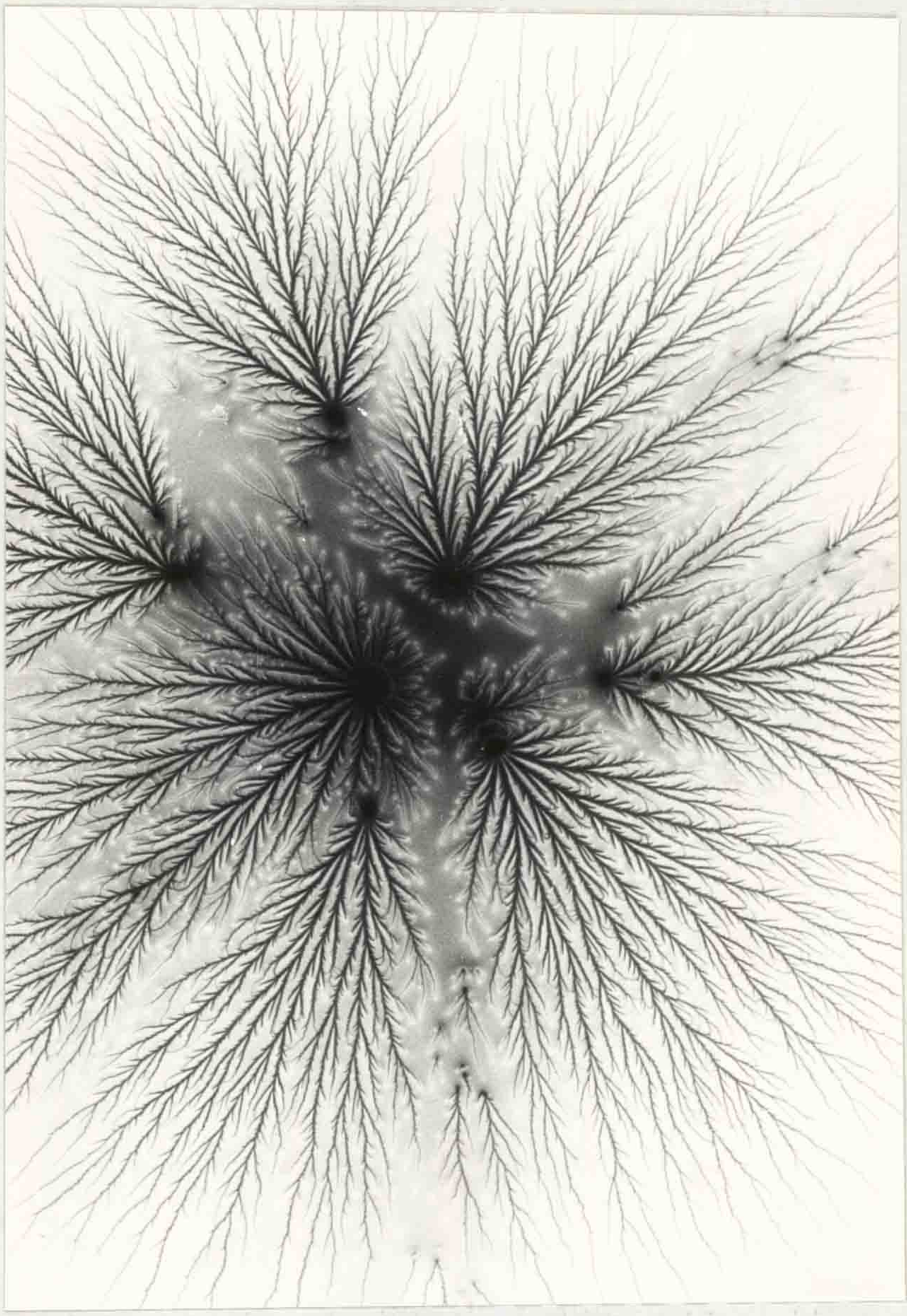

FIG. 52 LICHTENBERG FIGURE 12 cm ABOVE THE PLANE WITH THE ROD END HEMISPHERICAL

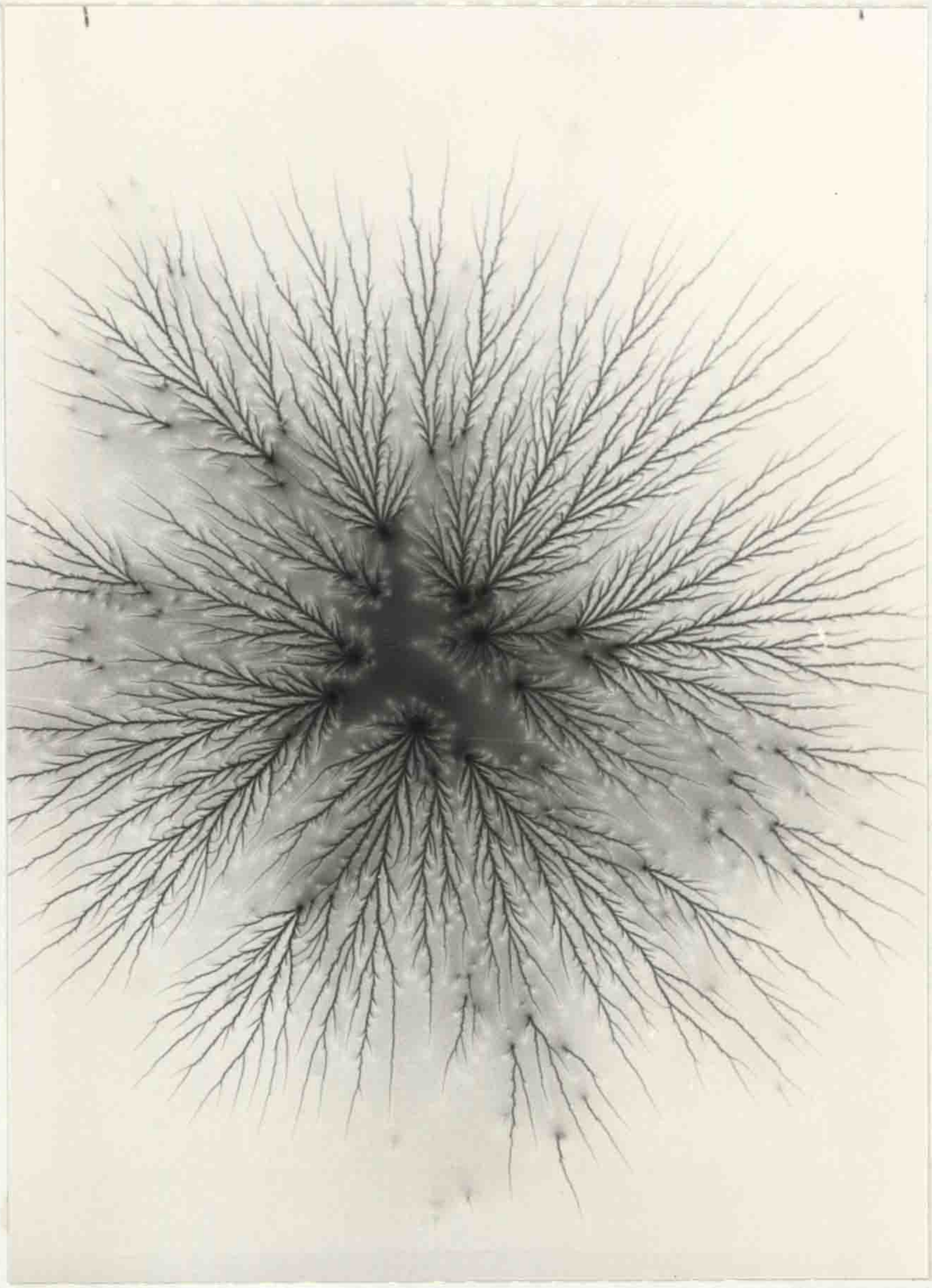

FIG. 53 LICHTENBERG FIGURE 12 cm ABOVE THE PLANE WITH THE ROD END A 30° CONE

(ii) Long Gaps

For the longer gaps it was not practical to use X-ray film to obtain Lichtenberg figures because of the large sizes required. Instead, Xerox powder on perspex was used to obtain the figures which were mainly used to determine how far the filaments progressed into the gap and how many reached the plane. In a 50 cm gap with an applied voltage of 240 kV the filaments spread horizontally approximately 20 to 25 cm which agrees with the initial corona filament growth deduced for barrier experiments outlined in Section III-(iii)-a. This shows that the space charge is in a cylindrical volume rather than a hemispherical volume as was the case for the 15 cm gap. The space charge was also shown to be in a roughly cylindrical volume for the 2 m gap by placing vertical barriers at various horizontal distances from the rod. For an applied impulse of 990 kV Lichtenberg figures showed that corona filaments reached the plane but only extended 75 to 100 cm in the horizontal direction. The exact extent of the corona in the horizontal direction could not be determined as the Lichtenberg figures on the vertical barriers were very faint, unlike those obtained on a horizontal barrier which were very clear. Better

sensitivity could no doubt be obtained using X-ray film but the problem of shielding the film from external light outweighed the advantage of increased sensitivity since the exact extent of the corona was not significant.

V. Measurement of Charge in Corona Filaments

Although the field measuring technique required that the current in the probe be purely a displacement current it was found that a conduction current to the probe was also useful in providing a measure of the charge associated with a corona filament.

With a 50 cm gap a $\frac{3}{4}$ mm diameter probe was constructed and mounted in the plane. The small size of the probe ensured that only one filament hit the probe at any one time and also made the voltage due to the displacement current small enough to be negligible compared with the voltage due to the conduction current. The results using this probe are shown in Fig. 54 and 55. Fig. 54 shows two oscillograms plotted as a percentage of full value against time, one being a charge of 2.24×10^{-10} coulombs and the other being a charge of 1.05×10^{-9} coulombs. From this it is seen that the larger charge takes longer to flow onto the probe. Fig. 55 shows four

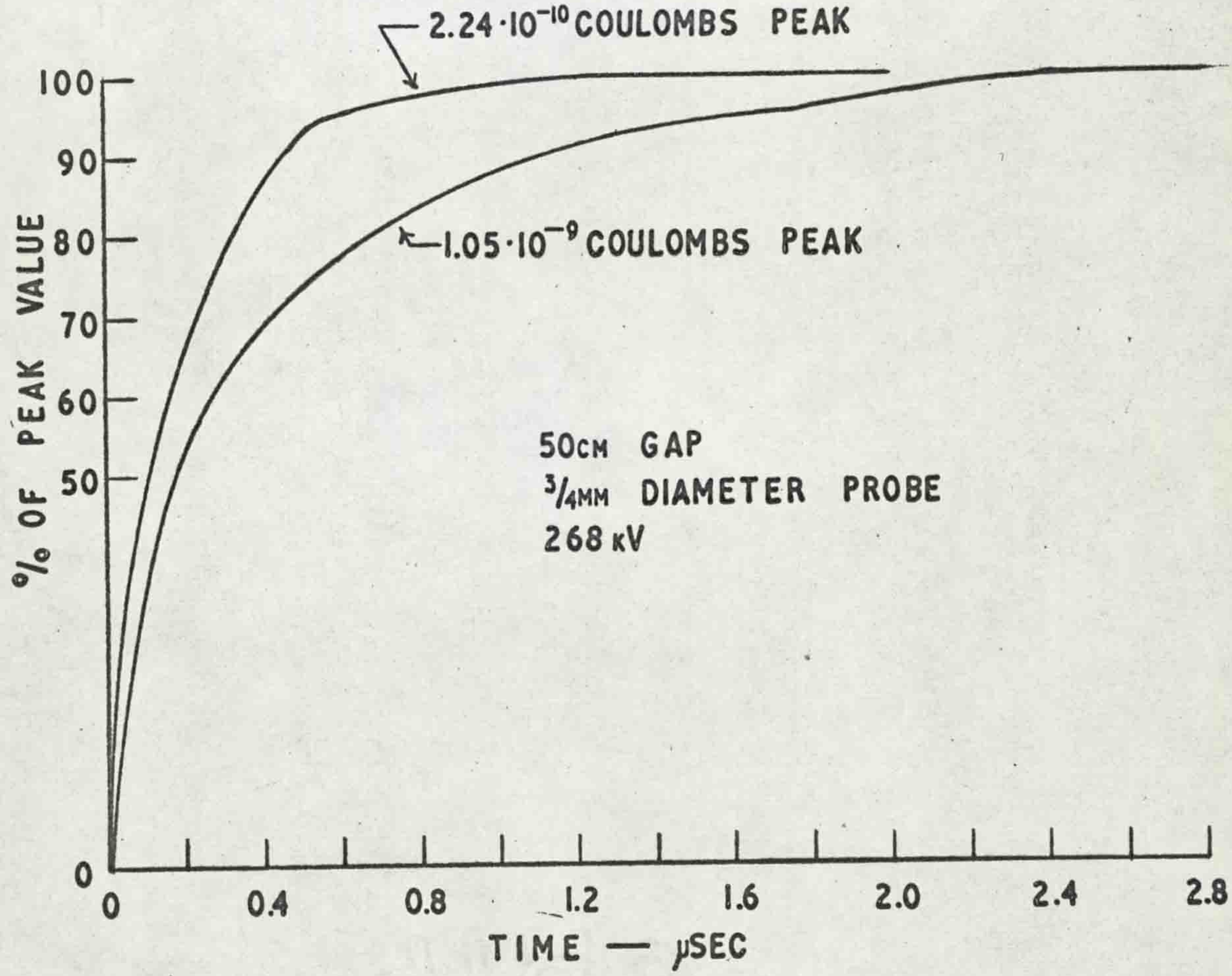

FIG. 54 CHARGING OF FIELD PROBE WHEN HIT BY A CORONA FILAMENT

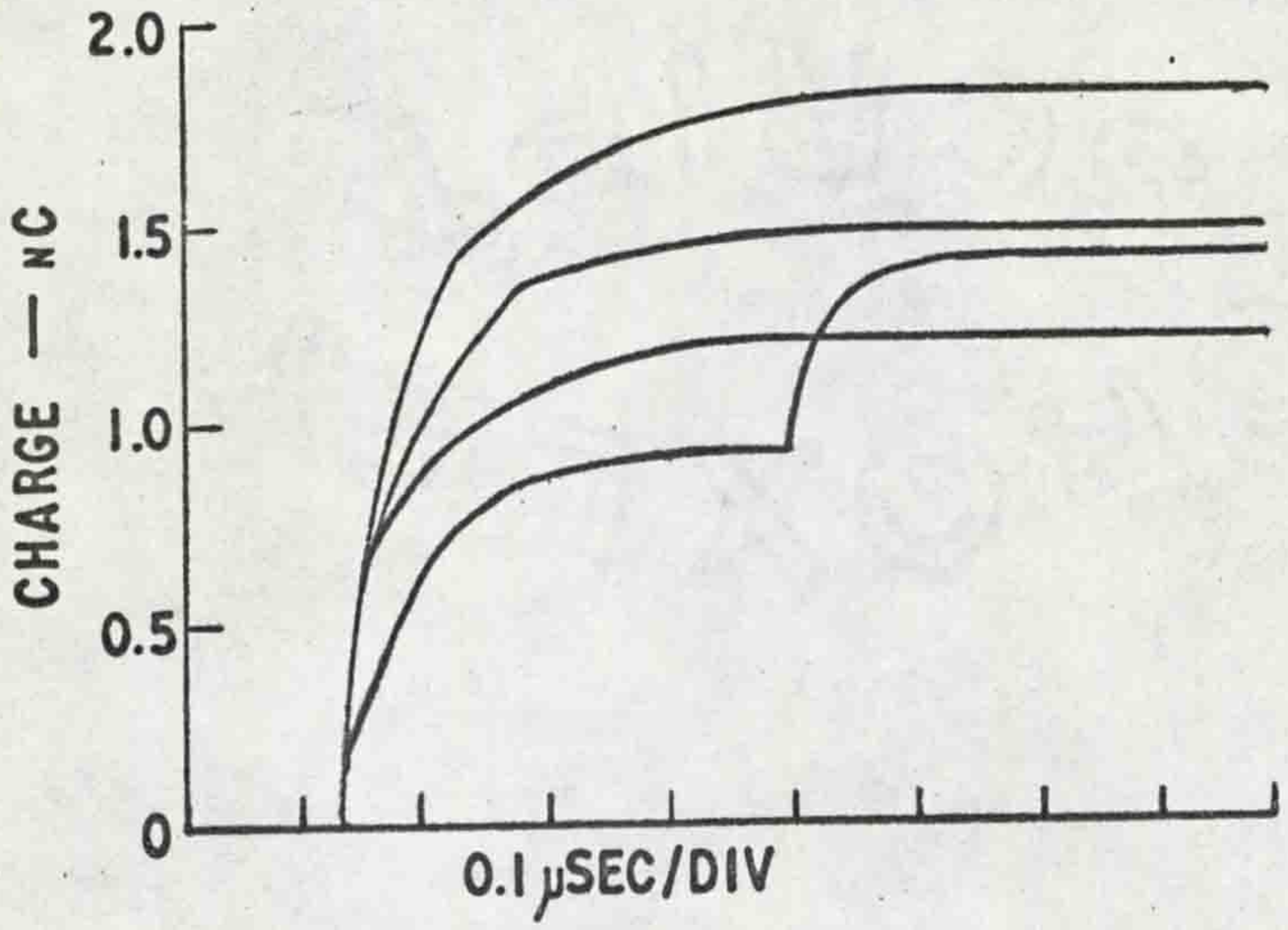

FIG. 55 CHARGING OF A 3/4MM DIAMETER PROBE WHEN HIT BY A CORONA FILAMENT. 4 SHOTS SUPERIMPOSED

50CM GAP
273 KV

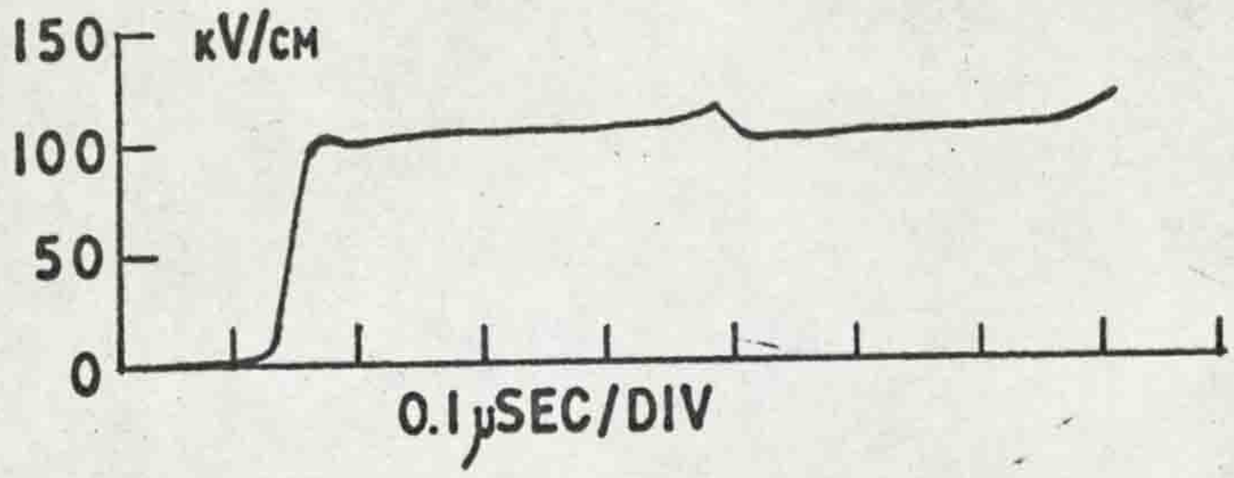

FIG. 56 FIELD ON A 2MM DIAMETER PROBE WHEN COVERED BY A 0.05MM BARRIER

25CM GAP
166 KV

oscillograms superimposed representing charges ranging from 9.00×10^{-10} coulombs to 1.77×10^{-9} coulombs. The second step on the lower oscillogram represents a charge of 5.10×10^{-10} coulombs. These oscillograms also show that in general the higher the step the longer the time required for the step to reach its maximum value. If this charge came solely from the head of a corona filament one would expect the times to be much more consistent. Therefore it would appear that the charge is coming from the channel behind the head as well as from the head of the corona filament. The brightening of the channel at the plane as observed by Park and Cones[32] and the "return globule" observed by Kritzinger[54] would be consistent with the charge being drawn from the channel. The double step on one oscillogram also suggests charge being drawn from the same channel in both steps. Since the probe was only $\frac{3}{4}$ mm in diameter it was hit in only one shot out of about 20 so that the chance of it being hit more than once in a single impulse unless the same channel were used seems quite remote. Further evidence supporting this is shown in Fig. 56 which is an oscillogram taken using a 2 mm diameter probe covered by a 0.05 mm thick polythene barrier. The slight rounding at the start is due to the induced

current as the filament approaches the plane. When the filament tip hits the barrier there is a step in the oscillogram but the sharp cut-off indicates no build up of charge on the barrier from the channel behind the tip. This is because the charge on the barrier prevents a high field from building up due to the charge in the channel which would occur if the charge in the tip had been neutralized on the plane. Similar results were obtained for 15 cm and 100 cm gaps so it was assumed that the gap length did not affect the charge on the corona filament.

Using a 100 cm gap with an applied voltage of 503 kV and using the 2 mm diameter probe, 20 shots were taken to determine the minimum value of charge hitting the probe which was 5.36×10^{-11} coulombs. The probe was then covered with a perspex cup so that the charge could not come within 0.14 mm of the probe and another 20 shots taken which gave a minimum value of field of 15.5 kV/cm. These two values were assumed to pertain to a corona filament just capable of reaching the plane and from calculations shown in Appendix I in which the charge is assumed to be in a spherical volume the radius of the volume was found to be 0.064 mm. The excess positive charge was found to be 3.35×10^{8} ions which gives an excess charge density of 3×10^{14} ions/cc.

Dawson and Winn[51] in their streamer propagation model give the minimum conditions for the propagation of a filament as a radius of 0.03 mm and an excess of charge of 10^8 ions. This is quite reasonable agreement and as the experimental values are higher it could be expected that a lower value might be obtained if more than 20 shots had been taken.

VI. Negative Rod-Positive Plane

(i) 50 cm gap

The negative rod-plane results differed in several respects from the positive rod-plane results, the most noticeable difference being the higher voltage required to cause breakdown for the negative case. Field measurements at the plane on the rod center-line show that the field is much lower for the negative case and the field value was much more consistent up to the point where a second discharge occurred. Fig. 57 shows the field as a function of voltage in curve 1 and the geometrical field in curve 2. The field is only that due to the first discharge and it was found that if several shots at the same voltage were superimposed on one oscillogram it was not possible to detect any difference in the initial field

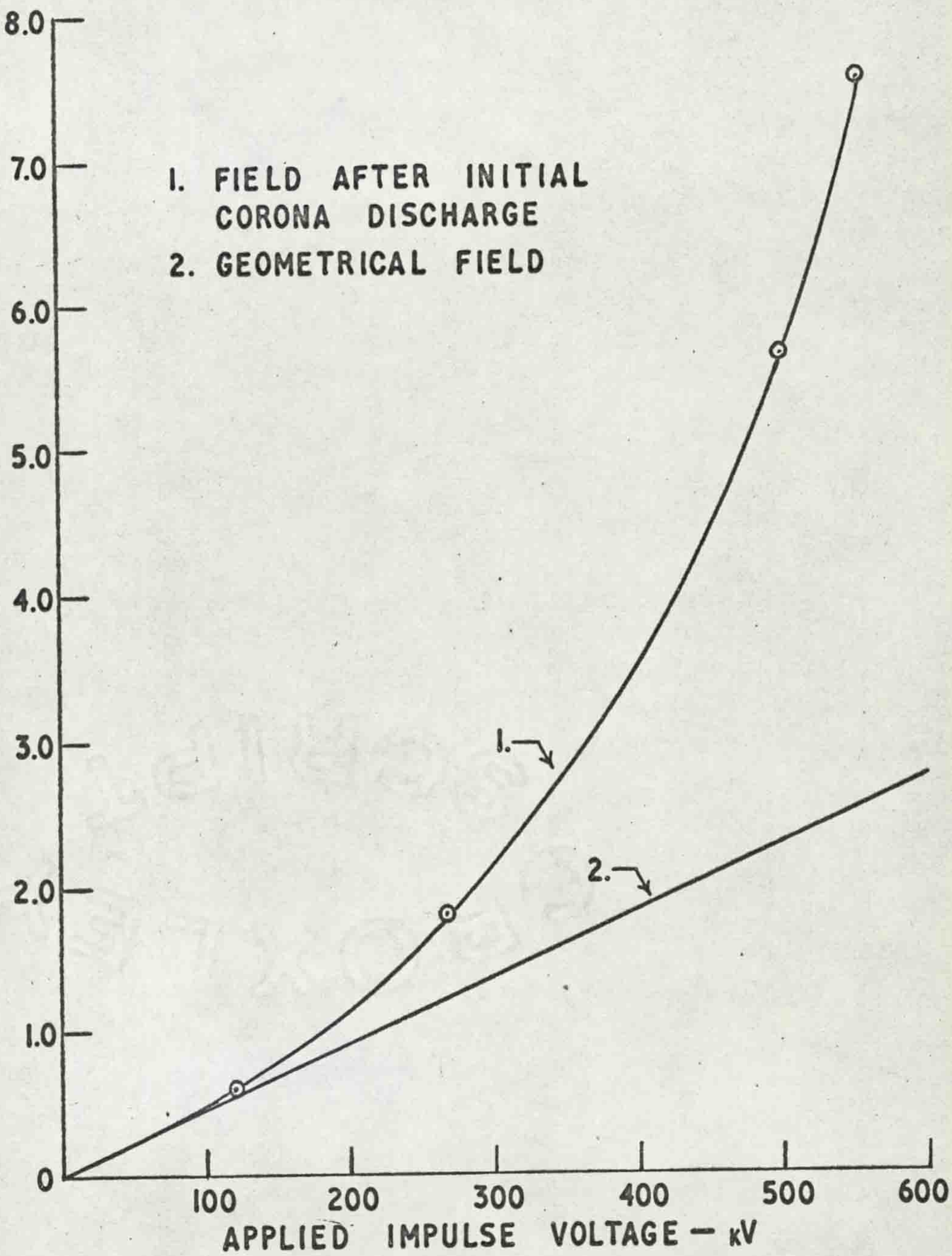

FIG. 57 FIELD AT THE PLANE WITH A NEGATIVE ROD

50CM GAP

rise. Example oscillograms are shown in Fig. 58. Fig. 58A shows the field with an applied voltage of 500 kV when no second discharge occurs. The rise time is, within the measuring limits, the same as that of the voltage wave which indicates that the corona pulse is very short and is over before the voltage crest is reached which is less than 0.5 μsec. Fig. 58B shows the field with an applied voltage of 510 kV and in this case a second discharge occurs causing a second rise in field.

The field distribution along the plane was measured at several voltages and the results are shown in Fig. 59. The values have all been converted to a 500 kV base so that the differences in amplitude are due to a change in space charge. As the voltage is raised the shape of the field distribution, shown in Fig. 60, with the values converted to a common peak amplitude, does not change greatly which is consistent with results obtained using Lichtenberg figures showing that the initial corona is confined to the upper part of the gap with a maximum extent of approximately 20 to 25 cm when 555 kV is applied.

Lichtenberg figures formed on barriers in the lower part of the gap showed that the second discharge consisted of a small number of corona filaments, which grew into the

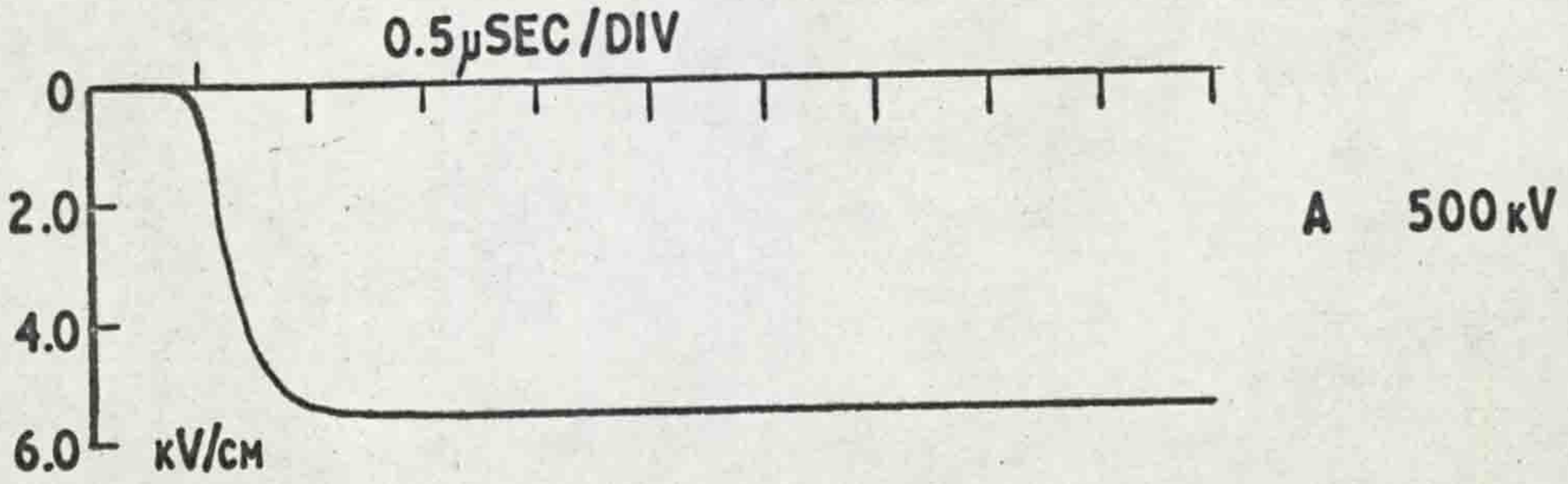

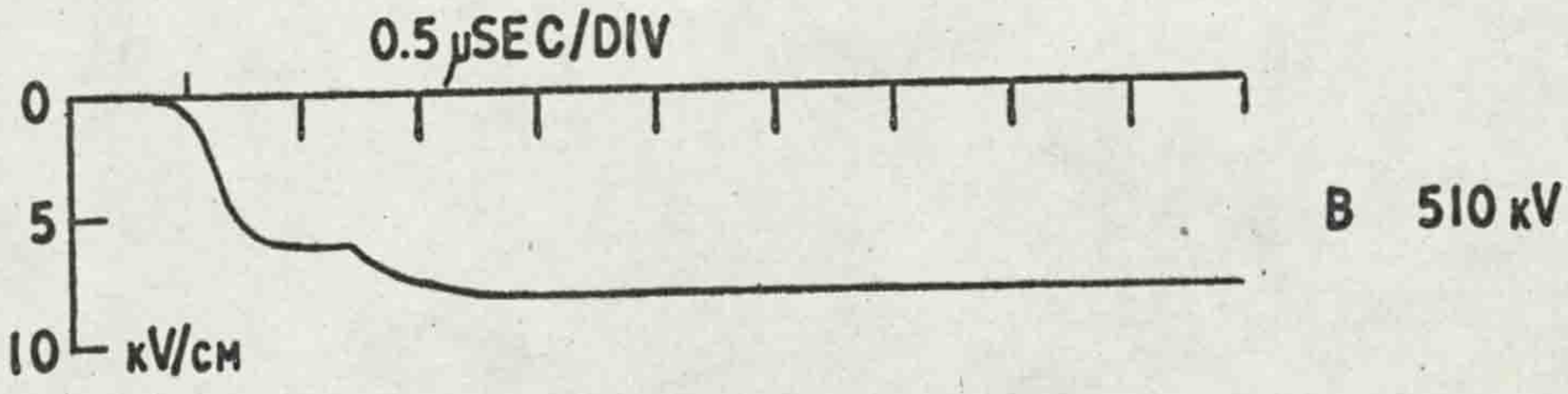

FIG. 58 FIELD AT THE PLANE WITH A NEGATIVE ROD

50cm GAP

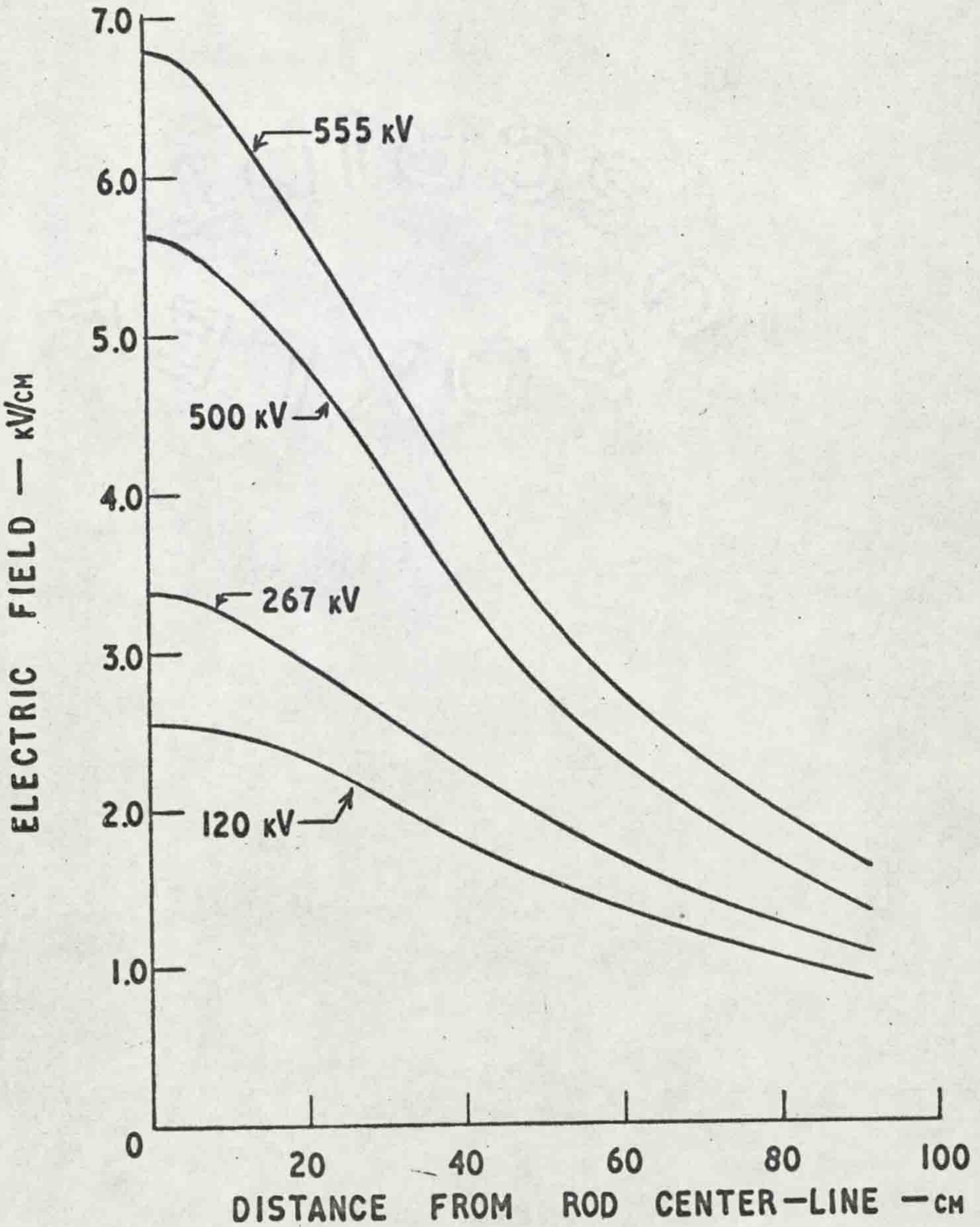

FIG. 59 FIELD DISTRIBUTION ALONG THE PLANE WITH A NEGATIVE ROD. FIELD VALUES CONVERTED TO A COMMON BASE OF 500 kV APPLIED IMPULSE

50cm GAP

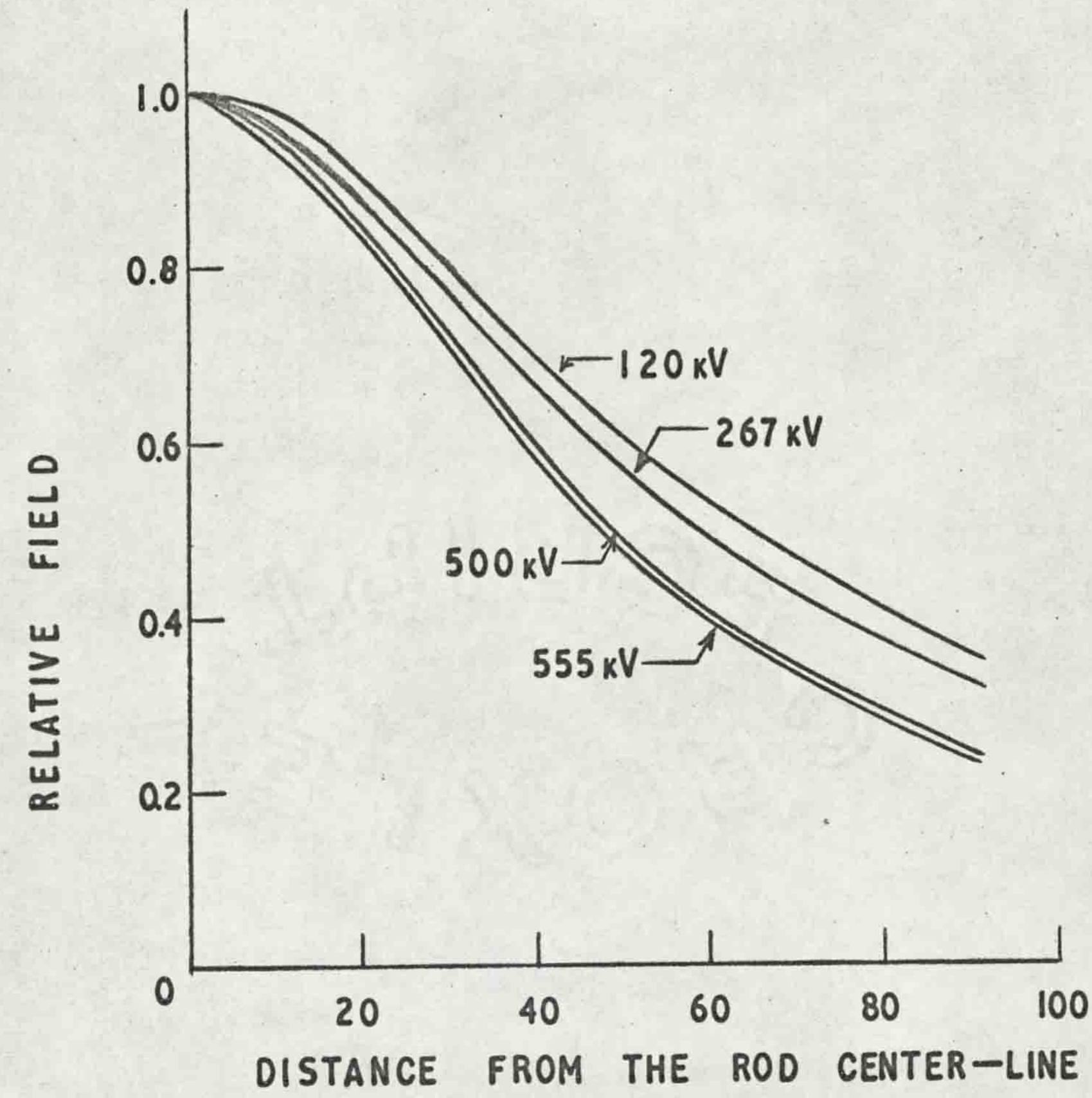

FIG. 60 RELATIVE FIELD DISTRIBUTION ALONG THE PLANE WITH A NEGATIVE ROD AND VARIOUS VOLTAGES

50CM GAP

lower gap. The field distribution along the plane confirms that the second discharge creates a space charge in the lower gap region as can be seen in Fig. 61. Curve 1 is the field distribution for the first discharge and curve 2 is the field distribution if a second discharge occurs. If the second discharge created a further space charge in the same region as the first space charge the two field distribution curves would be similar but the much sharper field distribution of the second discharge shows that the space charge is in the lower part of the gap. Sample oscillograms are shown in Fig. 62 where part A is the field at the rod center-line, part B the field 30½ cm from the rod center-line and part C the field 61 cm from the rod center-line. In each case the field when no second discharge occurs is also shown.

Previous workers[27,33] have shown that the corona completely crosses the gap before a positive leader is initiated from the plane and this work tends to confirm that result. From these field measurements it is obvious that the field which is sufficient to initiate a positive leader from the plane does not occur over a large area since the maximum field measured on a 2 cm diameter probe was less than 16 kV/cm.

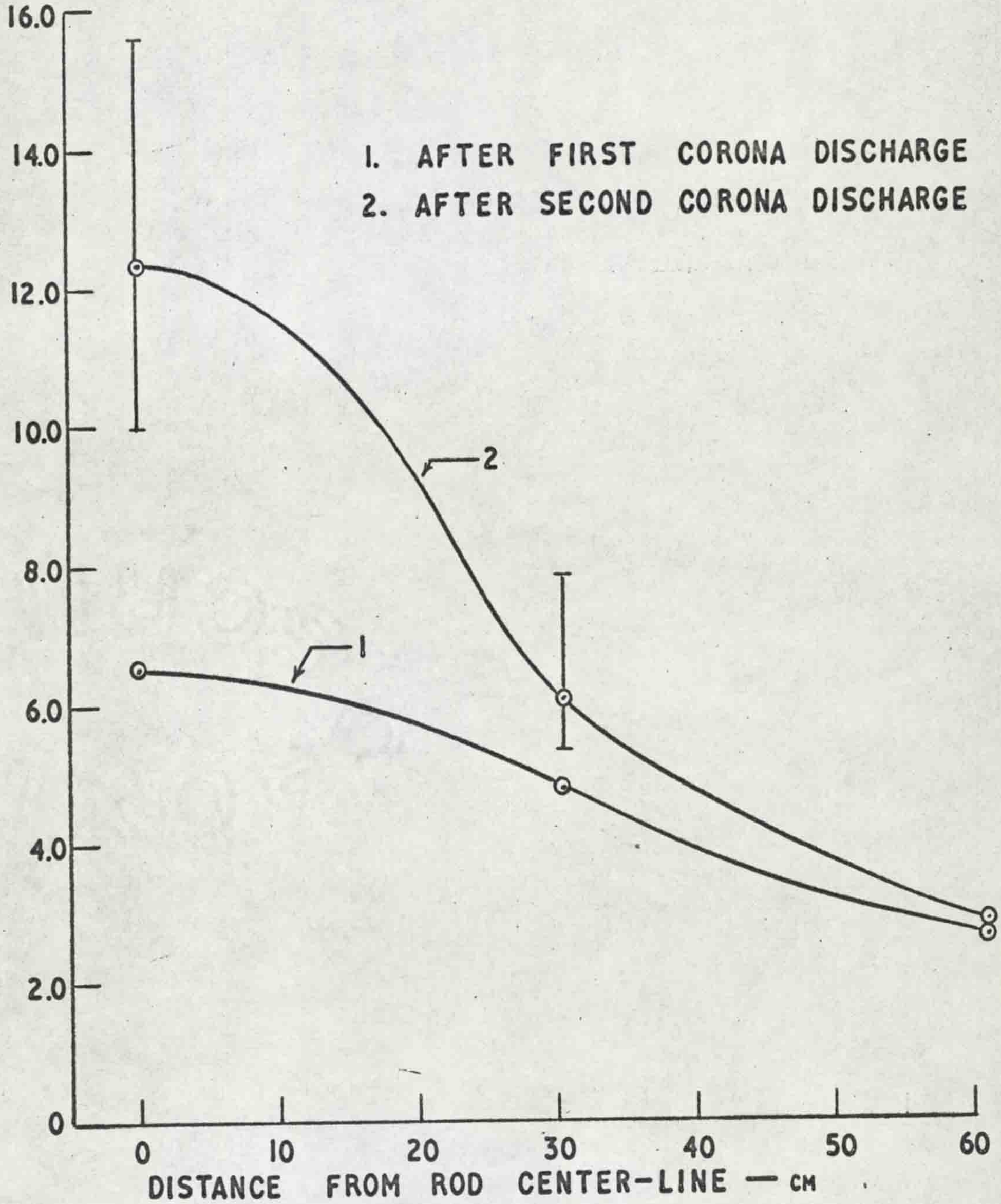

FIG. 61 FIELD DISTRIBUTION ALONG THE PLANE WITH A NEGATIVE ROD

50cm GAP
525 kV

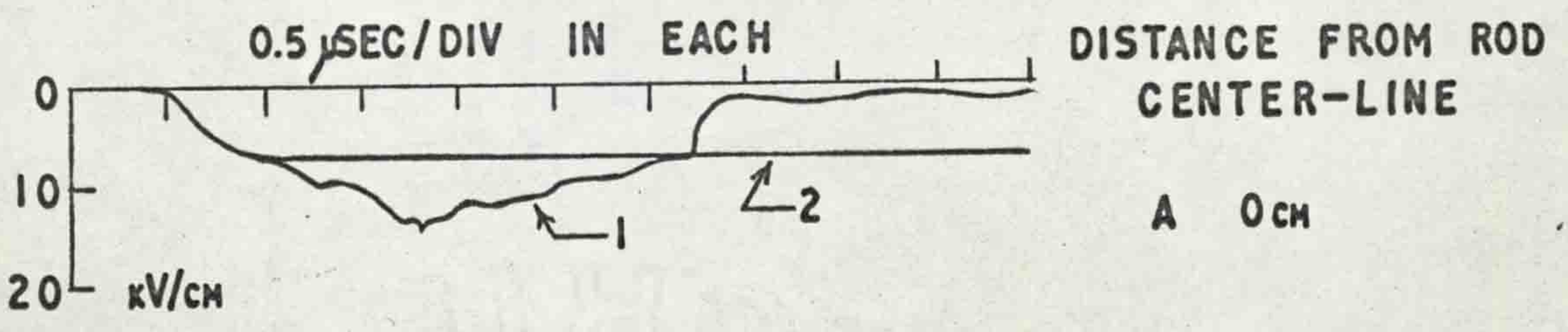

FIG. 62 FIELD AT THE PLANE WITH A NEGATIVE ROD

1. FIELD WITH A SECOND CORONA DISCHARGE
2. FIELD WITHOUT A SECOND CORONA DISCHARGE

50 cm GAP
525 kV

(ii) 100 cm gap

In order to determine the maximum field at the head of the negative corona filament it was necessary to use a smaller probe so the 2 mm diameter probe was tried. With the 1 m gap an applied impulse of 1,030 kV produced breakdown about 60% of the time in a series of 25 impulses. The field when no second discharge occurred reached a value of 9.6 kV/cm and a sample oscillogram is shown in Fig. 63, trace 1. When a second discharge occurred breakdown always followed and a peak field of from 13.5 to 27.2 kV/cm was measured. Trace 2 of Fig. 63 shows a sample oscillogram with breakdown occurring. The field rises to a peak value and then decreases slowly until breakdown when a sharp decrease in field occurs. The slow decrease in field is similar to that which occurs at the rod, in a positive rod gap, when the leader starts from the rod. This indicates that a positive leader starts from the plane causing the initial decrease in field. It was also noted that the higher the peak field the greater the drop due to the leader formation. The high field is due to the corona filament coming near to the probe and since the leader would have a greater shielding effect on the probe the nearer it is to the probe, this is further evidence that the leader starts from the point on the plane which is hit by the corona.

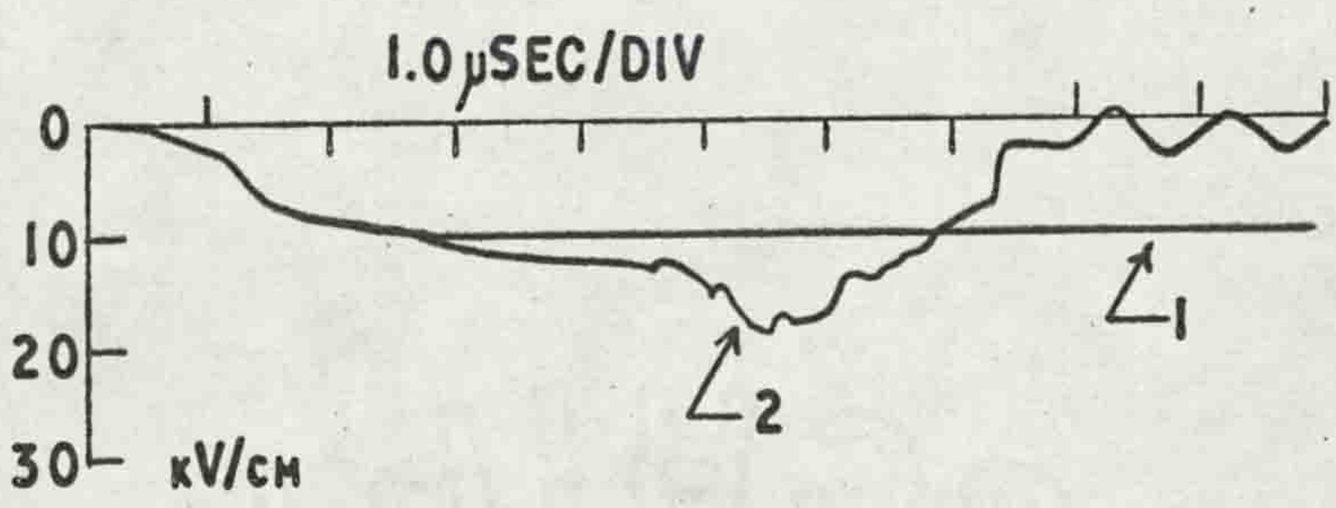

FIG. 63 FIELD AT THE PLANE WITH A NEGATIVE ROD

1. WITHOUT BREAKDOWN
2. WITH BREAKDOWN

100cm GAP
1030 kV

CHAPTER V

DISCUSSION AND CONCLUSIONS

Most of the results have been fully discussed and correlated with earlier work in the previous chapter, but a brief summing up is necessary to round off the work. There are two main contributions of this work which are the development of a new field measuring technique and the use of this technique to give a new perspective to the study of the spark breakdown of a rod-plane gap. From this study the following picture of the breakdown mechanism has emerged.

Considering first of all the positive rod case, the initial stage of breakdown, (1) the corona, is initiated with a varying time lag at the low voltages which indicates a statistical time lag but as the voltage is raised so (2) that corona starts on the wave front with very little time variation it starts at a reasonably constant field which indicates that the initiating electrons are produced by the high field from negative ions. It has been shown that the corona propagates in a low overall field, in the order of 5 kV/cm in the long gaps, and that the field at the tip of the corona filament is high, well in excess of

30 kV/cm and values have been measured up to 200 kV/cm. Field measurements at the rod have shown that the field rises as the corona propagates towards the plane which indicates that the space charge is associated with the tip of the corona filament. These facts support the theory[32,51] that the corona filament is a region of high space charge density which propagates due to its own high field and that it is not connected by a conducting channel to the rod.

Earlier work[23] indicated that the initial visible corona filled a roughly hemispherical volume which this work shows to be true for short gaps of about 15 cm but for longer gaps it would appear that the corona tends to fill a more cylindrical volume. There is however some evidence which suggests that the initial corona consists of two stages, the first being filaments directed radially from the rod end which would fill a hemispherical volume and the second being a downward directed corona starting from the surface of the hemispherical volume and tending to produce a cylindrical volume. Work is at present under way to calculate the field distribution along the plane due to various space charge distributions, then by comparing the calculated and measured values it is hoped that the actual space charge distribution can be found.

When the corona space charge has propagated a sufficient distance from the rod or when the space charge has been neutralized at the plane the field at the rod rises sufficiently to initiate a new discharge. This discharge, which is the leader channel, is different in character because it grows into a much more uniform field. The leader channel conducts along its length and from its tip the conduction is carried out by a succession of corona filaments which carry charge to the plane as did the initial corona. It is the sum of these small charges, generally in the order of 5×10^{-9} coulombs, which makes up the rising prebreakdown current. Final breakdown and collapse of voltage then occurs when the leader channel reaches the plane.

Turning to the negative rod case, there is again an initial radially directed corona from which a further, downward directed, corona may grow. The downward directed corona in this case differs greatly from the positive case in that it consists of only a few filaments rather than the several hundred of the positive case. When one of these filaments reaches the plane it causes a positive leader to grow from the plane which in turn leads to complete breakdown of the gap. The actual charge and field

associated with the negative corona were not measured but the acquisition of a new double beam oscilloscope should enable a two probe experiment to be done to determine these factors.

Further work using the field measuring technique is in progress to study the effect of wave front duration on the field at the plane and to study the field when various gases are used but there still remains considerable new work to be initiated. In order to get more information about breakdown in gaps several metres long it will be necessary to measure the field at the rod and for this the ideal technique would be to measure the field at the high voltage electrode using a Faraday cage to house an oscilloscope. This has the advantage that simultaneous measurements can be made at the rod and at the plane so there is no question about correlating results obtained by earthing each electrode in turn. It is also expected that much useful information could be obtained by extending the field measurement technique to the study of breakdown in other gap geometries and to the study of field distortion due to the effect of neighbouring objects.

Finally, it is noted that two papers have been prepared during the course of this work. One was published in

"Electronics Letters" and the second was read at the VIIth International Conference on Phenomena in Ionized Gases, Belgrade, August, 1965. Copies of these papers are appended inside the back cover of this thesis.

APPENDIX I

The minimum charge measured when a corona filament hit the 1 mm radius probe was 0.536×10^{-10} coulombs and the minimum field, due to a corona filament, which was measured when a 0.14 mm barrier was over the probe was 15.5 kV/cm. Assuming that the charge is in a spherical volume and, neglecting the charge distribution in the volume, that it acts as a point charge at the center of the volume the following result is obtained.

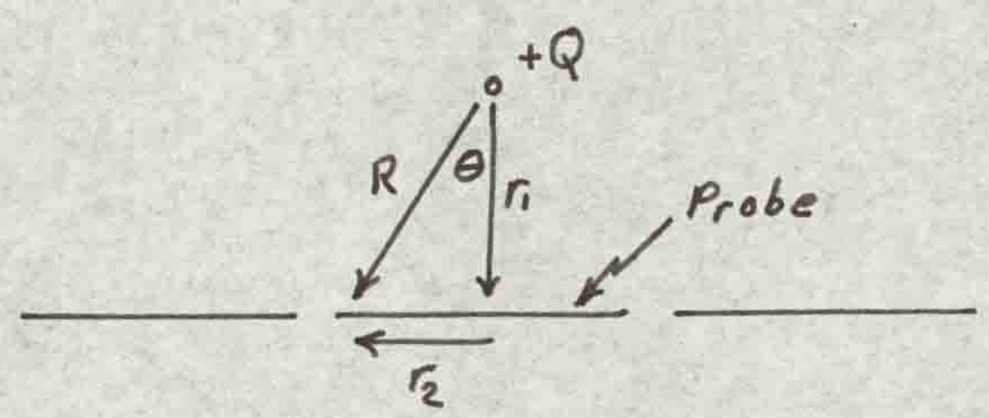

The average flux density, $D_{AV} = \dfrac{\int_{probe} \frac{2Q}{4\pi R^2} \cos\theta \, ds}{\text{Probe Area}}$

$$E_{AV} = \frac{D_{AV}}{\epsilon_0} = \frac{2Q}{4\pi\epsilon_0}\left[\int_0^{2\pi}\int_0^{r_2} \frac{1}{(r_1^2+r_2^2)} \cdot \frac{r_1}{(r_1^2+r_2^2)^{1/2}} \cdot r_2 \, dr_2 \, d\phi\right] \cdot \frac{1}{\pi r_2^2}$$

$$E_{AV} = \frac{2Q \cdot 2\pi r_1}{4\pi\epsilon_0 \pi r_2^2}\left[\frac{1}{r_1} - \frac{1}{(r_1^2+r_2^2)^{1/2}}\right]$$

Substituting the known values of E_{AV}, Q and r_2 and solving for r_1 gives r_1 = 0.204 mm. This gives a charge radius of 0.064 mm. The excess charge is

$$\frac{0.536 \times 10^{-10}}{1.6 \times 10^{-19}} = 3.35 \times 10^{8} \text{ ions}$$

which gives an excess charge density of

$$\frac{3.35 \times 10^{8}}{4/3\pi(6.4)^{3} \times 10^{-9}} \simeq 3 \times 10^{14} \text{ ions/c.c.}$$

These values compare to the theoretical values of Dawson and Winn of 10^{8} ions in a volume of radius 3×10^{-3} cm which gives charge density of approximately 10^{15} ions/c.c.

REFERENCES

1. Miller, S.L.: Production of Some Organic Compounds Under Possible Primitive Earth Conditions: J. Am. Chem. Soc., 77, 2351-60 (1955).
2. Urey, H.C.: The Early Chemical History of the Earth and the Origin of Life: Proc. Natl. Acad. Sci. U.S., 38, 351-63 (1952).
3. Schonland, B.F.J.: The Flight of Thunderbolts: Oxford (Clarendon) 1950.
4. Chalmers, J.A.: Atmospheric Electricity: Pergamon Press, 1957.
5. Franklin, B.: Experiments and Observations in Electricity: A Collection of Letters and Notes: London, 1769.
6. Hoffert, H.H.: Proc. Phys. Soc., 10, 176 (1889).
7. Walter, B.: Ann. Physik, 10, 176 (1903).
8. Boys, C.V.: Nature, 118, 749 (1926) and 122, 310 (1928).
9. Schonland, B.F.J. and Collens, H.: Proc. Roy. Soc. A., 143, 654 (1934)
   152, 595 (1935).
10. Harris, W.S.: Phil. Trans., 124, 213 (1834).
11. Faraday, M.: Experimental Researches in Electricity, Series 12, 1837.

12. Steinmetz, C.P.: Dielectric Strength of Air: AIEE, 15, 327 (1898).

13. Townsend, J.S.: Electrons in Gases: Hutchinson, 1947.

14. Loeb, L.B. and Meek, J.M.: The Mechanism of the Electric Spark: Stanford Press, 1941.

15. Marx, E.: Elektrotech. Z., 45, 652 (1924).

16. Craggs, J.D. and Meek, J.M.: High Voltage Laboratory Technique: Butterworths, London, 1954.

17. Meek, J.M. and Craggs, J.D.: Electrical Breakdown of Gases: Oxford, 1953.

18. Gorin, B.N. and Stekolnikov, I.S.: Reverse Discharges and Their Application to Lightning: Soviet Physics - Doklady, 9, 812 (Mar., 1965).

19. Nakaya, V. and Yamasaki, F.: Proc. Roy. Soc. A., 148, 446 (1935).

20. Beams, J.W.: Rev. Sci. Inst., 1, 780 (1930).

21. White, H.J.: Rev. Sci. Inst., 6, 22 (1935).

22. Komelkov, V.: Structure and Parameters of the Leader Discharge: Bull. Ac. Sci. U.S.S.R. Dept. Tech. Sci., 8, 955 (Aug., 1947). (BEAIRA Trans./IB871).

23. Meek, J.M. and Saxe, R.F.: BEAIRA Technical Report L/T183, 1948.

24. Meek, J.M. and Craggs, J.D.: Nature, 152, 538 (1943).

25. Allibone, T.E.: Nature, 161, 970 (1948).

26. Norinder, H. and Salka, O.: Mechanism of Positive Spark Discharges with Long Gaps in Air at Atmospheric Pressure: Arkiv för Fysik, 3, 347 (1951).

27. Norinder, H. and Salka, O.: Mechanism of Long-Gap Negative Spark Discharges in Air at Atmospheric Pressure: Arkiv för Fysik, 5, 493 (1952).

28. Norinder, H. and Salka, O.: Screens in Long Discharge Gaps: Arkiv för Fysik, 6, 151 (1953).

29. Norinder, H. and Salka, O.: Long Sparks from Negative Electrode with Limited Current in Air at Atmospheric Pressure: Arkiv för Fysik, 10, 397 (1956).

30. Allibone, T.E. and Meek, J.M.: The Development of the Spark Discharge:
Proc. Roy. Soc. A, 166, 97 (May, 1938)
169, 246 (Dec., 1938).

31. Saxe, R.F. and Meek, J.M.: The Initiation Mechanism of Long Sparks in Point-Plane Gaps: Proc. IEE, C, 102, 221 (1955).

32. Park, J.H. and Cones, H.N.: Surge Voltage Breakdown of Air in a Non-Uniform Field: J. of Res. N.B.S., 56, 201 (April, 1956).

33. Waters, R.T. and Jones, R.E.: The Impulse Breakdown Voltage and Time-Lag Characteristics of Long Gaps in Air - I The Positive Discharge, II The Negative Discharge: Phil. Trans. Roy. Soc. A, 256, 185 (April, 1964). High Voltage Impulse Breakdown of Rod-Plane Gaps in Air: Vth Int. Conf. on Ionization Phenomena in Gases, Munich, 1, 992 (1961).

34. Baatz, H., Böcker, H. and Fischer, A.: The Development of the Impulse Breakdown in Rod Spark Gaps: E.T.Z.-A, 83, 909 (Dec., 1962) CERL Translation.

35. Hudson, G.G. and Loeb, L.B.: Streamer Mechanism and Main Stroke in the Filamentary Spark Breakdown in Air as Revealed by Photomultipliers and Fast Oscilloscopic Techniques: Phys. Rev., 123, 29 (July, 1961).

36. Nasser, E. and Loeb, L.B.: Impulse Streamer Branching from Lichtenberg Figure Studies: J. App. Phys., 34, 3340 (Nov., 1963).

37. Dawson, G.A.: Temporal Growth of Suppressed Corona Streamers in Atmospheric Air: J. App. Phys., 36, 3391 (Nov. 1965).

38. Stekolnikov, I.S. and Shkilev , A.V.: Soviet Physics - Doklady, 6, 139 (Aug., 1961).

39. Stekolnikov, I. S.: New Information on Initial Stages of a Spark: Soviet Physics - Doklady, 6, 1085 (June, 1962).

40. Stekolnikov, I.S. and Shkilev, A.V.: New Data on Negative Spark Development and Its Comparison with Lightning: Gas Discharges and the Electricity Supply Industry - J.S. Forrest: Butterworths, London, 1962.

41. Stekolnikov, I.S. and Shkilev, A.V.: Investigation of Negative Spark Mechanisms: Soviet Physics - Doklady, 8, 829 (Feb., 1964).

42. Bazelyan, E.M., Brago, E.N. and Stekolnikov, I.S.: The Large Reduction in Mean Breakdown Gradients in Long Discharge Gaps with an Oblique-Sloping Voltage Wave: Soviet Physics - Doklady, 5, 794, (1970).

43. Stekolnikov, I.S., Brago, E.N. and Bazelyan, E.M.: Decrease of Discharge Potentials over Wide Gaps by Use of Oblique Angle Waves: Soviet Physics - Technical Physics, 7, 722 (Feb., 1963).

44. Stekolnikov, I.S. and Shkilev, A.V.: Development of a Long Positive Spark in the Case of an Exponential Voltage Wave Front: Soviet Physics - Doklady, 8, 825 (Feb., 1964).

45. Bazelyan, E.M.: Measurement of Space Charge in the Initial Stages of a Positive Long Spark: Soviet Physics - Technical Physics, 9, 370 (Sept. 1964).

46. Bazelyan, E.M. and Stekolnikov, I.S.: Change in the Mechanism of a Spark Several Metres Long Produced by Artificially Introducing a Space Charge into the Insulating Gap: Soviet Physics - Doklady, 9, 308 (Oct., 1964).

47. Gorin, B.N. and Inkov, A. Ya.: Investigation of a Spark Channel: Soviet Physics - Technical Physics, 7, 235 (Sept. 1962).

48. Wright, J.K.: Proc. Roy. Soc. A, 280, 23 (1964) CERL Laboratory Report RD/L/R 1202.

49. Kritzinger, J.J.: Nature, 197, 1165 (1963).

50. Aleksandrov, G.N.: Mechanism of Corona-to-Spark Transition in Long Air Gaps: Soviet Physics - Technical Physics, 10, 948 (Jan. 1966).

51. Dawson, G.A. and Winn, W.P.: A Model for Streamer Propagation: Zeit. für Physik, 183, 159 (1965).

52. Dawson, G.A.: The Lifetime of Positive Streamers in a Pulsed Point-to-Plane Gap in Atmospheric Air: Zeit. für Physik, 183, 172 (1965).

53. Kritzinger, J.J.: The Relation Between Impulse Corona and Breakdown: Proc. VIth Int. Conf. on Phen. in Ionized Gases, Paris, 2, 295 (1963).

54. Kritzinger, J.J.: Impulse Corona and the Breakdown Mechanism of Non-Uniform Gaps: CERL Laboratory Report No. RD/L/R 1197.

55. Loeb, L.B.: Electrical Coronas: University of California Press, 1965.

ACKNOWLEDGMENTS

The author is most grateful to Professor J. M. Meek for the guidance and instruction provided during the many hours of discussion on this investigation.

For financial assistance the author is indebted to the National Research Council of Canada for granting educational leave and to the Central Electricity Generating Board for providing the research contract under which this program was carried out.

Finally, the author is indebted to the technical and secretarial staff of the Department of Electrical Engineering and Electronics for their co-operation and assistance.

Reprinted from 'Electronics Letters', 1965, Vol. 1, p. 110.

MEASUREMENT OF ELECTRIC FIELDS AT ELECTRODE SURFACES

A new technique for determining the field at the surface of the earthed electrode of a gap subjected to an impulse voltage is described. An example is given of the results obtained when the technique is applied to the study of the field variation during the initial stages of spark breakdown in a rod–plane gap, showing, in particular, the influence of space charges.

A new technique for determining the field at the surface of the earthed electrode of a gap subjected to an impulse voltage has been developed. The technique involves the measurement of the charge induced on a small probe mounted flush with the surface of the electrode and is based on the principle that the field is proportional to the electric flux density. It differs in principle from a technique developed by Kritzinger[1] in which the field is determined from the voltage developed on a probe projecting into the gap.

Consider a probe of area A with an electric flux of ψ coulombs entering it. Since $\epsilon_0 E = D = \psi/A$ and $\psi = \int i\,dt$, where i is the displacement current in the probe, it follows that $E = \int i\,dt/\epsilon_0 A$. Using this relationship, the field can be obtained by taking an oscillogram of the current in the probe and by finding the integral mechanically. It is, however, more expedient to integrate using a capacitor C, as shown in Fig. 1. An oscillogram of the voltage V across the capacitor then enables the field to be calculated

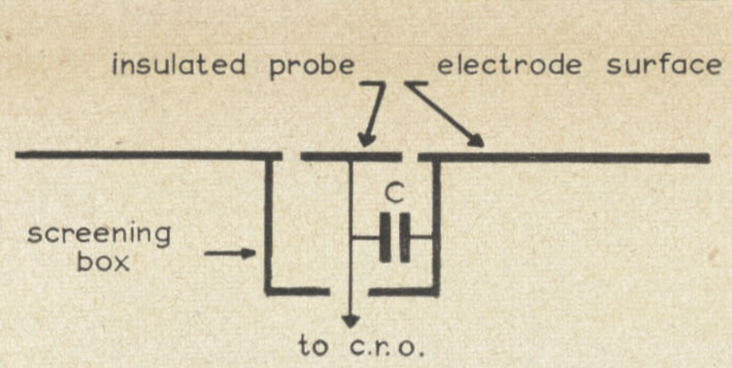

Fig. 1 *Diagram of probe connection*

from $E = CV/\epsilon_0 A$. As C, A and ϵ_0 are all constant, the voltage oscillogram can be calibrated directly in terms of E.

Experiments have been carried out with a circular probe mounted in the earthed-plate electrode of a uniform-field gap. The results show that allowance has to be made for the insulation thickness between the probe and the surrounding electrode, as the insulation increases the effective radius of the probe by approximately one half the insulation thickness. For a 1 cm-radius probe the insulation thickness can be made negligible, and the electric field determined by the probe agrees with that obtained from the applied voltage and gap length within the limits of error of the voltage divider used to measure the impulse voltage.

The effect of voltage on the probe was investigated by decreasing C by a factor of 10, which increased V from 20 to 200 V for a field of 22 kV/cm. This resulted in a $2\frac{1}{2}\%$ decrease in the measured field, which indicates the importance of keeping C at the maximum value consistent with obtaining a voltage which can be accurately measured on the oscilloscope.

Two other points must be considered when interpreting the results. Firstly, the technique gives the average field over the surface of the probe, and consequently, for nonuniform fields, the probe must be made small, if accurate values of localised fields are to be obtained. This is also true for uniform fields if local nonuniformities of field due to space charge are to be investigated. Secondly, the time constant of the measuring circuit will introduce error for measurements involving long times. From this point of view a high C and a high-input-impedance oscilloscope are desirable.

The technique has been applied to the study of the field variation during the initial stages of spark breakdown of rod–plane gaps and in particular to determine the influence on the field of space charges introduced by corona streamers. It has been used both at the rod and at the plane, depending on which was the earthed electrode, for both positive and negative rod–plane gaps. Fig. 2 gives an

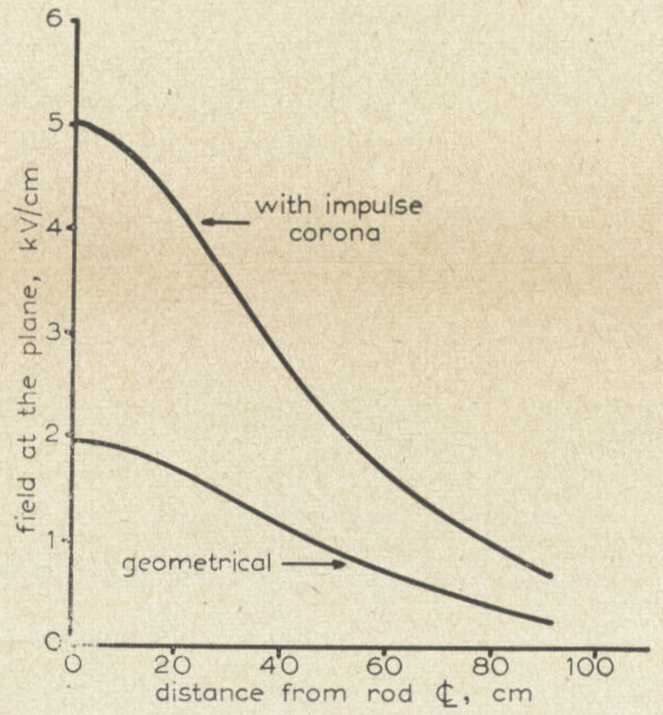

Fig. 2 *Field distribution at the plane for a 50 cm rod–plane gap with a 500 kV negative impulse applied to the rod*

example of the results for a 50 cm rod–plane gap with a negative impulse of 500 kV applied to the rod, which is sufficient to cause impulse corona at the rod without breakdown of the gap. The geometrical field, i.e. the field due to the geometry of the gap in the absence of a discharge, was obtained by scaling up the result for an applied voltage below the corona-onset voltage. The results show that the field at the plane is greatly increased by the development of the impulse corona discharge at the rod. A further substantial increase in the field at the plane occurs at higher voltages, sufficient to cause ultimate breakdown of the gap. A comprehensive account of this work will be published in the near future.

This technique can be applied to the study of the field at either electrode of any gap configuration, with or without space charge, provided that the probe is so positioned that the conduction current to it is zero. For example, it may be used to determine the field distortion at the electrode surface in parallel-plane gaps or sphere gaps due to the presence of neighbouring objects, or it may be used to study the field distortion caused by the firing of the trigger gap in a trigatron. These are only two of the many applications envisaged by the authors.

During the preparation of this note, the authors found that Bazelyan[2] and Bazelyan and Stekolnikov[3] have used another technique based on the same principle to measure more accurately than has been done previously the amount of charge injected into a gap by the corona from the sphere in an inverted sphere–plane gap.

Acknowledgment

Acknowledgment is made of the financial assistance given to this project by the Central Electricity Generating Board.

J. M. MEEK
M. M. C. COLLINS*
Department of Electrical Engineering
The University of Liverpool
Liverpool 3, England

31st May 1965

References

1 KRITZINGER, J. J.: 'The relation between impulse corona and breakdown', VI Conf. Int. sur les Phenomenes d'Ionization dans les Gaz, Paris 1963, **2**, p. 295
2 BAZELYAN, E. M.: 'Measurement of space charge in the initial stages of a positive long spark', *Soviet Physics—Technical Physics*, 1964, **9**, p. 370
3 BAZELYAN, E. M., and STEKOLNIKOV, I. S.: 'Change in the mechanism of a spark several meters long produced by artificially introducing a space charge into the insulating gap', *Soviet Physics—Doklady*, 1964, **9**, p. 308

* On leave of absence from the National Research Council, Ottawa, Canada

Adlard & Son, Ltd., Bartholomew Press, Dorking